R93-970104-2

(2)

AFOSR-TR- 93 0082

PROCESSING AND PROPERTIES OF COATED HPZ FIBER REINFORCED GLASS-CERAMIC MATRIX COMPOSITES

Prepared by

John Brennan
William Allen
Philip McCluskey
David Jarmon

FINAL REPORT

Contract F49620-88-C-0062

for

Air Force Office of Scientific Research
Bolling Air Force Base
Washington, DC 20332

MARCH 31, 1993

UNITED TECHNOLOGIES RESEARCH CENTER
East Hartford, Connecticut 06108

REPORT DOCUMENTATION PAGE

Form Approved
OMB No 0704-0188

1. AGENCY USE ONLY (Leave blank)	2. REPORT DATE	3. REPORT TYPE AND DATES COVERED
	31 March 1993	Final Report 5/88-1/93

4. TITLE AND SUBTITLE

PROCESSING AND PROPERTIES OF COATED HPZ FIBER REINFORCED GLASS-CERAMIC MATRIX COMPOSITES

5. FUNDING NUMBERS

F49620-88-C-0062

61102F

2306/A2

6. AUTHOR(S)

John Brennan, William Allen, Philip McCluskey, David Jarmon

7. PERFORMING ORGANIZATION NAME(S) AND ADDRESS(ES)

United Technologies Research Center
East Hartford, CT 06108

8. PERFORMING ORGANIZATION REPORT NUMBER

R93-970104 2

9. SPONSORING / MONITORING AGENCY NAME(S) AND ADDRESS(ES)

Lt Col Larry W. Burggraf
Air Force Office of Scientific Research/NE
Building 410, Bolling Air Force Base
Washington, DC 20332-6448

10. SPONSORING / MONITORING AGENCY REPORT NUMBER

F49620-88-C 0062

11. SUPPLEMENTARY NOTES

12a. DISTRIBUTION / AVAILABILITY STATEMENT

Unlimited

12b. DISTRIBUTION CODE

13. ABSTRACT *(Maximum 200 words)*

The main objective of this program was to utilize fiber coatings to tailor, or "engineer", the chemistry and bonding characteristics of the fiber/matrix interface in glass-ceramic matrix composites reinforced with Dow Corning's polymer derived Si-N-C-O "HPZ" fibers such that relatively weak bonding exists at the interface to allow matrix crack deflection to occur, thus increasing the toughness and damage tolerance of the composite, while at the same time maintaining the high temperature oxidative stability of the matrix/coating/fiber interfacial region. In addition, for this particular system which is inherently reactive, the fiber coating must also act as a barrier to interdiffusion and reaction. A secondary objective of this program is to investigate advanced composite processing methods other than the traditional hot-pressing, such as hot isostatic pressing (HIP) and glass matrix transfer molding into integrally woven fiber preforms.

During the performance of this contract, the microstructure and properties of HPZ fibers, CVD BN and SiC/BN coatings on HPZ fibers, and barium magnesium aluminosilicate (BMAS) glass-ceramic composites fabricated with these coated fibers were investigated. It was found that the HPZ fibers exhibit a porous, oxygen rich surface that appears to enhance their reactivity at elevated temperatures, either by themselves or with the BMAS composite matrix. Early experiments with BN and SiC/BN coated HPZ fibers in BMAS glass-

14. SUBJECT TERMS

Ceramic composite interfaces, HPZ fiber microstructure, BMAS glass-ceramic matrix/coated HPZ fiber composites

15. NUMBER OF PAGES

117

16. PRICE CODE

17. SECURITY CLASSIFICATION OF REPORT	18. SECURITY CLASSIFICATION OF THIS PAGE	19. SECURITY CLASSIFICATION OF ABSTRACT	20. LIMITATION OF ABSTRACT
Unclassified	Unclassified	Unclassified	SAR

13. ABSTRACT (Cont'd)

in BMAS glass-ceramic matrices resulted in relatively poor composite performance due to non-uniform BN coatings leading to subsequent fiber/matrix reactivity. More recent experiments with HPZ fibers that exhibited better handleability during the BN coating process, yielding more uniformly coated fibers, resulted in BMAS matrix composites that exhibited much improved flexural and tensile properties to temperatures of 1200°C. Alternate processing experiments utilizing coated fibers in BMAS matrices demonstrated the viability of composite processing by both hot isostatic pressing (HIP) and matrix transfer molding.

UNITED TECHNOLOGIES RESEARCH CENTER
East Hartford, Connecticut 06108

R93-970104-2

Processing and Properties of Coated HPZ Fiber Reinforced Glass-Ceramic Matrix Composites

FINAL REPORT

Contract F49620-88-C-0062

APPROVED BY: K. M. Prewo

K. M. Prewo, Manager of
Materials Sciences

DATE: 3/31/93

TABLE OF CONTENTS

TABLE OF CONTENTS (Cont'd)

PROCESSING AND PROPERTIES OF COATED HPZ FIBER REINFORCED GLASS-CERAMIC MATRIX COMPOSITES

SUMMARY

The main objective of this program was to utilize fiber coatings to tailor, or "engineer", the chemistry and bonding characteristics of the fiber/matrix interface in glass-ceramic matrix composites reinforced with Dow Corning's polymer derived Si-N-C-O "HPZ" fibers such that relatively weak bonding exists at the interface to allow matrix crack deflection to occur, thus increasing the toughness and damage tolerance of the composite, while at the same time maintaining the high temperature oxidative stability of the matrix/coating/fiber interfacial region. In addition, for this particular system which is inherently reactive, the fiber coating must also act as a barrier to interdiffusion and reaction. A secondary objective of this program was to investigate advanced composite processing methods other than the traditional hot-pressing, such as hot isostatic pressing (HIP) and glass matrix transfer molding into integrally woven fiber preforms.

The fiber chosen for this study was the polymer derived (hydridopolysilazane) Si-N-C-O HPZ fiber from Dow Corning. The primary glass-ceramic matrix utilized is based on the barium-magnesium aluminosilicate (BMAS) system that crystallizes to barium osumilite ($BaMg_2Al_6Si_9O_{30}$). A magnesium aluminosilicate (MAS) matrix that crystallizes to cordierite ($Mg_2Al_4Si_5O_{18}$) has been utilized for the glass transfer molding studies. The fiber coatings are based on BN, with and without a SiC diffusion barrier overlayer. 3M was chosen as the primary fiber coating source, utilizing their CVD coating technology. The chemistry and structure of the resultant composite interfacial region was studied utilizing surface science techniques such as the scanning Auger depth profiling of coated fiber and composite fracture surfaces, and high resolution TEM for interface structure and phase determination. The fiber/coating/matrix bonding and chemistry were then related to the resultant composite properties.

Past studies on this contract have shown that BN coatings of ~200-400nm in thickness on Nicalon Si-C-O fibers in BMAS matrices have yielded composites with excellent strength and moderate toughness characteristics. Maximum high temperature composite strength and oxidative stability was achieved utilizing an overcoat of ~200nm of SiC to prevent boron diffusion from the BN layer into the BMAS matrix. Interfacial TEM and Auger analysis has shown that the SiC/BN layer on the fibers can prevent the oxidatively unstable carbon layer from forming on the Nicalon fiber surface during composite fabrication.

In contrast, from the current studies it has been found to be very difficult to prevent fiber/matrix reactions from occurring in the HPZ fiber/BMAS matrix system, utilizing the same types of fiber coatings. The HPZ fibers themselves have been found from TEM analysis to have a microporous oxygen rich surface layer of ~200-300nm in thickness that is extremely reactive when in contact with aluminosilicate glass-ceramic matrices at elevated temperatures. Diffusion of matrix elements (Ba, Mg, O, Al, Si) through this surface layer occurs very rapidly, with the result being crystallization of the underlying HPZ fiber to silicon oxynitride (Si_2N_2O). In the BN and SiC/BN coated HPZ fiber composites, it has been found from TEM and scanning Auger studies that at the usual processing temperature of 1430°C for 5 min, matrix element diffusion through the CVD BN layer to the HPZ fiber surface will result in reacted fiber surfaces if the BN layer is less than ~200nm in thickness or if it detaches from the fiber surface. In the SiC overcoated BN coated HPZ fiber composites, the SiC will prevent matrix element diffusion into the BN layer, but it has been found that a number of the coated fibers exhibited detached SiC layers during composite processing, which can exacerbate the reactivity problem.

A number of factors may be responsible for the observed results. Certain lots of HPZ fibers appear to shrink during composite processing. Evidence of this has been seen in SEM examination of composite fracture surfaces and TEM replicas of polished composite cross-sections. If the HPZ fibers do shrink, the stresses set up may detach the BN and/or SiC coatings, which then can fracture easily during composite processing leading to the observed matrix/fiber reactions. Since most of the coating detachment observed has been related to the SiC coatings, it may be a result of either the less compliant nature of the SiC vs the BN coating, or the higher thermal expansion of the SiC compared to the BN or the HPZ fiber itself leading to stresses in the SiC layer during processing, or a combination of the two.

In addition to coating fracture or spallation during composite processing, uniform coating thicknesses has been found to be a concern. It has been found by 3M that the HPZ fiber tow, unlike Nicalon fiber, tends to fray and become very fuzzy when the sizing is removed prior to coating deposition. This fuzziness is related to broken fibers which curl away from the rest of the 500 filament tow. During the CVD coating deposition process, these fibers are the first to become coated and wind up with a very thick coating while the interior fibers in the tow do not receive the necessary gas compositions to insure proper coating deposition. The result is thinner than anticipated BN layers which then lead to HPZ fiber/matrix reactions as discussed previously. The fuzzy nature of the HPZ fiber tow also causes clogging of the CVD reactor orifices through which the tows pass. This causes tow breakage and coating damage.

While a significant number of composites were fabricated that exhibited excessive fiber/matrix reaction and thus low composite properties, due to the above factors, improvements in the handleability of the HPZ fibers towards the end of the program resulted in much improved and more uniform BN coatings and, subsequently, much improved composite properties. Flexural strengths for 0/90° BMAS matrix composites of over 50 ksi (345 MPa) from RT to 1100°C were routinely achieved with the improved coated fibers. Only a slight amount (<5%) of the BN coated fibers showed evidence of fiber/matrix reaction. While SiC layer detachment was still a problem, the more uniform BN layers resulted in much less reactivity. For use temperatures to 1100°C, the SiC overcoat layer may not be necessary. The key to fabricating composites without matrix/fiber reaction is to insure that the BN coating thickness is at least 300nm. Additional work may be necessary to achieve this for 100% of the coated fibers in the composites.

As mentioned previously, a secondary objective of this program was to investigate alternate composite processing methods such as HIP and glass transfer molding. Experiments conducted in these areas were first focused on uncoated Nicalon fiber composites and, when these proved successful, on SiC/BN coated Nicalon fiber composites. Coated HPZ fiber composites processed by HIP or glass transfer molding were not able to be fabricated since, by the time an optimized coated HPZ fiber was obtained, the program schedule could not accommodate further processing studies.

HIP studies in the past at UTRC have shown that low temperature fiber reinforced borosilicate glass composites could be successfully HIP'd into tubular or L-bracket structures utilizing sheet steel canning methods. A higher temperature glass-ceramic system such as BMAS cannot use steel cans without melting due to the Fe-C eutectic. Experiments under this program demonstrated that, utilizing titanium canning, BMAS matrix/coated Nicalon fiber composite articles could be successfully densified using the HIP processing method. Two L-brackets of ~13 cm x 4 cm x 4 mm wall thickness were fabricated in the UTRC HIP. This was the first time a high temperature BMAS matrix composite article was densified using the HIP process. Although this size composite could be fabricated in a hot-press, larger sizes (up to one meter in length) that could not be hot-pressed could be HIP'd in a facility that UTRC has used in the past with minimum scale-up required.

Glass transfer molding of a MAS matrix/SiC/BN coated woven Nicalon fiber composite has also been demonstrated under this program. A 3D angle interlock preform of coated fiber was woven at Techniweave, Inc. Subsequent glass transfer molding of the MAS glassy matrix into this preform was done at a temperature of ~1480°C, a temperature where the glass viscosity was low enough so that flow into and around all the fiber tows could take place. From mechanical property testing and TEM analyses, however, it was found that a significant amount of coating damage occurred

either during the weaving of the coated fiber tow, or during composite fabrication, or both. Refinement of this technique by utilizing sizing on the coated fiber tows to minimize damage during the weaving process, or by batch coating pre-woven fiber preforms should be explored. If successful, this method of composite processing could be applied to fabricate very intricate shapes, which could not be fabricated by the usual uniaxial hot-pressing methods.

I. INTRODUCTION

Fiber reinforced glasses and glass-ceramics have been under study at UTRC and other research organizations for a number of years as possible high temperature, lightweight, structural materials[1-41]. For the past few years this research at UTRC has concentrated on the study of the fiber/matrix interface and the relationship of the interfacial morphology, chemistry, and degree of bonding to the resultant composite mechanical and environmental properties[13,14,17,20,36]. From the results of these studies, it has been found that polymer derived Si-C-O or Si-C-N-O fibers such as Nicalon (Nippon Carbon Co.), Tyranno (Ube Industries), and Dow Corning's MPDZ (methylpolydisilylazane), that contain excess carbon and oxygen over stoichiometric SiC, form a carbon rich fiber/matrix interfacial layer when incorporated into glass-ceramic matrices at elevated temperatures. The exact mechanisms for the formation of this layer are not totally defined, but may be related to diffusion of oxygen and silicon ions down the silica activity gradient that exists from fiber to matrix, as proposed by Cooper and Chyung[19]. The formation of this weak interfacial zone in these composites is responsible for the high toughness observed, in that it allows crack deflection to occur along the fiber/matrix interface and also allows load transfer from matrix to fiber to occur so that strengthening by traditional composite theory can take place. Unfortunately, it has also been found that those composites with a carbon rich fiber/matrix interfacial layer undergo an embrittlement and concurrent strength and toughness degradation when either stressed at elevated temperatures in an oxidizing environment or thermally aged in an unstressed condition for relatively long periods of time in an oxidative environment at temperature.

In the case of fibers that do not form an *in situ* carbon rich interface during glass-ceramic matrix composite processing, such as the high nitrogen HPZ (hydridopolysilylazane) fibers from Dow Corning, or oxide fibers such as the mullite based Nextel fibers from 3M or the alumina based FP and PRD-166 fibers from DuPont, the fiber/matrix interfacial bonding is strong, with resultant composite behavior that is weak and brittle. An example of a typical brittle fracture surface of an LAS matrix/HPZ fiber composite is shown in Fig. 1. In the case of HPZ fibers, a reaction occurs during composite processing that forms silicon oxynitride at the fiber/matrix interface[20], similar to that seen for silicon nitride whiskers in LAS (lithium aluminosilicate) glass-ceramic matrices[40]. A large amount of fiber/matrix interdiffusion also occurs for the above systems, contributing to weakening of the fibers.

The main objective of this program is to utilize fiber coatings to tailor, or "engineer", the chemistry and bonding characteristics of the fiber/matrix interface in

glass-ceramic matrix composites reinforced with Dow Corning's polymer derived Si-N-C-O "HPZ" fibers such that relatively weak bonding exists at the interface to allow matrix crack deflection to occur, thus increasing the toughness and damage tolerance of the composite, while at the same time maintaining the high temperature oxidative stability of the matrix/coating/fiber interfacial region. In addition, for this particular system which is inherently reactive, the fiber coating must also act as a barrier to interdiffusion and reaction. A secondary objective of this program is to investigate advanced composite processing methods other than the traditional hot-pressing, such as hot isostatic pressing (HIP) and glass matrix transfer molding into integrally woven fiber preforms.

II. BACKGROUND

During the past few years, the interest in fiber coatings as a means of controlling the fiber/matrix interfacial properties in ceramic matrix composites has increased[41-52]. Studies conducted at UTRC in this area in the past few years have consisted of an investigation as a subcontractor to Dow Corning Corp. on a DARPA/AFML program to evaluate a variety of fiber coatings on Nicalon and HPZ fibers[43], an ONR program studying the effect of coatings on monofilament boron and SiC fibers in glass matrices[45], as well as an ONR program to investigate BN coatings on Nicalon fibers in a chemically vapor infiltrated (CVI) SiC matrix[46]. An example of an early coated HPZ fiber composite fracture surface from work conducted in 1987 under the DARPA/AFML program[43] is shown in Fig. 2. This figure shows that utilizing a 3000Å thick carbon coating on the HPZ fibers in an LAS matrix composite prevents the usual fiber/matrix interaction, with the result being a strong, tough, composite with good interfacial debonding characteristics. Unfortunately, the carbon interface is not oxidatively stable, rendering it ineffective at elevated temperatures in oxidizing environments.

From the work conducted under the current AFOSR program in 1991[41], it was found that fiber coatings, such as CVD BN and CVD SiC over BN, deposited on small diameter fibers such as the SiC based Nicalon fiber from Nippon Carbon Co. and the Si-N-C based HPZ fiber from Dow Corning Corp., can result in strong, tough, and oxidatively stable high temperature structural composites when these coated fibers are incorporated into glass-ceramic matrices such as lithium aluminosilicate (LAS) and barium-magnesium aluminosilicate (BMAS).

BN coated Nicalon fibers were investigated from two sources: General Atomics (GA) in San Diego, CA, and 3M in St. Paul, MN. Most of the GA BN coatings evaluated were deposited at low temperatures (500°-550°C) from diborane plus ammonia precursors and were totally amorphous with relatively stoichiometric BN chemistry. The 3M BN coatings were deposited at higher temperatures (~1000°C) utilizing a 3M proprietary precursor and were amorphous to partly turbostratic in nature with a chemistry close to stoichiometric BN with ~15 at% C included. The morphology of the BN coatings from GA was, in general, much smoother than that of the 3M coatings, although the measured tensile strength and handleability of the 3M coated fibers was usually much better than that of the GA coated fibers.

Most of this previous work focused on LAS matrix composites that were fabricated from both the GA and 3M BN coated Nicalon fibers. In general, the flexural strength of the 3M coated fiber composites was significantly higher than the GA coated fiber composites, although above ~1000°C the strength decreased significantly. Interfacial analysis of the BN coated Nicalon fiber composites, utilizing both scanning Auger microprobe (SAM) depth profiling of fracture surfaces and transmission electron microscopy (TEM) of thin foils, indicated that during composite fabrication the BN coating next to the LAS matrix crystallized with concurrent Si and Al matrix element diffusion into it, and a significant amount of boron diffusion occurred from the BN coating into the LAS matrix. The boron diffusion into the LAS matrix prevented complete crystallization of the matrix to the high temperature β-spodumene structure, with the residual boron containing glassy regions contributing to the low elevated temperature strength of the composites. From the SAM analyses, the higher temperature CVD 3M BN coatings appeared to be more resistant to matrix element diffusion through them than did the lower temperature CVD GA BN coatings. Interfacial debonding appeared to be enhanced in those regions of the BN coating where no matrix element diffusion occurred.

In order to prevent boron diffusion into the matrix during composite fabrication, a thin (2000-4000Å) diffusion barrier SiC overcoat was applied to the BN coated Nicalon fibers by 3M. From SAM and TEM analyses, it was found that this SiC layer prevented boron diffusion into the matrix and matrix element diffusion into the BN, thus resulting in composites with superior elevated temperature properties compared to BN coated Nicalon fiber composites. Both LAS and BMAS matrix composites were fabricated with the 3M SiC/BN coated Nicalon fibers, with the LAS and BMAS matrix composites resulting in high strengths and thermal and oxidative stability to ~1100°C and 1200°C, respectively.

Only a brief study was conducted into the interfacial properties, microstructure, and strength vs temperature for BN and SiC/BN coated HPZ fiber/BMAS matrix composites. As in the coated Nicalon fiber composites, it was found that the best elevated temperature properties were obtained with the dual SiC/BN coated HPZ fibers. Respectable flexural strength to 1200°C in air was obtained for this composite system. Similar to coated Nicalon fiber composites, interfacial debonding occurred in the BN layer that did not contain diffused matrix elements such as Si, Al, and Ba.

It thus appeared that the BMAS matrix composite systems with both Nicalon and HPZ fibers coated with SiC over BN offer significant potential as tough, thermally stable, structural ceramic composites for applications to ~1200°C. A new AFOSR contract (F49620-92-C-0001) has continued with the emphasis focused primarily on BN based coatings for Nicalon fibers in glass-ceramic matrix composites[53]. The AFOSR contract

(F49620-88-C-0062) discussed in this report was redirected in September, 1991, to concentrate on BMAS glass-ceramic matrices reinforced with BN based coatings on HPZ fibers. This final report will cover the work performed on this contract from September 1, 1991 through January 31, 1993.

III. TECHNICAL DISCUSSION

The research under this program is divided into six main tasks: I. HPZ Fiber/Coating/Matrix Predictive Modelling; II. Coated and Uncoated HPZ Fiber Characterization; III. Glass-Ceramic Matrix/Coated Fiber Composite Fabrication; IV. Composite Mechanical and Thermal Testing; V. Microstructural and Microchemical Analysis of Composites; and VI. Alternate Processing of Glass-Ceramic Matrix/Coated Fiber Composites. These tasks are set up to run concurrently and are iterative with one another.

During the period of performance covered in this report, studies under this program have dealt with the composite system consisting of a barium-magnesium aluminosilicate (BMAS) matrix that contains either BN or SiC over BN coated HPZ fibers. The HPZ fibers[54] were obtained from the Dow Corning Corporation, Midland, Michigan. The fiber coatings have been applied by a chemical vapor deposition process at 3M Co., St. Paul, MN. A portion of Task VI was performed with a magnesium aluminosilicate (MAS) matrix and both coated and uncoated Nicalon fibers.

A. Fiber/Coating/Matrix Predictive Modelling Studies - W. Allen

The thermodynamic stability and compatibility of phases comprising the matrix, fiber, and fiber coatings are important considerations in the development of high-temperature composite materials. Although chemical interactions are often suppressed at lower temperatures due to kinetic constraints, thermodynamic stability is the primary concern for high-temperature materials since reaction rate kinetics in condensed systems (which are usually diffusion controlled) tend to increase exponentially with increasing temperature. Thermodynamic calculations were performed as part of this investigation to address stability and compatibility issues and thereby predict chemical interactions which may occur during composite processing. In the analyses which follows, therefore, calculations were performed assuming temperatures typically used for hot pressing and ceraming of glass-matrix composites (1400°C [1673K] and 1200°C [1473K] *respectively*[37]).

1. Thermodynamic Analysis

(a) Si-N-O-C Phase Equilibria

The HPZ fibers used in this investigation consist of an amorphous mixture of Si-N-O-C with an approximate composition of 43at% Si-36at% N-16at% C-5at% O[55]. The thermal stability of HPZ fibers can be assessed by calculating the Si-O-N-C quaternary

system. Assuming that condensed phases exist in either the elemental form or as stoichiometric compounds, ternary and quaternary phase equilibria can be predicted by writing possible displacement reactions[56]. Consideration of the free energy change associated with a given reaction involving competing equilibria then defines the equilibrium phase mixture for a given composition.

Using available thermodynamic data[57-59], equilibria between vapor and condensed phases can be calculated for the four three component (ternary) systems which comprise the Si-N-O-C quaternary system. A composite representation of the calculated ternary systems illustrating their relationship to the resulting quaternary system is shown in Fig. 3. Each of the unshaded triangles would be folded along the edge adjacent to the shaded triangle to form the quaternary tetrahedron. Although the phase diagram shown in Fig. 3, represents equilibrium at 1473K, equilibria at 1673K is identical. It should be noted that this diagram is constructed assuming unit activity of components and compounds.

(b) Si-N-O Phase Stability Diagrams

Phase stability diagrams were calculated to provide a more detailed assessment of the stability of condensed phases in the presence of vapor. These calculations do not assume unit specie activities in the vapor phase and therefore provide a more accurate description of thermodynamic stability.

Three-phase equilibrium between two solid phases and the vapor phase was calculated using available thermodynamic data. For example, equilibrium between Si_3N_4, Si_2N_2O and vapor phase can be represented by:

$$2Si_3N_{4(s)} + 3/2O_{2(v)} = 3Si_2N_2O_{(s)} + N_{2(v)} \qquad (1)$$

with a corresponding Gibbs free energy change, $DG_1\circ$, of -960-0.0153T kJ. This free energy change can also be expressed as:

$$\Delta G_1\circ = -RT\ ln\ [(a_{Si_2N_2O})^3 P_{N_2} / a_{Si_3N_4}(P_{O_2})^{3/2}] \qquad (2)$$

where a_i and P_i represent the activity of species i and RT has the usual meaning. Assuming unit activity of condensed phases, this equilibrium can then be rewritten as:

$$log\ [(P_{O_2})^{3/2}/(P_{N_2})] = (-50{,}110/T) - 0.800 \qquad (3)$$

where P_{O_2} and P_{N_2} represent the partial pressures of O_2 and N_2 respectively.

Expressions similar to Equation 2 were generated for the three-phase equilibria, $Si+SiO_2$+vapor, $Si+Si_2N_2O$+vapor, $Si+Si_3N_4$+vapor and $SiO_2+Si_2N_2O$+vapor. Using these expressions, stability diagrams illustrating the relationship between P_{O_2}, P_{N_2} and the stability various condensed phases in the Si-N-O system can be calculated. Stability diagrams at 1473K (1200°C) and 1673K (1400°C) are shown in Fig. 4 by the solid and dashed lines respectively. The intersections between the lines representing 3-phase equilibria define the invariant 4-phase equilibria.

(c) Thermal Stability of Si_3N_4 and Si_2N_2O

The thermal stability of Si_3N_4 and Si_2N_2O can also be assessed by calculating the equilibrium vapor pressures of species released by these compounds during exposure to elevated temperatures in a vacuum or inert gas atmosphere. Sublimation of Si_3N_4 can be represented by:

$$Si_3N_{4(s)} = 3Si_{(v)} + 2N_{2(v)} \quad (4)$$

with a corresponding free energy change, $\Delta G_4°$, of

$$\Delta G_4° = \log [P_{Si}{}^3 P_{N_2}{}^2] \quad (5)$$

where P_{N_2} and P_{Si} represent the partial pressures of N_2 and Si vapor. Due to the stoichiometric constraints imposed by Equation (4), P_{N_2} can also be expressed as $P_{N_2}=(3/2)P_{Si}$. The equilibrium vapor pressure generated by pure Si_3N_4 as a function of temperature can then be calculated on substitution of an appropriate expression for $\Delta G_4°$. Using this approach, calculated values for P_{Si} and P_{N_2} are 1.1×10^{-4} and 1.6×10^{-4} torr at 1473K and 6.2×10^{-3} and 9.4×10^{-3} torr at 1673K, respectively.

Although thermodynamic prediction of the sublimation behavior of Si_3N_4 is relatively simple since it involves a binary system, sublimation of pure Si_2N_2O is more difficult to evaluate due to the introduction of oxygen and the likelihood of $SiO_{(v)}$ formation. If the various chemical reactions involved with sublimation of Si_2N_2O are written in matrix form, reduction to an echelon matrix can be used to show that only two reactions are linearly independent [60]. These reactions can be written as:

$$Si_2N_2O_{(s)} = 2Si_{(v)} + N_{2(v)} + 1/2O_{2(v)} \quad (6)$$

and

$$Si_{(v)} + 1/2O_{2(v)} = SiO_{(v)} \quad (7).$$

The Gibbs phase rule can then be applied to show that two degrees of freedom are available to this system even under isothermal conditions. Therefore, the equilibrium partial pressure of Si_2N_2O cannot be predicted unless an additional constraint is imposed on the system.

As will be discussed in a later section, HPZ fibers are comprised of Si_3N_4(+C) with a thin oxygen rich surface layer. If one treats the fibers as consisting of a two-phase mixture of Si_3N4 and Si_2N_2O, the presence of two condensed phases can be used as an additional thermodynamic constraint limiting the system to only one degree of freedom. In this case, the predicted sublimation behavior of HPZ fibers reduces to the lines shown in Fig. 4 representing three-phase equilibrium between Si_3N_4, Si_2N_2O and vapor.

(d) Matrix/Fiber Interactions

Thermodynamic calculations were also performed to assess likely chemical interactions between uncoated HPZ (Si_3N_4) fibers and a barium-magnesium aluminosilicate (BMAS) matrix. In this case, since no thermodynamic data exists for BMAS, this phase was modeled using a thermodynamic description of magnesium aluminosilicate (MAS). After consideration of several possible reactions, involving formation of various mixed oxides and nitrides, it is predicted that contacting BMAS and Si_3N_4 will likely result in formation of Si_2N_2O with concomitant SiO_2 depletion of the matrix. Such a reaction can be represented by:

$$Mg_2Al_4Si_5O_{18(s)} + 5Si_3N_{4(s)} = 2MgAl_2O_{4(s)} + 10Si_2N_2O_{(s)} \quad (8)$$

with a corresponding Gibbs free energy change, $\Delta G_8{}^\circ$, of -500 and -566 kJ at 1473K and 1673K, respectively. Thermodynamics would predict, therefore, that a two-phase mixture of Si_3N_4 and MAS is unstable and will transform to a mixture of Si_2N_2O and a low-silica mixed oxide such as $MgAl_2O_4$.

2. Discussion

(a) Thermal Stability of Fibers

The calculated phase diagram shown in Fig. 3 provides a first order assessment of equilibria expected in the Si-N-O-C quaternary system. The two-phase and three-phase equilibria, represented by tie lines and triangles respectively in Fig. 3, remain very stable with increasing temperature with one notable exception. Although a tie line exists between Si_3N_4 and C at both 1473K and 1673K, the free energy difference between Si_3N_4+C and the competing SiC+N_2 equilibrium is relatively small (72 kJ at 1473K and only 10 kJ at 1673K). In fact, at temperatures above 1706K (1433°C) two-phase equilibrium between Si_3N_4 and C is replaced by SiC+N_2 equilibrium, i.e.:

$$Si_3N_{4(s)} + 3C_{(s)} = 3SiC_{(s)} + N_{2(v)} \qquad (9).$$

This change in equilibrium, which results in N_2 evolution, is indicated by the dashed line in Fig. 3. Although this analysis suggests that the stability of Si_3N_4+C is marginal at the temperatures used for hot pressing glass-ceramic matrix composites, the thermal stability will be enhanced by a low C activity and a high partial pressure of N_2.

As discussed previously, equilibrium specie vapor pressures generated by pure Si_3N_4 at 1673K (1400°C) have been estimated as $P_{Si}=6.2\times10^{-3}$ and $P_{N_2}=9.4\times10^{-3}$ torr for a total pressure of 1.6×10^{-2} torr. These predictions are consistent with the extensive outgassing of N_2 and $Si_{(v)}$ observed during exposure of Si_3N_4 to elevated temperatures[55,61]. Based upon the above thermodynamic assessment, formation of $SiO_{(v)}$ is aiso expected to occur during annealing of HPZ fibers, and this phenomena has been observed experimentally[55].

(b) Fiber/Matrix Interaction

The free energy change associated with reaction (8) indicates that Si_3N_4 and MAS (and likely BMAS) cannot coexist in equilibrium. Therefore, thermodynamics would predict that Si_2N_2O and a low-silica mixed oxide (e.g. $MgAl_2O_4$ [spinel] or $Mg_4Al_{10}Si_2O_{23}$ [sapphirine]) will then form at the Si_3N_4/MAS interface. Such a reaction will likely result in formation of separate $MgAl_2O_4$ and Si_2N_2O layers as the MAS becomes depleted of SiO_2 and the Si_3N_4 transforms to Si_2N_2O. Continued reaction will likely require diffusion of SiO_2 through these interfacial reaction layers.

This behavior can be illustrated by rewriting reaction (8) as two separate reactions. The first reaction,

$$Mg_2Al_4Si_5O_{18(s)} = 2MgAl_2O_{4(s)} + 5SiO_{2(s)} \quad (10)$$

results in liberation of SiO_2 and would occur initially at the MAS/Si_3N_4 interface and later at the MAS/$MgAl_2O_4$ interface. The second reaction,

$$5SiO_{2(s)} + 5Si_3N_{4(s)} = 10Si_2N_2O_{(s)} \quad (11)$$

results in formation of Si_2N_2O at the Si_2N_2O/Si_3N_4 interface. The SiO_2 liberated by reaction (10) must then diffuse through the $MgAl_2O_4$ and Si_2N_2O reaction layers to result in further transformation.

The reaction sequence discussed above would be driven by differences in SiO_2 activity in the HPZ fibers and glass-ceramic matrix. The MAS (as well as BMAS) matrix is expected to possess a relatively high activity of $SiO_2$53. On the other hand, HPZ fibers will likely exhibit a relatively low SiO_2 activity. In fact, since HPZ fibers actually exhibit an oxygen rich surface film that can be approximated as Si_2N_2O, an estimate of the SiO_2 activity in the HPZ fiber can be evaluated based upon consideration of the SiO_2 activity required for two-phase equilibrium between Si_3N_4 and Si_2N_2O. This equilibrium can be written as:

$$Si_3N_{4(s)} + SiO_{2(ss)} = Si_2N_2O_{(s)} \quad (12)$$

where the subscript ss denotes SiO_2 in solid solution. The free energy change associated with this reaction can be written as:

$$\Delta G_{11}^{\circ} = -RT \ln (a_{Si_2N_2O}/a_{Si_3N_4}\, a_{SiO_2}) \quad (13)$$

where $a_{Si_2N_2O}$ and $a_{Si_3N_4}$ are unity. Substitution of the appropriate expression for this free energy change yields a calculated value of the a_{SiO_2} of 5.8×10^{-4} and 5.1×10^{-4} at T=1473K and 1673K, respectively.

Coatings (such as BN/SiC) can be applied to HPZ fibers to suppress chemical reaction with the matrix. Differences in specie activity between the matrix and fiber provides driving force for diffusion of matrix species (such as SiO_2) through these coatings. In the case of SiO2 diffusion, Fick's first law of can be written as:

$$J_{SiO_2} = - D_{SiO_2} (d\mu_{SiO_2}/dX) \quad (14)$$

where J_{SiO_2} is the SiO_2 flux, $DSiO_2$ is the chemical diffusion coefficient, and $d\mu_{SiO_2}/dX$ is the gradient in the of SiO_2 chemical potential. Since the chemical potential is defined as:

$$\mu SiO_2 = \mu_{SiO_2}^{\circ} + RT \ln (a_{SiO_2}) \quad (15)$$

where $\mu_{SiO_2}^{\circ}$ is the chemical potential of the chosen standard state[62], large differences in matrix and fiber SiO_2 activity will increase the flux of SiO_2 through the coating and could promote more rapid chemical reaction. Use of fibers and matrices possessing a similar SiO_2 activity would likely decrease chemical interaction during processing/service.

B. Uncoated and Coated HPZ Fiber Characterization

During the course of this program, a number of different lots of HPZ fibers were received from Dow Corning. In addition, a number of different BN and SiC/BN CVD coating deposition runs were performed at 3M on many of the different lots of HPZ fibers. The following sections will examine the unique microstructure found for the HPZ fibers, as well as the differences noted between the various lots of fiber and between the different BN and SiC/BN coating deposition runs performed at 3M.

1. As-Received HPZ Fiber Characterization

A scanning Auger depth profile performed on a relatively recent lot (#100173) of HPZ fiber is shown in Fig. 5. As seen previously for HPZ fibers[41,43], the near-surface region is very oxygen rich to a depth into the fiber of ~200nm (2000Å). While the composition of the bulk of the fiber is ~43 at% Si, 34% N, 19% C, and 4% O, the surface region is ~40% Si, 34% O, 14% C, and 12% N. The fiber surface is quite smooth, with an average UTS of 339 ksi (2.34 GPa).

TEM thin foil analysis of a longitudinal section of lot #100173 HPZ fiber was done by mounting the fibers in an epoxy resin, followed by ion beam thinning. As shown in Fig. 6, the oxygen rich surface layer on these fibers appears to be microporous, with a very abrupt transition to the dense bulk fiber. From the EDX spectra (Fig. 7) taken from a

similar thinned HPZ fiber lot (#92372-16), the porous surface region is obviously oxygen rich, while the denser bulk region is high in nitrogen and very low in oxygen. At higher magnifications (Fig. 8), the microporosity and abrupt transition region can be seen more clearly.

While no TEM analysis was performed on early HPZ fibers during the previous DARPA/AFML program[43], scanning Auger analysis done then indicated that the earlier HPZ fibers had a much thinner oxygen rich surface region. This was verified on the current program by TEM thin foil analysis of a vintage 1986 HPZ fiber (lot #34916-45) and the most recent lot (#062984-07) of HPZ fiber delivered to UTRC by Dow Corning in the fall of 1992. From Fig. 9, it can be seen that the earlier HPZ fiber exhibits a much thinner (~1130Å) and finer microporous oxygen rich surface region than the latest HPZ fiber lot. The thickness and structure of this surface oxygen rich layer may play an important role in the reactivity of the HPZ fibers, not only with glass-ceramic matrices but just for the fibers themselves as a function of heat-treatment. The effect of a 1430°C, 10 minute heat-treatment in nitrogen inside a graphite die in the hot-press chamber on the tensile strength of three different lots of HPZ fiber is shown in Table I. It can be seen that the UTS of the heat-treated fibers degraded significantly, except for the older lot #7370-78-1C, which was relatively low strength to start with and had a significantly thinner oxygen rich surface layer (similar to lot #34916-45 shown in Fig. 7).

The cause of this degradation in tensile strength can be seen in Fig. 10, which shows the fracture surface of a lot #03028013 HPZ fiber after the 1430°C, nitrogen heat-treatment, as well as a TEM thin section of the surface region of this fiber. It can be seen that the fiber has a definite surface layer on it that exhibits a significant number of pits. From the TEM analysis, it is evident that the oxygen rich surface layer has crystallized to a rather uneven layer of crystalline silicon oxynitride (Si_2N_2O).

Another batch of HPZ fibers, including the most recent lot #062984-07, were subjected to the same heat-treatment and sent to Dow Corning for evaluation. Tensile tests done at Dow Corning confirmed the severe strength degradation that occurred as a result of this heat-treatment, although Dow Corning found that the early lot #7370-78-1C also was degraded severely in strength. Similar heat-treatments (1400°C, 2 hrs, Ar) at Dow Corning on a variety of HPZ fiber lots also showed distinct, pin-holed surface layers had formed on the fibers as a result of heat-treatment, with resultant loss in fiber UTS. However, the surface region on HPZ fibers previously heat-treated at Dow Corning at 1400°C, 2 hrs, Ar, was found to consist of a relatively pure silica layer, not crystalline silicon oxynitride[63].

2. Coated HPZ Fiber Characterization

As discussed in the previous Annual Report on this program[41], early deposition runs at 3M of BN and SiC/BN coatings on HPZ fibers resulted in rather "sooty", or rough, coating morphologies. The compositions of these coatings, especially the BN, varied considerably through the coating thickness, with areas of very high carbon content being found from scanning Auger analyses. Nevertheless, these coated HPZ fibers did result in BMAS matrix composites with reasonable strengths to temperatures approaching 1200°C.

During the past eighteen months of this program, over ten different BN and SiC/BN coating deposition runs on various HPZ fiber lots were performed at 3M. These coated HPZ fibers were then subjected to a variety of analyses at UTRC, including tensile testing, SEM analysis, scanning Auger depth profiling, and TEM replica and thin foil characterization. Most of these coated HPZ fibers were then utilized for the fabrication of BMAS matrix composites. The following discussion of the characteristics of a selected number of these BN and SiC/BN coated HPZ fiber lots will illustrate the similarities, and differences, noted between different coating runs.

(a) Coated Lot #9545-20 HPZ Fibers

Figure 11 shows typical morphologies of SiC over BN coated HPZ fibers (3M run #92172:57) that were received at UTRC in late 1991. This coating run, and a companion run (#92172:56) utilizing only a BN coating, were deposited on lot #9545-20 HPZ fibers. Most of the coated fibers in run #92172:57 appeared similar to that shown in the top SEM photo in Fig. 11, in that most of the coatings were quite smooth and most of the fibers were oval in cross-section. However, some of the SiC/BN coatings were still quite rough, or "sooty", as shown for the other fiber in Fig. 11, and some of the HPZ fibers were not oval in cross-section, but round and hollow. The round, hollow fibers in recent lots of HPZ fibers constitute ~5% of the fibers within a 500 filament tow. 3M utilized a modified "low soot" deposition process to coat these fibers, which did result in much smoother coatings than previously[41], but did not insure that all fibers within the tow had smooth coatings. It has been found that some of the fibers (~5%) around the periphery of the tow were still coated with a rather rough, or "sooty", coating.

A scanning Auger depth profile of a SiC/BN coated HPZ fiber from run #92172:57 is shown in Fig. 12. The particular fiber analyzed had a relatively smooth coating, which consisted of ~2000Å of slightly carbon rich SiC over ~5000Å of relatively stoichiometric BN with the usual 10-15% carbon and 3-5% oxygen. The oxygen rich surface region of the HPZ fiber is quite evident under the BN layer in Fig. 12.

The measured average tensile strength of this coated fiber run was only 137 ksi (945 MPa), which is significantly less than the measured strength of the uncoated HPZ fiber from lot #9545-20-12 of 289 ksi (1980 MPa). While the SiC/BN coating thickness of 7000-8000Å can be expected to carry essentially no load and is measured as part of the fiber diameter to determine UTS, this still would not account for a drop in tensile strength of this magnitude. As will be discussed later, a BN coating on a similar lot of HPZ fiber resulted in essentially no decrease in UTS, so the SiC overcoating must either be weakening the fiber or increasing its notch sensitivity, so that when the SiC coating cracks, the crack propagates directly through the BN into the fiber.

TEM thin foil analysis was performed on the as-received SiC/BN coated HPZ fiber lot #92172:57 by mounting the coated fibers in an epoxy resin, grinding into a thin disc, and then ion beam thinning into a foil. The surface region of a coated fiber can be seen in Fig. 13. The individual coating layers are quite evident, with no visible interaction between the BN layer and the porous oxide surface of the HPZ fiber. The Mo seen in the EDX spectra is an artifact from the ion beam thinning process, in which Mo holders are utilized to hold the sample in place.

As mentioned previously, a coating run (#92172:56) was done by 3M that consisted of just BN on HPZ fibers. The only analysis performed on this coated fiber sample was a scanning Auger depth profile, as well as tensile testing. As shown in Fig. 14, the ~4000Å thick BN coating was somewhat boron rich for much of its thickness, with somewhat higher oxygen content than the BN in run #92172:57, and a slightly carbon rich surface. The measured average tensile strength was quite high at 286 ksi (1980 MPa), which is approximately that measured for the HPZ fiber lot (#9545-20-5A) utilized for this coating run. It appears that, unlike the SiC/BN coated HPZ fibers, the BN coated fibers retain their strength as a result of the coating process.

(b) Coated Lot #100173-1 HPZ Fibers

In early 1992, a lot of HPZ fiber was received from Dow Corning that was considerably stronger [UTS = 340 ksi (2.34 GPa)] than previous lots of HPZ. A SAM depth profile and TEM thin foil of this fiber lot was previously shown in Figs. 5 and 6, respectively. This fiber was sent to 3M for coating with a dual layer of SiC over BN. As shown in Fig. 15, the morphology of this lot of coated fiber (#92172:74) was quite smooth, with very few "sooty" coated fibers. The SAM depth profile of this coated fiber lot, as shown in Fig. 16, is quite similar to that for the previous lot #92172:57 fibers (Fig. 12), except that the carbon content of the BN is somewhat less. TEM thin foil analysis of lot #92172:74 SiC/BN coated HPZ is shown shown in Fig. 17. As can be seen from Fig. 17, the particular coated fiber analyzed had coating thicknesses of ~2000Å for both the

SiC and the BN. The nominal desired thickness for the BN layer was 4000Å, similar to that for lot #92172:57 as was shown in Fig. 13.

In order to determine the variation in SiC/BN coating thickness for lot #92172:74, several coated fiber tows were mounted in resin, polished transversely, and subjected to TEM replica analysis. It was found that the SiC/BN coating thicknesses varied widely from the center to edge of the 500 filament tows, and from tow to tow. An example of this is shown in Fig. 18, where the SiC/BN coating thicknesses on one fiber from the center of the tow were ~1300Å (130nm) for the SiC and ~1550Å (155nm) for the BN, while the thicknesses for the coatings on a fiber from near the outside of the fiber tow were ~1800Å (180nm) for the SiC, and 6700Å (670nm) for the BN. From this information, it can be seen that the SiC thickness does not vary widely, but the BN thickness does. As will be shown in a later section of this report dealing with BMAS matrix composites, the thin BN layers on many of the fibers from this coating run resulted in severe reactivity between the BMAS matrix and the HPZ fibers.

One of the reasons that these fiber coatings were so non-uniform was that 3M experienced a considerable amount of difficulty in running the lot #100173-1 HPZ fiber through their continuous coating CVD reactors. Even though the individual filament tensile strengths of this fiber lot were quite high, the overall handleability of the fiber tows was very poor. According to 3M, the fiber tows would often break when they were being unwound from the spools, and would also tend to break upon removal of the PVA sizing. It was determined that these problems were a combination of the sizing continuing to cure after the sized tows were wound onto the spools, and damage to the tows at the ends of the spools due to poor packaging procedures at Dow Corning. All of the breakage experienced from these causes during fiber coating resulted in interruptions during the coating process that led to the non-uniform coating of the first coating layer, ie, the BN.

(c) Coated Lot #062984-07 HPZ Fibers

In mid-1992, Dow Corning produced a lot of HPZ fiber (#062984-07) that incorporated improvements in both sizing application and packaging. A small amount (400m) of this lot of HPZ fiber was sent to 3M for coating with BN and their evaluation as to its handleability compared to previous lots of HPZ fiber. The nominal coating thickness was requested to be ~5000Å.

The SAM depth profile and TEM replica analyses of this run of BN coated HPZ (#97037:23) are shown in Figs. 19 and 20, respectively. From Fig. 19, it can be seen that the coating thickness of the fiber analyzed is ~5000Å, with the B/N ratio being quite close to 1/1. The carbon and oxygen contents of the BN vary somewhat through the coating thickness, but average ~15% C and 8% O, which are within acceptable levels.

The average measured tensile strength for 15 of the coated fibers was 229 ksi (1578 MPa), which is less than that measured on the lot #062984-07 HPZ fiber of 330 ksi (2.3 GPa), but with the thick BN layer being measured to determine fiber cross-section, this amount of measured strength reduction is acceptable.

The two examples of BN coated HPZ fibers from this coating run that are shown in Fig. 20 represent the thinnest (4600Å) and thickest (6600Å) BN coatings found from the TEM replica analysis. This represents a marked improvement in coating thickness variation compared to previous coating runs, and is due to the much improved handleability of this lot of HPZ fiber, as was found by 3M.

The remaining amount of lot 062984-07 HPZ fiber (2000m), was sent to 3M for coating; half with BN and half with SiC/BN. The SAM depth profiles for these coated fiber runs (#97037:69-1 & -2) are shown in Figs. 21 and 22. From these figures, it can be seen that, while some of the coatings appear to be slightly "sooty", the coating thicknesses are ~2000Å for the SiC and ~6000Å for the BN. TEM replica analysis of the as-received coated fibers verified that, like run #97037:23, the coating thicknesses were quite uniform throughout the coated HPZ tows, with the outside of the 500 filament tows tending to exhibit more of the slightly "sooty" coatings than the inside of the tows. As usual, the measured tensile strengths for the SiC/BN coated HPZ fibers were significantly less than the BN coated fibers. These coated fibers, along with the smaller lot #97037:23 BN coated fibers, were utilized to fabricate a number of BMAS matrix composites, the results of which will be discussed in a following section of this report.

C. BMAS Glass-Ceramic Matrix/Coated Fiber Composite Fabrication

During the course of this program, over twenty 0/90° ply layup BMAS glass-ceramic matrix composites of dimensions 1.5" x 3.0" (3.8 x 7.6 cm) or 4"x4" (10 x 10 cm) were fabricated with 3M BN and SiC/BN coated HPZ fibers. The smaller composites were utilized for flexural screening studies, while the larger ones were used to obtain additional mechanical and thermal property data. Most of the composite panels were hot-pressed at maximum temperatures of 1400°-1450°C, 6.9 MPa pressure, for times of 5 to 20 min. One was pressed at a lower temperature (1050°C) in order to study the effect of temperature on the reactivity of the BMAS matrix with the coated HPZ fibers.

After hot-pressing, the composite panels were then cut into either flexural test samples of dimensions ~0.2 x 0.1 x 4.0" (0.51 x 0.25 x 10 cm), or tensile samples of dimensions ~0.5 x 0.1 x 4.0" (1.25 x 0.25 x 10 cm) with a dogbone gage section of 0.2 " (0.51 cm) in width and 1.0" (2.54 cm) in length. Those composites to be tested in the "cerамed" or matrix crystallized condition were heat-treated in argon to 1200°C for 24 hrs in order to crystallize the BMAS matrix to the barium osumilite phase.

D. Composite Mechanical and Microstructural Characterization

This section will cover the results obtained on this program from Tasks IV - Composite Mechanical and Thermal Testing, and V - Microstructural and Microchemical Analysis of Composites, since the mechanical properties of these composites are so intimately related to their microstructural characteristics. The discussion will commence with the results obtained from uncoated HPZ fiber composites, and progress to results obtained on the various BN and SiC/BN coated HPZ fiber composites.

1. BMAS Matrix/HPZ Fiber Composites

As was shown in Fig. 1, it was found that the fracture surface of an early HPZ fiber composite utilizing an LAS (lithium aluminosilicate) glass-ceramic matrix was extremely brittle, with little evidence of the fibers contributing to either the composite strength or toughness. A more recent BMAS matrix/uncoated HPZ fiber composite (#349-91) fracture surface is shown in Fig. 23. This composite exhibited a RT flexural strength of 23 ksi (159 MPa), which is comparable to that for an unreinforced BMAS glass-ceramic. As in the composite of Fig. 1, the fracture characteristics are that of a monolithic glass-ceramic, with obviously strong bonding between the fibers and matrix. The oval shape of the more recent HPZ fibers (lot # 9545-20-12), along with the few round but hollow fibers, can be seen in Fig. 23.

A TEM replica characterization of a transversely polished cross-section of composite #349-91 is shown in Fig. 24. It can be seen that a tremendous amount of reaction has occurred between the HPZ fibers and the BMAS matrix during composite fabrication. From X-ray and electron diffraction analysis, the reaction product around the periphery of the HPZ fibers was found to be crystalline Si_2N_2O, the same reaction product found previously[20] for HPZ fibers in LAS matrices. As can be seen in Fig. 24, the remnants of the oxygen rich surface layer on the HPZ fibers are visible as thin "stringers" that are often detached from the rest of the fiber.

In an attempt to determine if the thicker oxygen rich porous surface layer found on recent HPZ fibers, compared to earlier vintage fibers (Fig. 9). is influencing the fiber/matrix reactivity in these composites, a BMAS matrix composite was fabricated with a mat of "old" lot #34916-45 HPZ fibers that were found previously (Fig. 9) to exhibit a much thinner oxygen rich surface layer. The TEM replica analysis of this composite (#245-92) is shown in Fig. 25. Comparing this figure to Fig. 24, it can be seen that while the reactivity of the older HPZ fibers appears to be much more irregular from fiber to fiber and also around the same fiber, the amount of overall reaction to silicon oxynitride is still significant.

In order to determine if the presence of the oxygen rich porous surface layer on the HPZ fibers, whether it is thick or thin, influences the reactivity of a Si-N based fiber with BMAS glass-ceramic matrices, a small pseudo-composite was fabricated utilizing a small amount of TONEN silicon nitride fiber. These fibers are amorphous with a composition very close to that of Si_3N_4 with very low oxygen content (<3 at%), and no high oxygen surface region. The TEM replica micrograph shown in Fig. 26 of the small BMAS matrix composite (#269-92) fabricated with these fibers indicates that while some reactivity appears to have occurred with the BMAS matrix during composite processing, the large amount of silicon oxynitride formation observed with the HPZ fibers does not occur in this system. Rather, it appears that the surface of the TONEN fibers acts as a nucleating site for mullite crystal formation from the BMAS matrix during cooling from the composite consolidation temperature. Some silicon oxynitride may have formed at the fiber/matrix interface as well, but not as much as with HPZ fibers. No other analysis of this composite was attempted.

From the results obtained on uncoated HPZ fibers in BMAS matrix composites, it is apparent that these fibers react very quickly with the BMAS matrix at the composite processing temperature of ~1430°C to form a rather thick (1-2μm) crystalline silicon oxynitride surface layer. This surface layer degrades the strength of the fibers and promotes very strong bonding between matrix and fiber, both of which contribute to the rather weak and very brittle composite properties. The presence of a porous, oxygen rich surface layer on the HPZ fibers appears to enhance their reactivity with the BMAS matrix during composite processing.

2. BMAS Matrix/BN and SiC/BN Coated HPZ Fiber Composites

As discussed in the previous annual report on this program[41], two small 0/90° ply layup BMAS matrix composites were fabricated utilizing very "sooty" BN and SiC/BN coated HPZ fibers. These composites (#5-91 and 12-91) gave quite good flexural strengths from RT to 1200°C considering the starting coated HPZ fibers only had average UTS values of 206 ksi (1420 MPa) and 150 ksi (1040 MPa), respectively. The mode of fracture of these composites, while not particularly fibrous, was certainly "tougher" than the totally brittle behavior of uncoated HPZ fiber/BMAS glass-ceramic matrix composites fabricated at UTRC, as was shown in Fig. 23.

Figure 27 shows the microstructure of composite #5-91. From the light microscopy and TEM replica micrographs of the composite cross-section, it can be seen that a significant amount of BN "sooting" can be seen on the coated fiber surfaces and in the composite matrix. From Fig. 28, which shows the SAM depth profile of the interfacial region of composite #5-91, it can be seen that the interfacial debonding occurred within the BN layer where no diffused Si was present. The high amount of carbon that had

been noted in the as-received BN coating can also be seen in the composite interface, but it was not evident that the high carbon levels in the BN influenced the composite debonding or fracture characteristics. Also of note is that boron diffusion from the BN layer into the BMAS matrix has occurred for composite #5-91. This boron diffusion into the BMAS matrix was not found for the SiC/BN coated HPZ fiber composite #12-91. The higher flexural strength at 1200°C found for composite #12-91 was likely due to the lack of boron in the BMAS matrix allowing complete crystallization to barium osumilite.

The flexural strength results as a function of temperature for the above two composites, as well as the uncoated HPZ fiber composite #349-91 are shown in Table II, along with more recent data obtained on composites fabricated with lots #9545-20 and #100173 HPZ fibers with "low soot" BN and SiC/BN coatings. As can be seen from this data, the composites fabricated with the "low soot" coated HPZ fibers ranged from relatively strong to very weak. A discussion of these results and their correlation to composite microstructure follows.

(a) Coated Lot #9545-20 HPZ Fiber Composites

The flexural strength of the BMAS matrix composite #415-91 fabricated with the smoother "low soot" BN coated HPZ fibers (3M run #92172:56) was relatively high from RT to 1200°C [38-44 ksi (262-303 MPa)], with a fracture mode that was indicative of a high toughness composite, as shown in Fig. 29. Comparing the RT calculated stress/strain behavior of this composite to that of the uncoated HPZ fiber composite #349-91, as shown in Fig. 30, illustrates the difference in both load carrying ability and mode of failure. The SiC/BN coated HPZ composite #452-91, while exhibiting reasonable strength at 1200°C, was not particularly strong or "tough" at lower temperatures. This could be related, as was discussed previously, to the low tensile strength measured for this SiC/BN coated fiber run (#92172:57). At low temperatures, the relatively rough, high modulus SiC coating may be causing the fibers to be notch sensitive. When the SiC coating cracks, the crack propagates directly through the fibers. At 1200°C, the softening of the BMAS matrix may result in crack blunting.

(b) SiC/BN Coated Lot #100173 HPZ Fiber Composites

As shown in Table II and discussed previously, the lot #100173 HPZ fibers were the strongest HPZ fibers used on this program, and the two SiC/BN coating runs on these fibers (#92172:74 & 78) produced the strongest SiC/BN coated HPZ fibers used for composite fabrication. However, the BMAS matrix composites fabricated from these coated fibers, utilizing the normal hot-pressing procedure, were the weakest coated HPZ fiber composites made on this program. Five BMAS matrix composites were fabricated

under the normal conditions, and all of them exhibited RT flexural strengths in the range of 19-25 ksi (131-172 MPa). Two of these composites (#53-92 and #88-92) are listed in Table II, both of which were utilized for extensive analytical characterization in order to discover the cause of the poor composite behavior.

A typical fracture surface of composite #53-92 is shown in Fig. 31. While there is some evidence of fiber/matrix debonding within the BN layer, many of the coated fibers fractured in the plane of the matrix crack with no evidence of interfacial debonding. A SAM depth profile of a fiber surface and matrix trough from a longitudinally fractured sample of this composite, as shown in Fig. 32, indicated that the fracture occurred within the BN layer, as expected. A significantly high carbon content within the BN layer near the fracture surface was found, which was not present in the as-coated BN layer (Fig. 16). The reason for this increase in carbon content could not be determined.

Optical and TEM replica microscopy was performed on composite #88-92, as shown in Figs. 33 and 34. This composite exhibited very similar strength and fracture behavior to composite #53-92, although it had a higher volume fraction fiber content. From Figs. 33 and 34, it can be seen that a significant number of the SiC/BN coated HPZ fibers in this composite have reacted in localized regions with the BMAS matrix during composite processing. The cause of this reaction to silicon oxynitride appears to relate to the debonding of the SiC layer from the BN layer during composite processing. Matrix element diffusion through the BN layer, as will be shown later, then causes the reaction with the HPZ fibers.

The reason for the SiC layer debonding from the BN layer during processing of these composites is not entirely clear. One reason could be that in composites with high volume fraction fibers, the coated fibers can often come in contact with one another during composite processing. This contact could then cause damage to the brittle SiC coating, allowing it to crack and then separate from the BN. This mode of coating damage has been seen in TEM replica analysis of these composites, but does not explain the coating damage and separation seen when fibers are separated by regions of BMAS matrix, as can be seen in Figs. 33 and 34.

Another possible explanation is that it has been noticed from both TEM replica analyses and SEM of composite fracture surfaces, that often at the smaller radius regions of the oval shaped HPZ fibers, the SiC (and BN) coatings appear to separate from the HPZ fibers, as if the fibers have shrunk, or contracted, during composite processing. This phenomenon can be seen in the TEM replicas of Figs. 33 and 34, and can also be seen in the SEM of the composite #53-92 fracture surface in Fig. 35. In many cases, as can be seen in Figs. 33 and 34, this apparent shrinkage does not cause the SiC/BN coating to fracture, but simply to detach and pull away form the fiber surface. However, it would seem that a detached coating would be more likely to fracture during

composite processing, leading to the observed reactions. It has been noticed that many of the reacted regions in these composites occur at, or appear to originate from, the small radius side of the HPZ fibers. Since the maximum processing temperature of the BMAS matrix composites (~1430°C) may be higher than the pyrolysis temperature of the HPZ fibers[54], additional shrinkage of the fibers during composite processing may indeed take place. The same comments also hold for Nicalon fibers, but no shrinkage has been noted for BMAS/SiC/BN/Nicalon fiber composites. This may be related to their round shape, compared to the oval shape of the HPZ fibers.

To investigate whether or not shrinkage of HPZ fibers above their pyrolyzation temperature may be leading to the reactivity problems noted for SiC/BN coated lot #100173 HPZ fibers, a BMAS matrix composite was fabricated at a maximum temperature of 1050°C, which is above the glass transition temperature but below the barium osumilite crystallization temperature. At this temperature, the BMAS glass particles do not flow around the fibers, as they do at the usual hot-pressing temperatures, but instead sinter together into an essentially fully dense matrix. This fabrication method is not normally used for glass or glass-ceramic matrix composites at UTRC because it is difficult to form the composite into shapes other than simple flat panels, and there is the potential for damage to the fibers from the glass particles.

From the composite results listed in Table I, it can be seen that the flexural strength of the 1050°C hot-pressed composite (#213-92) was not particularly high [~30 ksi (207 MPa)], but was constant as a function of temperature to 1200°C. In addition, the elastic modulus remained relatively high at 1100° and 1200°C, compared to previous HPZ composite results. The fracture surface of this composite is shown in Fig. 36. It can be seen that fiber/matrix debonding did occur for most of the fibers, and appeared to take place within the BN layer. While not evident from Fig. 36, no visible indication of HPZ fiber shrinkage could be seen in the SEM analysis of the composite fracture surface.

TEM replica analysis and light microscopy of a polished section of composite #213-92 in the as-pressed condition is shown in Fig. 37. From this analysis, no evidence of HPZ fiber shrinkage could be seen, nor was there any indication of debonded or fractured fiber coatings or reactivity of the fiber to form silicon oxynitride. The unusual crystals that can be seen within the predominantly glassy matrix were identified from X-ray diffraction analysis as being primarily the hexacelsian form of BAS ($BaAl_2Si_2O_8$), with minor amounts of the monoclinic celsian BAS phase, as shown in Fig. 38. Upon ceraming at 1200°C, the matrix crystallized to essentially pure barium osumilite, with only a minor amount of hexacelsian remaining.

The above experiment appeared to substantiate the possibility of shrinkage of the HPZ fibers during composite processing leading to damage of the SiC/BN coatings, which then can result in severe HPZ fiber reaction with the BMAS matrix. The relatively low strength of composite #213-92 is surprising, given the fact that no fiber/coating/matrix reactivity was seen. Although it could not be determined from the analyses conducted on this composite, fiber damage during composite processing could be a factor. Additional low temperature fabrication experiments should be an area for future work in this composite system.

(c) TEM Thin Foil Analysis of Reactions in BMAS/BN and SiC/BN Coated HPZ Fiber Composites

TEM thin foil analysis was conducted on BMAS matrix composites with BN and/or SiC/BN coated HPZ fibers that showed evidence from TEM replica analysis of either reacted or non-reacted HPZ fibers, in order to determine the mechanisms of reaction. As shown in Figs. 39 and 40 for BMAS matrix/BN coated HPZ fiber composite #5-91, the normally turbostratic BN fiber coating crystallizes from the matrix towards the fiber during composite processing, due to matrix element (Al, Ba, Mg, Si, O) diffusion into the BN. This effect was found previously for BN coated Nicalon fiber composites, as well[41,53]. This recrystallized BN region has been found to be ~1500-2000Å thick for BMAS matrix composites processed at a maximum temperature of ~1430°C. From Fig. 40B, it can be seen that this recrystallized BN contains a significant amount of matrix elements, while the turbostratic, or fine grain BN (Fig. 40C), shows very little evidence for matrix elements, except for Si. The Si may represent a small amount of Si diffusion into the BN from the fiber, as was found from the SAM depth profile conducted on this composite (Fig. 28). Very small amounts of Si give very large Si signals in the EDX analysis. Some Al may also be diffusing into the fine grained BN. As was found from SEM and SAM analyses, fracture and fiber/matrix debonding in this type of composite occurs within the fine grained BN layer.

The porous oxygen rich HPZ fiber surface remained relatively unreacted, except for a slight change in its morphology next to the BN layer. From EDX analysis (Fig. 40D), a very small amount of Al may have diffused through the BN layer into the oxygen rich HPZ fiber surface region. As will be discussed shortly for composite #88-92, this change in the oxygen rich region appears to be a densification phenomenon, with the BMAS matrix element diffusion actually filling the porous structure. Definitive characterization of the change in this region would require high resolution TEM (HRTEM) analysis.

Composite #88-92, which utilized SiC/BN coated HPZ fiber (Run #92172:78), was very weak and exhibited quite brittle fracture behavior and a significant amount of

matrix/fiber interaction, as was shown in Figs. 33 and 34. TEM thin foil analysis was performed on this composite, as shown in Figs. 41 and 42. In these figures, two coated fibers are shown with BMAS matrix in between. The SiC/BN coatings on the top fiber have remained intact during composite processing, with the result that no reaction has occurred between matrix and fiber and the BN coating has retained its turbostratic structure. On the bottom fiber, however, it can be seen that the SiC layer has debonded from the BN layer at some point during composite processing, allowing BMAS matrix to penetrated between the SiC and BN layers. Matrix element diffusion has then occurred into the BN layer, and since the thickness of the BN was only on the order of 1500Å, the total thickness of BN has crystallized. From Fig. 41, it can be seen that matrix element diffusion (primarily Al, Mg, and Ba) has occurred into the oxygen rich porous HPZ fiber surface layer and apparently caused it to densify. A higher magnification view of this progressive matrix element diffusion and densification of the oxygen rich zone is shown in Fig. 43. Diffusion through this region into the HPZ fiber itself has also occurred, causing formation of crystalline Si_2N_2O (Fig. 42). This, in turn, weakens the fibers and bonds them tightly to the BMAS matrix, thus resulting in the weak and brittle fracture behavior observed for this composite.

An interesting comparison can be made between SiC/BN coated HPZ fiber composites and SiC/BN coated Nicalon fiber composites, where in both composites the SiC layer has detached from the BN layer during composite processing. Figure 44 shows TEM thin foil comparisons between the aforementioned BMAS matrix/SiC/BN coated HPZ fiber composite #88-92 and a similar composite with coated Nicalon fibers. The detachment of the SiC layer in both cases has resulted in the BN layer crystallizing through its thickness. In contrast to the HPZ fiber composite where severe reaction then occurred between the diffusing matrix elements and the HPZ fiber, no reaction occurs with the Nicalon fiber, except for the formation of an extremely thin (<100Å) carbon rich layer between the Nicalon fiber surface and the crystallized BN layer[53]. The strength of the Nicalon fiber composite remains high, and the fracture behavior consists of fiber/matrix debonding with resulting high toughness, as seen in Fig. 45.

It appears that, in order to fabricate coated HPZ fiber/BMAS matrix composites with high strength and fracture toughness, certain criteria must be satisfied. The primary criteria is that, due to the extreme reactivity of the HPZ fibers with glass-ceramic matrices during composite processing, the BN layer on the fibers must be thick and uniform enough so that if matrix element diffusion does occur into this layer, it is thick enough so that this diffusion and crystallization of the BN does not occur through its total thickness. Secondly, if SiC overlayers are necessary to prevent boron diffusion into the matrix and matrix diffusion into the BN, they must be remain bonded to the BN layer during composite processing. Other areas of concern, such as the possible shrinkage of the HPZ fibers during composite fabrication and the possible elimination of the very reactive

porous oxygen rich surface layer on the HPZ fibers, may or may not be able to be dealt with.

As was discussed in a previous section of this report, one of the major problems in CVD coating HPZ fibers with uniform coatings of SiC and, in particular, BN, was the poor handleability of the HPZ fibers during the coating process. This problem, it is believed, led to the non-uniform BN coatings on runs #92172:74 and 78, and thus the resulting poor composite properties obtained for these composites. Improvements in the sizing and packaging of lot #062984-07 HPZ fibers, as was shown previously, led to much improved BN coating uniformity for CVD runs #97037:23, 69-1, and 69-2. The following section will present and discuss the results obtained on BMAS matrix composites fabricated with these more uniform coated fibers.

(d) BN and SiC/BN Coated Lot #062984-07 HPZ Fiber Composites

As mentioned previously, a small amount (~400m) of this HPZ fiber lot was coated with ~5000Å of BN at 3M (#97037:23), followed by a larger amount (1000m each) of BN (#97037:69-1) and SiC/BN (#97037:69-2) coated fiber. It was found that the BN layers in all of these coating runs were much more uniform than previously, with thickness variations found from TEM and SAM analyses being between ~4000Å and ~7000Å. This does not guarantee, however, that some fibers may not be coated with such thick and uniform BN layers. However, as will be discussed, BMAS matrix composites fabricated with these coated fibers demonstrated much improved mechanical properties compared to previous composites fabricated under this program.

Eight BMAS matrix composites were fabricated with the improved uniformity BN and SiC/BN coated HPZ fibers. These composites were subjected to flexural testing at RT, 1100°, and 1200°C. A selected number of these composites were also subjected to tensile testing at 1100° and 1200°C, and stepped tensile stress-rupture testing at 1100°C.

The results of composite flexural testing are shown in Table III. One of the goals of this series of composites was to keep the volume fraction fibers in the range of 30-40%, in order to minimize fiber-to-fiber contact, and thus coating damage, during composite fabrication. This was accomplished except for composite #334-92.

From Table III, it can be seen that the RT flexural strengths measured for the five BN coated HPZ fiber composites are, in general, quite a bit higher than that measured for previous BN coated HPZ fiber composites. The elevated temperature properties of these composites were also relatively high, especially for the last three composites

(#392-92, 397-92, and 17-93) where a small change in the ceraming, or matrix crystallization, heat-treatment resulted in an improved composite microstructure.

The microstructure of composite #334-92 in the ceramed condition is shown from TEM replica analysis (Fig. 46) to consist primarily of unreacted fibers, as shown in the top micrograph, with a few regions in the composite having slightly reacted fibers, as shown in the lower micrograph. As was shown in Fig. 20, this lot of BN coated HPZ fibers (#97037:23) was coated quite uniformly with ~5000Å of BN. Since past TEM thin foil analyses have shown that the matrix element diffusion zone, and subsequent BN crystallization zone, is on the order of ~2000Å thick, the BN layer on this lot of fibers should have protected the fibers from reactivity with the matrix. In most cases, it did. However, a small number of fibers (<10%) did show some indications of reaction, so the BN uniformity must not have been quite as good as initially thought.

While the RT flexural strength of the two composites (#301 & 334-92) fabricated with the lot #97037:23 BN coated HPZ fibers were the highest ever measured for BMAS matrix composites (0/90°) with coated HPZ fibers, the elevated temperature properties were not as high as expected. It was determined by examining the fracture characteristics of these composites that shear failure within the BMAS matrix was the primary mode of failure. For composites fabricated with the subsequent 1000m length of BN coated HPZ fiber (#97037:69-1), an adjustment to the composite ceraming heat-treatment schedule was made that appeared to eliminate the tendency for composite shear failure at elevated temperatures.

TEM replica analysis of composite #392-92 in the ceramed condition is shown in Fig. 47. This composite, with a BN coating on the HPZ fibers, appeared to crystallize almost completely to barium osumilite with very little residual glassy phase. The amount of reaction with the HPZ fibers was very little (<5%), and was not very severe, as seen in Fig. 47. This may be an effect of both the more uniformly coated fibers and the lower volume fraction fibers in the composite resulting in less fiber-to-fiber interaction. The revised matrix crystallization heat-treatment resulted in much improved elevated temperature flexural strengths, with tensile failure occurring for both the 1100° and 1200°C tested samples. The mode of fracture for this composite was quite "tough", with measured flexural strain-to-failures of 0.64% at RT, 0.89% at 1100°C, and 1.06% at 1200°C.

Elevated temperature (1100° & 1200°C) tensile testing was also performed on the BN coated HPZ fiber composites #392-92 and #397-92, as well as the SiC/BN coated HPZ fiber composite #393-92, as shown in Table IV. These tests were performed in air on dog-boned specimens with a gage length of 1" (2.54 cm) and a gage cross-section of ~0.1" x 0.2" (0.25 x 0.51 cm). On average, the tensile strengths

measured at 1100° and 1200°C for these samples were on the order of one-half of the flexural strengths measured at these temperatures for the same composites. For comparison purposes, the 1100° and 1200°C flexural and tensile strengths measured on BMAS matrix/SiC/BN coated Nicalon fiber composites are from 50 to 100% higher than the strengths measured for composites #392-92 and #397-92. The proportional limit (deviation from linearity) stress and elastic modulus measured for the SiC/BN coated Nicalon fiber composites are also significantly higher than that measured for these two BN coated HPZ fiber composites, but very similar to that measured for the SiC/BN coated HPZ fiber composite #393-92.

The reasons for the lower proportional limit stress and elastic modulus for the BN coated HPZ fiber composites at elevated temperatures may very well relate to boron diffusion into the matrix causing glassy phase formation with incomplete crystallization to barium osumilite, although TEM and X-ray analyses have not shown this to be a major problem compared to earlier results with LAS matrix composites[41]. The fact that the SiC/BN coated HPZ fiber composites have higher proportional limits and elastic modulus values lends credence to this scenario. The lower ultimate elevated temperature flexural and tensile strengths of these composites (compared to SiC/BN coated Nicalon fiber composites) may be related to the slight amount of fiber/matrix reaction still present in these composites, or may be related to thermal degradation of the HPZ fibers themselves. The low tensile strengths measured for the SiC/BN coated composite #393-92 are undoubtedly due to the amount of reactivity noted for this composite and the problems with matrix crystallization, as will be discussed below.

Figure 48 shows the optical and TEM replica characterization of the SiC/BN coated HPZ fiber composite #393-92. It can be seen that, while the amount of reaction with the fibers is not as severe as was seen for composite #88-92 (Figs. 33 & 34), a significant number of the fibers (~20%) showed some reaction and a majority of them showed debonding of the SiC layer. Changes incorporated in the processing of composite #19-93, which also had a SiC/BN coating, resulted in an improved composite microstructure and improved composite properties. However, as can be seen in Fig. 49, there still is some evidence of fiber/matrix reactivity and a considerable amount of SiC layer detachment. Interestingly, the more "sooty", or rougher coated fibers did not show any evidence of SiC layer detachment, compared to the smoother, or "low soot", coatings, as shown in Fig. 50. The "sooty" coated fibers tended to be near the edge of each individual fiber tow, and comprised less than 5% of the total coated fibers. The fracture surface of this composite (Fig. 51) showed a considerable amount of fiber/matrix debonding within the BN layer, especially for the 90° layers, with short, but consistent fiber pullout in the 0° layers. The degree and uniformity of fiber/matrix debonding for this composite was significantly better than that shown in Figs. 31 and 35 for composite #53-92, which is reflected in the much improved strength of composite #19-93.

While time constraints did not permit the tensile testing of composites #17-93 and #19-93, which were fabricated utilizing improvements in processing, tensile samples are available from these composites. It is planned that these tensile samples and others from previous composites (#392-92 & #397-92) be incorporated into the ongoing work being conducted under the related AFOSR contract F49620-92-C-0001[53]. Tensile and tensile stress-rupture testing will then be performed, with the results being compared to results for coated Nicalon fiber/BMAS matrix composites currently being studied under this program. Contrasting the effect of elevated temperature stress states on the fiber/coating(s)/matrix interfacial chemistry and structure for the two different fiber systems should be of great benefit to the development of these systems for high temperature, lightweight, structural applications.

E. Alternate Processing of Glass-Ceramic Matrix/Coated Fiber Composites

While the predominant glass and glass-ceramic matrix composite fabrication technique utilized at UTRC has been hot-pressing of glass powder infiltrated tape layups, other fabrication techniques such as hot isostatic pressing (HIP) and glass transfer molding may allow more complex shapes and/or reduced cost of processing for these types of composites. Under this program, an effort was made to evaluate these two types of alternate processing methods utilizing refractory glass-ceramic matrices and coated fibers.

1. Hot Isostatic Pressing (HIP) Processing - P. McCluskey

(a) Introduction

In HIP'ing, the part to be consolidated is loaded into an expendable container which is evacuated and sealed. By applying an isostatic load through a high pressure, high temperature gas, the container deforms and consolidates the part.

While several different composite shapes such as thin walled tubes and L-beams have been fabricated by HIP at UTRC utilizing graphite fibers and borosilicate glass matrices, higher temperature systems utilizing glass-ceramic matrices and fibers such as HPZ have not been demonstrated. The much higher temperature required for processing of these composites required a study to determine a compatible containment and die material.

Due to difficulty in obtaining a consistent source of HPZ fiber, the high cost of HPZ fiber, and difficulty in CVD coating these fibers, this task of the program was altered to include CVD coated Nicalon yarn as the reinforcing fiber. Processing temperatures are

a function of the matrix only. The temperatures required for processing glass-ceramic materials are several hundred degrees higher than used for borosilicate glass matrices. Since the expected difficulties in HIP'ing glass-ceramic matrix materials were associated only with the matrix and not the fiber, it was determined that switching fibers would not detract form the value of the study.

(b) Die and Tool Compatibility

The initial part of this task was concerned with determining compatible die and tool materials for processing composites in the HIP at temperatures required for glass-ceramics. The die materials used in this study were fabricated from graphite due to UTRC's experience in using graphite dies to form glass-ceramic matrix composites, its high degree of machinability, and its low cost. The need to find a compatible tool or can material was necessitated by the eutectic that many materials form with carbon at elevated temperature. Previous work at UTRC on HIP consolidation of glass matrix composites used stainless steel tooling due to the low (less than 1150°C) processing temperatures. Iron and carbon form a eutectic melt at approximately 1150°C. In addition, stainless steel melts at approximately 1350°C. For composites that utilize more refractory glass-ceramic matrices, processing temperatures in excess of 1400°C are commonly used. This necessitates the need to find a containment material that can be used with carbon at these temperatures.

A survey of available metallic materials was performed, and the promising containment materials are listed below. Materials were determined to be promising if available in a variety of forms, i.e. tubes and plate stock, readily formed and welded, and compatible with carbon dies to elevated temperature. Glass containment systems were not surveyed.

Material	Eutectic Temp. with Carbon	Comment
Iron	1150°C	Melts at 1350°C
Nickel	1316°C	
Molybdenum	2210°C	Embrittlement
Titanium	1650°C	

Titanium was selected as the primary material for containment from the materials listed above. Nickel was dismissed due to the eutectic at 1316°C, and molybdenum was dismissed due to the inherent problems that are associated with welding and the embrittlement that molybdenum materials undergo after heating. Titanium is readily formed into tubes and flat stock, and is easily welded in inert atmospheres. The titanium-carbon eutectic is well above any foreseeable processing temperatures for glass-ceramic matrix composites.

(c) HIP Consolidation of BMAS Matrix/SiC/BN Coated Nicalon Fiber Composites

HIP consolidation was performed utilizing a BMAS matrix and SiC/BN coated Nicalon fibers. Two composites were fabricated using a similar process and HIP'ed together.

The unsized coated fiber was drawn through an aqueous slurry containing the matrix powder and a fugitive binder, and collected on a rotating drum. The prepreg tape was cut into individual plies of the size needed for the particular composite. Binder removal was performed in an oxidizing atmosphere at a temperature sufficient to decompose the binder. The burned off tape was loaded into the graphite die which was then loaded into the titanium can. The cans were welded closed, helium leak checked, vacuum degassed at approximately 400°C and sealed. HIP consolidation was accomplished at UTRC under time and temperature conditions very similar to that utilized for normal hot-pressing.

The composites fabricated are shown in Fig. 52. Both composites are 16 ply, unidirectional, L-beam shapes, having leg lengths of 2.5 cm and 4.0 cm. Both composites are 12.5 cm long and nominally 0.3 cm thick. The polished micrograph shown in Figure 52 shows good fiber distribution and matrix densification, and no damage to the fiber coatings. These samples have been retained as demonstration articles and no further testing or analysis was done on them.

(d) Conclusions

Titanium canning materials were successfully employed in the HIP consolidation of a BMAS glass-ceramic matrix/SiC/BN coated Nicalon fiber composite at temperatures in excess of 1400°C. Multiple part fabrication in a single HIP run was demonstrated. No damage to the fiber coating was seen as a result of HIP densification, and fiber distribution and matrix densification were good.

2 Glass Transfer Molding of Integrally Reinforced Composites - D. Jarmon

(a) Introduction

Fiber reinforced glass-ceramic composites can obtain significant benefits in mechanical performance from integral reinforcement due in part to the fundamental nature of their fiber/matrix interface. The fiber/matrix interface in these composites required a weak to moderate bond strength to produce strong composites with

increased toughness and fiber pullout[14,17]. A crack propagating through a ceramic matrix will be deflected at a fiber if the fiber and matrix are weakly bonded. If the fiber and matrix are strongly bonded the crack will propagate straight through the fiber. The result is that a weak to moderate strength bond at the fiber/matrix interface increases the energy absorbing capability of the ceramic matrix composite in the direction perpendicular to the fiber reinforcement.

While the weak/moderate strength interface bond is necessary for increased fracture toughness, it also is a limiting factor for composite through-thickness properties in 1-D and 2-D reinforced composites. One method of increasing the through-thickness properties is to provide fiber reinforcement in the through-thickness direction. The use of integrally woven (3-D) fiber preforms is a practical method of obtaining this through-thickness fiber reinforcement and glass transfer molding is an ideal method of consolidation for integrally reinforced composites. UTRC has been investigating glass transfer molding for the consolidation of 3-D preforms since 1986[64,65]. The majority of UTRC's investigation of glass transfer molding has been performed with low temperature glasses such as borosilicates. Limited work in glass transfer molding with lithium aluminosilicate (LAS) glass-ceramic has been unsuccessful due to the high viscosity of this composition in the glassy state.

Under this program, UTRC investigated glass transfer molding with magnesium aluminosilicate (MAS) glass-ceramics. Nicalon reinforced MAS composites have potential use temperatures in excess of 1200°C. The ability to glass transfer mold with high temperature glass-ceramics should be beneficial in the fabrication of gas turbine engine components such as complex nozzle components.

(b) Processing and Materials Utilized for Glass Transfer Molding

Glass transfer molding involves the injection of a glass into a fiber array at elevated temperatures. The processing is schematically illustrated in Fig. 53. Glass transfer molding will generally be performed at the maximum temperature which does not severely degrade the fibers. The objective is to obtain the lowest possible viscosity of the glass in order to facilitate injection into the fiber array while not significantly degrading the reinforcing fibers. The viscosity of the glass must be less than 10^3 poise for glass transfer molding to be a viable processing method. The processing is similar to resin transfer molding of fiber reinforced plastics except that it is performed at higher temperatures and higher viscosities. The viscosity of resins during resin transfer molding is generally less than one poise.

A feature of glass transfer molding is that the fibers do not move substantially during processing. This is extremely attractive for the consolidation of 3-D fiber arrays

since processing 3-D preforms using compression techniques, such as hot pressing and hot isostatic pressing, will results in damage to the fibers in at least one direction of reinforcement. Glass transfer molding has the advantage of enabling fabrication of complex shapes without fiber movement.

Glass transfer molding of an integrally fiber reinforced glass composite involves relatively few processing steps, as shown in Fig. 53. The first step is to weave an integrally reinforced fabric. An orthogonal weave was chosen for this investigation because it should provide the maximum benefit to through-thickness reinforcement. Techniweave Inc. of Rochester, N.H. was selected to weave the material required for this program. Figure 54 illustrates the orthogonal woven structures that Techniweave prepared and labels the nomenclature/orientation used to identify the various fibers.

Techniweave fabricated preforms which were approximately 102 mm X 102 mm (4" X 4"). Hand weaving was selected over machine weaving due to the low volume of material being woven. JTRC's processing started by heating a preform in air at 500°C to thermally decompose any fiber sizing, fiber serving, or organic binder that may have existed in the preform. After heat treatment, the preform was loaded into tooling for the glass transfer molding operation. The glass transfer molding operation involves heating the tooling to the desired temperature (1400°C to 1500°C) and applying pressure to the ram. The ram travel was controlled so that the glass flows from the glass reservoir into the molding cavity containing the fiber preform at a moderate rate. After ram travel has stopped, the tooling was cooled to room temperature and the composite was removed.

Magnesium aluminosilicate (MAS) glass-ceramic from Ferro Corporation (SG266M) was selected for this investigation. The viscosity of this glass-ceramic decreases rapidly above 1400°C and is approximately 1 X 10^2 poise at 1450°C. Past experience had shown that it is possible to achieve good infiltration in this viscosity range.

(c) Results

Using the orthogonal woven preforms from Techniweave, two composites were fabricated by glass transfer molding with MAS glass-ceramic. The first composite (#102-92) was fabricated with a preform woven with standard ceramic grade Nicalon fiber and the second composite (#186-92) was woven with SiC/BN coated Nicalon. Table V provides information on the fiber architectures of these composites and the mechanical properties measured. A Nicalon fiber/aluminosilicate glass matrix composite (#319-90) which was fabricated on a previous Office of Naval Research contract is included in Table V for comparison.

(i) Uncoated Nicalon Fiber Composite #102-92

Composite #102-92 was fabricated by glass transfer molding using the preform woven with ceramic grade Nicalon fiber. The preform woven by Techniweave was of excellent quality. It had a uniform thickness of 0.64 cm (0.25") and even fiber spacing. The fiber volume was 41% with the following fiber distributions: X direction - 31%, Y direction - 46% and Z direction - 23%. Cross sections of composite #102-92 in the Y-Z, X-Z and X-Y directions are shown in Figs. 55, 56, and 57, respectively. The fiber tows are straight with no evidence of compaction of the overall preform. Individual tow bundles, shown in Fig. 58A, also do not show evidence of compaction. The degree of consolidation on this composite was fair. Figure 58B shows some porosity inside a tow bundle and the apparent porosity (surface connected) measured on the composite was 2.2%. Based on past experience, UTRC has achieved the highest mechanical properties on glass transfer molded composites when the apparent porosity levels are below 1.5%. The desired goal on UTRC glass transfer molded composites is to have the apparent porosity less than 1%.

The mechanical properties measured on composite #102-92 are summarized in Table V. The tensile strength of 93 MPa (13.5 ksi) measured in the Y direction was approximately one third of strength measured on hot pressed 2D BMAS matrix/SiC/BN coated Nicalon fiber composites with similar fiber volume loadings. The low strength may be related to: (1) fiber degradation due to high processing temperatures, (2) high porosity and/or (3) reaction between the fiber and the MAS matrix. In past work at UTRC, Nicalon fiber reinforced SG266M MAS composites fabricated by hot pressing have had low flexural strengths (140 to 200 MPa). The fracture surfaces on these specimens have exhibited brittle failure and fibers leached from these composites have been very weak. Scanning Auger studies showed that a considerable amount of Mg had diffused into the near-surface region of the fibers. This data indicates excessive reaction between the MAS and Nicalon fibers during processing.

(ii) SiC/BN Coated Nicalon Fiber Composite #186-92

In order to increase the mechanical properties, Techniweave Inc. wove an orthogonal preform according to UTRC specifications using SiC/BN coated Nicalon fiber. Hot pressed SiC/BN coated Nicalon reinforced BMAS composites have exhibited good oxidative stability and mechanical properties to 1200°C[53]. In hot pressed composites, the BN layer provides a weak interface and the SiC overcoat layer inhibits reaction between the matrix glass-ceramic and the boron nitride layer. The goal of using SiC/BN coated Nicalon for glass transfer molding was also to have the SiC overcoat inhibit reaction between the matrix and BN layer.

Nicalon fiber was coated with SiC/BN by 3M Corporation based on UTRC specifications. The thickness of the BN layer was ~4000Å and the SiC layer was ~2000Å. UTRC supplied this fiber to Techniweave with instructions to weave a preform similar to the preform used to fabricate composite #102-92. The fiber was supplied to Techniweave with no sizing and Techniweave did not size the fiber prior to weaving. Organic sizings are commonly applied to the surface of fiber tows to improve handling and minimize fiber degradation due to self abrasion.

Techniweave had more difficulty in weaving the SiC/BN coated fiber than they did the uncoated Nicalon fiber; however, they believe these problems could be significantly reduced in future work. The resultant preform was of poor quality due to the weaving problems. The thickness ranged from 0.70 cm to 0.80 cm and the fiber spacing was not consistent. Techniweave had to reduce the volume percent of fibers in the X direction in order to weave the preform. The total fiber volume was 38% with the following fiber distributions: X direction - 25%, Y direction - 50% and Z direction - 25%. Figure 59 provides a surface view of the as-received woven preform. Some breakage of the Z fiber loops and SiC/BN coating was observed by SEM examination.

Composite #186-92 was fabricated by glass transfer molding using the preform described above. The Y-Z cross section of this composite is presented in Fig. 60 and mechanical data is provided in Table V. The composite was thicker than the desired goal of 0.64 cm (0.25") due to the variation in the preform thickness. The composite had an apparent porosity of 3.5% which is significantly higher than the desired goal of less than 1%. The location of this porosity is shown in Figs. 60 and 61. Some of the porosity is associated with the matrix rich areas and some is located between filaments in the fiber tows. The porosity within the tows is the most detrimental to mechanical performance.

The goal of using SiC/BN coated fibers was to inhibit fiber matrix reaction and increase mechanical performance; however, the mechanical properties measured on composite #186-92 were approximately the same as those measured on composite #102-92 (see Table V). In the Y direction, the tensile strength was 90 MPa (13 ksi) and the flexural strength was 205 MPa (30 ksi). As mentioned previously, these low strengths may be related to: (1) fiber degradation due to high processing temperatures, (2) high porosity and/or (3) reaction between the fiber and the MAS matrix. Reaction between the fiber and the MAS matrix is the most likely source of degradation because of evidence of damage to the SiC/BN coating during weaving and subsequent composite processing. The TEM replica micrographs shown in Figs. 62 and 63 of longitudinally polished sections of composite #186-92 show that separation of the SiC/BN coating at regions of both inward and outward curvature of the integrally woven preform was significant. This coating damage undoubtedly occurred during the preform

weaving and may have been exacerbated during composite processing. With coating damage, the MAS matrix can then lead to significant degradation of the Nicalon fibers during composite processing, due to excessive Mg diffusion into the fibers. To avoid coating damage of integrally woven preforms, approaches such as sizing the coated fibers prior to weaving or batch coating pre-woven fiber arrays should be explored.

(iii) Through-thickness Composite Tensile Strengths

As discussed in the Introduction, one of the primary reasons for incorporating 3-D fiber reinforcement into a ceramic matrix composite is to increase the through-thickness strength. For composite #102-92, a through-thickness strength of 20 MPa (2.9 ksi) was measured. Based on 23% of the reinforcing fiber oriented in the Z direction, one could expect that for a composite with little or no fiber degradation during composite processing, the through-thickness UTS should be in the range of 100 to 170 MPa (15 to 25 ksi). Instead, the through-thickness tensile strength of this composite was similar to that of a 2-D composite. The through-thickness tensile strength of 0°/90° Nicalon fiber reinforced glass-ceramics is typically 15 to 25 MPa (2.2 to 3.6 ksi). No through-thickness tensile testing was done for the coated fiber composite #186-92.

The lack of increase in through-thickness strength could be a function of the test specimen design as well as the degradation of fiber strength during composite processing. The tensile strength was measured on a 2.54 cm diameter disc machined from the composite panel, with 0.13 cm machined from both sides of this disc in order to remove the surface loops on Z direction fibers. The disc was bonded with adhesive between two metal attachment fixtures. This assembly was loaded into a test machine and stressed in tension. The through-thickness tensile specimen for composite #102-92 failed near the adhesive bond line. In future through-thickness testing, a machined slot in the edge of the disc to reduce the area of the gage section and achieve tensile failure of the composite, rather than the adhesive bond, will be utilized.

(d) Summary

3-D reinforced MAS composites were successfully fabricated by glass transfer molding with both Nicalon fiber and SiC/BN coated Nicalon fiber. The microstructures of these composite was good except for excessive porosity. The apparent porosity was in the 2 to 3% range which is higher than the goal porosity level of less than 1%. The mechanical properties of the composite were low, which may be related to: (1) fiber degradation due to high processing temperatures, (2) high porosity and/or (3) reaction between the fiber and the MAS matrix. For the composite made with SiC/BN coated Nicalon fiber there was evidence of damage to the fiber coating which undoubtedly occurred during the weaving process. These damaged areas appear to have rendered

the SiC/BN coating ineffective in inhibiting reaction between the MAS matrix and the Nicalon fibers.

Future investigation should include the following:

- Investigation of fiber sizings for the coated Nicalon fiber to minimize coating damage during weaving.
- Glass transfer molding with barium magnesium aluminosilicate (BMAS) matrices. These matrices have historically produced SiC/BN coated Nicalon reinforced hot pressed composites with excellent properties.
- Investigation of processing parameters, such as injection rate and temperature, in order to reduce porosity and minimize fiber degradation.
- Investigation of through-thickness tensile specimen design for integrally reinforced composites.

IV. CONCLUSIONS

From the work conducted under this program, it has been demonstrated that BMAS glass-ceramic matrix composites (0/90°) reinforced with BN coated HPZ fibers can be fabricated with minimal fiber/matrix reactivity, resulting in composites with flexural strengths over 50 ksi (345 MPa) from RT to 1100°C and a fair degree of fracture toughness. These results have been achieved only after significant improvements in the handleability of the HPZ fiber itself by Dow Corning that then led to much improved BN coating uniformity by 3M. Previously utilized HPZ fiber tows would often break when being unspooled, due to improper sizing application and/or packaging methods, which would lead to non-uniform and damaged BN and SiC/BN coatings during the continuous CVD deposition process.

From TEM and scanning Auger studies conducted under this program, it was found that during composite processing, matrix element diffusion through the CVD BN layer to the HPZ fiber surface (which was found to consist of a microporous, oxygen rich layer ~300nm thick) would result in reacted fiber surfaces, with crystalline silicon oxynitride formation and weak and brittle composites, if the BN layer thickness was less than 200-300nm. Uniform BN coatings that were in excess of the minimum thickness produced relatively strong BMAS matrix composites, with minimum reaction between the matrix and HPZ fibers. While SiC layer detachment during composite processing remained a problem for the dual coated SiC/BN HPZ fibers, the SiC overcoat may not be necessary if the composite use temperature is projected to be 1100°C or less. For higher temperature composites where the SiC layer may be necessary as a boron diffusion barrier, additional work is needed to determine the mechanisms causing SiC layer detachment.

The investigation of alternate processing techniques other than traditional hot-pressing has demonstrated the viability of composite processing by both hot isostatic pressing (HIP) and glass matrix transfer molding into integrally woven fiber preforms. These experiments were performed utilizing SiC/BN coated Nicalon fibers, due to the lack of suitable coated HPZ fibers in time to meet the program schedule. In addition to demonstrating these processes with coated HPZ fibers, future work needs to be done in scaling up the HIP process to larger sizes, and in weaving coated fiber tows and/or coating pre-woven fiber preforms without inflicting damage to the fiber coatings, so that glass transfer molding can be utilized to fabricate composites with improved properties.

V. ACKNOWLEDGEMENTS

The authors would like to thank Mr. Rick Jones of Dow Corning for coordinating the delivery of the HPZ fibers to UTRC, Mr. Jim O'Kelly of 3M for coating the HPZ fibers under study, Dr. Bruce Laube of UTRC for the SAM analyses, Mr. Gerald McCarthy of UTRC for the TEM analyses, Mr. Stan Kustra of UTRC and Mr. Gary Linsey of P&W for the composite mechanical testing, and Ms. Laura Austin, Mr. Steve Gore, and Mr. Dom Malaquias of UTRC for the fabrication of the coated fiber composites, and to Lt. Col. Larry Burggraf of AFOSR for his sponsorship of this program.

Papers published to date under AFOSR support include:

1. "SiC-Whisker-Reinforced Glass-Ceramic Composites: Interfaces and Properties", John J. Brennan and Steven R. Nutt, J. Am. Ceram. Soc. 75, [5] 1205-16 (1992)

Papers presented at meetings dealing with the subject matter of this contract:

1. "Interfacial Studies of Coated Nicalon and HPZ Fiber/Glass-Ceramic Matrix Composites", John J. Brennan, presented at the 16th Annual Conference on Composites, Materials, & Structures, Cocoa Beach, Fla., January 15, 1992.

2. "Interfacial Reactions in BN Coated HPZ Fiber Reinforced Glass-Ceramic Matrix Composites", John J. Brennan, presented at the 17th Annual Conference on Composites, Materials, & Structures, Cocoa Beach, Fla. January 14, 1993.

REFERENCES

1. Prewo, K.M. and Bacon, J.F.: Proc. of Second Int. Conf on Composite Materials, Toronto Canada (AIME New York 1978) 64.

2. Prewo, K.M., Bacon, J.F. and Dicus, D.L.: SAMPE Q (1979) 42.

3. Prewo, K.M.: Development of a New Dimensionally and Thermally Stable Composite, Proceedings of "The Conference on Advanced Composites-Special Topics", (Dec 4-6, 1979) El Segundo CA.

4. Prewo, K.M. and Minford, E.J.: Graphite Fiber Reinforced Thermoplastic Matrix Composites for Use at 1000°F, SAMPE J. Vol 21-1 (March 1985).

5. Prewo, K.M.: A Compliant, High Failure Strain Fibre Reinforced Glass Matrix Composite, J. Mat. Sci. 17 (1982) 3549-3563.

6. Bacon, J.F. and Prewo, K.M.: Proc. Second Intl. Conf. on Composite Materials, Toronto Canada (AIME New York 1978) 753.

7. Prewo, K.M. and Brennan, J.J.: High Strength Silicon Carbide Fiber-Reinforced Glass Matrix Composites, J. Mat. Sci. 15 (1980) 463-468.

8. Prewo, K.M. and Brennan, J.J.: Silicon Carbide Yarn Reinforced Glass Matrix Composites, J. Mat. Sci. 17 (1982) 1201-1206.

9. Brennan, J.J. and Prewo, K.M.: Silicon Carbide Fiber Reinforced Glass-Ceramic Matrix Composites Exhibiting High Strength and Toughness, J. Mat. Sci. 17 (1982) 2371-2383.

10. Chyung, K., Cooper, R.F., Gadkaree, K.P., Stewart, R.L., Taylor, M.F.: Reinforcement of Alkaline Earth Aluminosilicate Glass-Ceramics, US Patent 4,615,987, Oct. 7, 1986.

11. Brennan, J.J., and Prewo, K.P.: Study of Lithium Aluminosilicate (LAS)/SiC Fiber Composites for Naval Gas Turbine Applications, Final Report R82-915778-4 on NASC Contract N00019-81-C-0136, Oct. 8, 1982.

12. Brennan, J.J., and Prewo, K.P.: Investigation of Lithium Aluminosilicate (LAS)/SiC Fiber Composites for Naval Gas Turbine Applications, Final Report R83-916232-4 on NASC Contract N00019-82-C-0438, Oct. 30, 1983.

13. Brennan, J.J.: Interfacial Studies of SiC Fiber Reinforced Glass-Ceramic Matrix Composites, Final Report R87-917546-4 on ONR Contract N00014-82-C-0096, October 15, 1987.

14. Brennan, J.J.: Interfacial Characterization of Glass and Glass-Ceramic Matrix/Nicalon SiC Fiber Composites, Proc. of the Conf. on Tailoring Multiphase and Composite Ceramics, Penn St. Univ. (July 1985). Materials Science Research Vol 20, Plenum Press, New York (1986) 549-560.

15. Minford, E.J. and Prewo, K.M.: Fatigue Behavior of SiC Fiber Reinforced LAS Glass-Ceramic, ibid.

16. Prewo, K.M., Brennan, J.J. and Layden, G.K.: Fiber Reinforced Glasses and Glass-Ceramics for High Performance Applications, Am. Cer. Soc. Bull. Vol. 65, No. 2 (Feb. 1986).

17. Brennan, J.J.: Interfacial Chemistry and Bonding in Fiber Reinforced Glass and Glass-Ceramic Matrix Composites, Proc. of the Conf. on Ceramic Microstructures '86: Role of Interfaces, Univ of Calif, Berkeley (July 1986) Materials Science Res Vol. 21, Plenum Press, NY (1987) 387-400.

18. Mah, T., Mendiratta, M.G., Katz, A.P., Ruh, R. and Mazdiyasni, K.S.: Room Temperature Mechanical Behavior of Fiber-Reinforced Ceramic-Matrix Composites, J. Am. Cer. Soc. 68 [1] (1985) C-27-30.

19. Cooper, R.F. and Chyung, K.: Structure and Chemistry of Fibre-Matrix Interfaces in SiC Fibre-Reinforced Glass-Ceramic Composites: An Electron Microscopy Study, J. Mat. Sci. 22 (1987) 3148-3160.

20. Brennan, J.J.: Interfacial Characteristics of Glass-Ceramic Matrix/SiC Fiber Composites, Journal de Physique, Colloque C5, supplement au n° 10, Tome 49, Oct. 1988, 791-809.

21. Prewo, K.M.: Tension and Flexural Strength of Silicon Carbide Fiber-Reinforced Glass-Ceramics, J. Mat. Sci., 21, 1986, 3590-3600.

22. Prewo, K.M.: Fatigue and Stress Rupture of Silicon Carbide Fiber-Reinforced Glass-Ceramics, ibid., 22, 1987, 2695-2701.

23. Michalske, T.A., and Hellman, J.R.: Strength and Toughness of Continuous Alumina-Fiber-Reinforced Glass-Matrix Composites, J. Am. Cer. Soc., 71 [9] 1988, 725-731.

24. Cho, K., Kerans, R.J., and Jepsen, K.A.: Selection, Fabrication, and Failure Behavior of SiC Monofilament-Reinforced Glass Composites, Cer. Engr. Sci. Proc., [9], 7-8, 1988, 815-824.

25. Lankford, J.: Strength of Monolithic and Fiber-Reinforced Glass-Ceramics at High Rates of Loading and Elevated Temperatures, ibid., 843-852.

26. Kim, R.Y., and Katz, A.P.: Mechanical Behavior of Unidirectional SiC/BMAS Ceramic Composites, ibid., 853-860.

27. Murthy, V.S.R., Jie, L., and Lewis, M.H.: Interfacial Microstructure and Crystallization in SiC-Glass Ceramic Composites, ibid., [10], 7-8, 1989, 938-954.

28. Pannhorst, W., Spallek, M., Bruckner, R., Hegeler, H., Reich, C., Grathwohl, G., Meier, B., and Spelmann, D.: Fiber-Reinforced Glasses and Glass-Ceramics Fabricated by a Novel Process, ibid., [11], 7-8, 1990, 947-963.

29. Zawada, L.P., Butkus, L.M., and Hartman, G.A.: Room Temperature Tensile and Fatigue Properties of Silicon Carbide Fiber-Reinforced Aluminosilicate Glass, ibid., 1592-1606.

30. Wang S.-W., and Parvizi-Majidi, A.: Mechanical Behavior of NICALON Fiber-Reinforced Calcium Aluminosilicate Matrix Composites, ibid., 1607-1616.

31. Parlier, M., Ritti, M.H., Stohr, J.F., and Vignesoult, S.: Silicon Carbide Fibre-Reinforced Glass-Ceramic Matrix Composites: A High Temperature Material for High Performance Application, Proc. of ICAS 90, Stockholm, Sweden, Sept. 9-14, 1990.

32. Hegeler, H., and Bruckner, R.: Fibre-Reinforced Glasses: Influence of Thermal Expansion of the Glass Matrix on Strength and Fracture Toughness of the Composites, J. Mat. Sci., [25], 1990, 4836-4846.

33. Phillips, D.C., Park, N., and Lee, R.J.: The Impact Behavior of High Performance, Ceramic Matrix Fibre Composites, Comp. Sci. & Tech., [37], 1990, 249-265.

34. Homeny, J., VanValzah, J.R., and Kelley, M.A.: Interfacial Characterization of Silicon Carbide Fiber/Lithia-Alumina-Silica Glass Matrix Composites, J. Am. Cer. Soc. 73 [7], 1990, 2054-59.

35. Ponthieu, C., Lancin, M.,Thibault-Desseaux, J., and Vignesoult, S.: Microstructure of Interfaces in SiC/Glass Composites of Different Tenacity, Colloque de Physique, C1, Supplement au n°1, Tome 51, Janvier 1990, 1021-1026.

36. Laube, B.L., and Brennan, J. J.: Scanning Auger Electron Spectroscopy of the Fiber/Matrix Interface of SiC Fiber/Silicate Glass Matrix Composites, J. Vac. Sci. Tech. A 81 (3) May/June 1990, 2096-2100.

37. Brennan, J. J.: Glass and Glass-Ceramic Matrix Composites, Chapter 8 in Fiber Reinforced Ceramic Composites, edited by K. S. Mazdiyasni, Noyes Publications, Park Ridge, NJ, 1990.

38. Bonney, L.A., and Cooper, R.F.: Reaction-Layer Interfaces in SiC-Fiber-Reinforced Glass-Ceramics: A High-Resolution Scanning Transmission Electron Microscopy Analysis, J. Am. Cer. Soc., 73 [10] (1990) 2916-21.

39. Prewo, K.M.., Johnson, B., and Starrett, S.: Silicon Carbide Fibre Reinforced Glass-Ceramic Composite Behavior at Elevated Temperature, J. Mat. Sci., 24, 1989, 1373-1379.

40. Brennan, J. J.: Interfacial Studies of Whisker and Coated Fiber Reinforced Ceramic Matrix Composites, Annual Rept. R90-918185-1 on AFOSR Contract F49620-88-C-0062, May 31, 1990.

41. Brennan, J. J.: Interfacial Studies of Coated Fiber Reinforced Glass-Ceramic Matrix Composites, Annual Report R91-918185-2 on AFOSR Contract F49620-88-C-0062, Sept. 30, 1991.

42. Rice, R. W.: BN Coating of Ceramic Fibers for Ceramic Fiber Composites, US Patent 4,642,271, Feb. 10, 1987.

43. Brennan, J.J.: The Evaluation of Dow Corning Fibers, UTRC Annual Report R86-917103-12 on Contract F33615-83-C-5006, Feb., 1986.

44. Singh, R.N.: Fiber-Matrix Interfacial Characteristics in a Fiber-Reinforced Ceramic-Matrix Composite, J. Am. Cer. Soc., 72 (9), 1989, 1764-1767.

45. Tredway, W.K., and Prewo, K.M.: Improved Performance in Monofilament Fiber Reinforced Glass Matrix Composites Through the Use of Fiber Coatings, Mat. Res. Soc. Symp. Proc. Vol. 170, 1990, 215-221.

46. Brennan, J.J.: Interfacial Studies of Chemical Vapor Infiltrated (CVI) Ceramic Matrix Composites, Final Report R90-917779-5 on ONR Contract N00014-87-C-0699, March 31, 1990.

47. Lowden, R.A., and Stinton, D.P.: Interface Modification in NICALON/SiC Composites, Ceram. Engr. Sci. Proc., 9 [7-8], 1988, 705-722.

48. Doughan, C.A., Lehman, R. L., and Greenhut, V.A.: Interfacial Properties of C-Coated Alumina Fiber/Glass Matrix Composites, Ceram. Engr. Sci. Proc. 10 [7-8], 1989, 912-924.

49. Jurewicz, A.J.G., Kerans, R.J., and Wright, J.: The Interfacial Strengths of Coated and Uncoated SiC Monofilaments Embedded in Borosilicate Glass, ibid, 925-937.

50. Hay, R.S., and Hermes, E.E.: Sol-Gel Coatings on Continuous Ceramic Fibers, ibid., 11 [9-10], 1990, 1526-1538.

51. Gulden, T.D., Hazlebeck, D.A., Norton, K.P., and Streckert, H.H.: Ceramic Fiber Coating by Gas-Phase and Liquid-Phase Processes, ibid., 1539-1553.

52. Bender, B.A., Jessen, T.L., and Lewis III, D.: Interfacial Microstructure and Mechanical Properties of SiC/$ZrTiO_4$ Composites Hot-Pressed in CO, ibid., [7-8], 964-973.

53. Brennan, J., Allen, W., Nutt, S., and Sun, Y.: Interfacial Studies of Coated Fiber Reinforced Glass-Ceramic Matrix Composites, Annual Report R92-970150-1 on AFOSR Contract F49620-92-C-0001, Nov. 30, 1992.

54. Legrow, G.E., Lim, T.F., Lipowitz, J., and Reaoch, R. S.: Ceramics from Hydridopolysilazane, Cer. Bull, Vol. 66, No. 2, 1987, 363-367.

55. Atwell, W.H., Jones, R.E., Lipowitz, J., and Salinger, R.M.: Advanced Ceramics Based on Polymer Processing, Final Report WRDC-TR-91-4058, DARPA Contract F33615-83-C-5006, Sept. 1990.

56. Van Loo, F.J.J., Van Beek, J.A., and Bastin, G.F.: On the Sequence of the Product Layers in Solid-State Displacement Reactions, Solid State Ionics, 16 (1985) 131-136.

57. Barin, I., Knacke, O., and Kubaschewski, O.: Thermochemical Properties of Inorganic Substances, Springer-Verlag, New York (1977).

58. JANAF Thermochemical Tables, edited by Chase, M.W., Davies, C.A., Downey, J.R., Frurip, D.J., McDonald, R.A., and Syverud, A.N.: Thermal Research Lab., DOW Chemical Corp., Midland, MI, third edition (1985).

59. Blegen, K.: Equilibria and Kinetics in the Systems Si-N and Si-N-O, Special Ceramics, 6 (1975) 223-238.

60. Hadley, G.: Linear Algebra, Addison-Wesley, Reading, MA (1973).

61. Yamawaki, M. and Hoch, M.: Vaporization Behavior of Silicon Nitride, Report AFML-TR-73-240, Contract No. F33615-69-C-1531, Dec. 1972.

62. Swalin, R.A.: Thermodynamics of Solids, John Wiley & Sons, New York (1972).

63. Zangvil, A., Chang, Y-W, and Finnegan, N.: Effect of Heat Treatment on the Elemental Distribution of Si, C, N, O Fibers, Ceramics International, 18 (1992), 271-277.

64. Jarmon, D.C., McCluskey, P.H., and Brennan, J. J.: Advanced Fabrication and Characterization of Fiber Reinforced Ceramic Matrix Composites, Final Report R89-917548-5 on ONR Contract N00014-86-C-0649, Feb. 15, 1991.

65. Cairo, R.R.: Advanced Turbine Rotor Design Program, Interim Tech. Report AFWAL-TR-88-2129, AFSC Contract F33615-85-C-2594, Feb. 1989.

Table I

Tensile Strength of HPZ Fibers Before and After Exposure in Nitrogen at 1430°C for 10 Minutes

Fiber Lot #	As-Received UTS - ksi (MPa)	Exposed UTS - ksi (MPa)
7370-78-1C	240 (1660)	208 (1430)
100173-16	339 (2340)	107 (740)
03028013	358 (2480)	128 (883)

Table II

Flexural (3-pt) Properties of BMAS Matrix/BN & SiC/BN Coated HPZ Fiber Composites (0/90°)

Comp. #	Fiber Lot	Fiber Coating	Ctg. Morph.	Vol. %	Composite σ - ksi (MPa)/E-msi (GPa)] RT	1100°C	1200°C
349-91	9545-20-20	none	-	30	23 (159) [14.3 (98)]	-	-
5-91	7370-78-1C (UTS=1.52 GPa)	BN (89030:90)	"sooty" (UTS=1.42 GPa)	41	55 (380) [15.1 (104)]	42 (290) [7.2 (50)]	28 (193) [5.6 (39)]
12-91	"	SiC/BN (89030:90)	"sooty" (UTS=1.03 GPa)	46	46 (317) [16.5 (114)]	44 (303) [9.6 (66)]	41 (283) [8.8 (61)]
415-91	9545-20-5A (UTS=2.0 GPa)	BN (92172:56)	"low soot" (UTS=1.97 GPa)	35	44 (303) [15.7 (108)]	38 (262) [8.0 (55)]	38 (262) [6.7 (46)]
452-91	9545-20-12 (UTS=1.98 GPa)	SiC/BN (92172:57)	"low soot" (UTS=0.95 GPa)	34	27 (186) [18.3 (126)]	28 (193) [10.4 (72)]	38 (262) [9.3 (64)]
53-92	100173-1,4 (UTS=2.34 GPa)	SiC/BN (92171:74)	"low soot" (UTS=1.62 GPa)	42	19 (131) [16.4 (113)]	-	-
88-92	"	SiC/BN (92172:78)	"low soot" (UTS=1.12 GPa)	61	22 (152) [19.4 (134)]	-	-
213-92 (1050°C Press)	"	SiC/BN (92172:74)	"low soot"	54	30 (207) [16.8 (116)]	30 (207) [13.7 (94)]	31 (214) [10.7 (74)]

Table III

Flexural (3-pt) Properties of BMAS Matrix/BN & SiC/BN Coated HPZ Fiber (Lot 062984-07) Composites (0/90°)

Comp. #	Fiber Lot	Fiber Coating	Ctg. Morph.	Vol. %	Composite σ - ksi (MPa)/[E-msi (GPa)] RT	1100°C	1200°C
301-92	062984-07 (UTS=2.3 GPa)	BN (97037:23)	"low soot" (UTS=1.58 GPa)	37	65 (448) [13.6 (94)]	42 (290) [11.0 (76)]	19 (131) [5.6 (39)]
334-92	"	"	"	45	65 (448) [15.0 (103)]	39 (269) [9.2 (63)]	29 (200) [8.2 (57)]
392-92	"	BN (97037:69-1)	"low soot" (UTS=1.71 GPa)	32	64 (440) [16.3 (112)]	56 (386) [10.2 (70)]	45 (310) [8.9 (61)]
393-92	"	SiC/BN (97037:69-2)	"low soot" (UTS=1.19 GPa)	28	43 (296) [15.3 (105)]	31 (214) [10.2 (70)]	23 (159) [8.1 (56)]
397-92	"	BN (97037:69-1)	"low soot"	30	52 (359) [16.5 (114)]	52 (359) [9.0 (62)]	37 (255) [7.4 (51)]
398-92	"	SiC/BN (97037:69-2)	"low soot"	28	41 (283) -	-	-
17-93	"	BN (97037:69-1)	"low soot"	33	67 (459) [15.9 (110)]	55 (378) [10.1 (69)]	37 (255) [6.4 (44)]
19-93	"	SiC/BN (97037:69-2)	"low soot"	36	55 (380) [16.1 (111)]	49 (337) [12.5 (86)]	46 (315) [10.1 (69)]

Table IV

Elevated Temperature Tensile Properties in Air for BMAS Matrix BN & SiC/BN Coated HPZ Fiber Composites (0/90°)

Comp. #	Fiber Coating	Temperature	UTS - ksi(MPa)	PL - ksi(MPa)	E - msi(GPa)	ε_1 - %
392-92	BN (97037:69-1)	1100°C	22.8 (157)	5.9 (41)	7.3 (50)	0.68
	"	1200°C	19.7 (136)	4.3 (30)	5.0 (35)	0.63
393-92	SiC/BN (97037:69-2)	1100°C	15.8 (109)	11.9 (82)	10.7 (74)	0.23
		1200°C	-	-	-	-
397-92	BN (97037:69-1)	1100°C	27.4 (189)	6.4 (44)	7.0 (48)	0.89
		1200°C	24.9 (172)	5.1 (35)	4.6 (32)	0.98

Table V

Properties of 3-D COMPGLAS Composites Fabricated By Glass Transfer Molding

Composite Number	# 102-92	# 186-92	# 319-90
Contract Number	F49620-88-C-0062	F49620-88-C-0062	N00014-86-C-0649
Materials			
Fiber	Nicalon	Nicalon	Nicalon
Fiber Coating	None	SiC / BN	None
Matrix Identification	Ferro SG266M	Ferro SG266M	CGW 1723
Matrix Type	MAS	MAS	aluminosilicate
Weave			
Type	Orthogonal	Orthogonal	Warp Interlock
Z or Warp Interlock Fiber Angle	90°	90°	30° to 35°
Fiber v/o			
Total Fiber %	41	38	34
Fiber Volume % of Total Volume			
X axis	31	25	40
Y axis	46	50	43
Z axis	23	25	15
Thickness (cm)	0.645	0.790	0.665
Liquid Displacement Properties			
Apparent Porosity (%)	2.2	3.5	0.3
Apparent Density (g/cc)	2.60	2.89	2.57
Bulk Density (g/cc)	2.55	2.79	2.56

Table V (Continued)

Properties of 3-D COMPGLAS Composites Fabricated By Glass Transfer Molding

Composite Number	# 102-92	# 186-92	# 319-90
Mechanical Properties			
Tensile: Y Direction			
Tensile Strength (MPa) {ksi}	93 {13.5}	90 {13.0}	195 {28.3}
Tensile Modulus (GPa) {Msi}	108 {15.6}	95 {13.7}	66 {9.6}
Strain to Failure (%)	0.3	1.4	0.57
Proportional Limit (MPa) {ksi}	10 {1.5}	20 {2.9}	39 {5.7}
0.02% Offset Stress (MPa) {ksi}	40 {5.7}	33 {4.7}	54 {7.8}
Tensile: Through-thickness Direction			
Strength: As-pressed Surf. (MPa) {k	-	-	7 {1.0}
Strength: Machined Surf. (MPa) {ksi	20 {2.9}	-	-
Flexural: Y Direction			
Max. Flexural Strength (MPa) {ksi}	204 {29.6}	205 {29.8}	173 {25.1}
Flexural Modulus (GPa) {MPa}	.73 {10.6}	-	57 {8.3}
Strain to Failure (%)	0.4	0.3	0.41
Proportional Limit (MPa) {ksi}	35 {5.1}	43 {6.3}	-
0.02% Offset Stress (MPa) {ksi}	57 {8.2}	89 {12.9}	-
Failure Mode	tensile	tensile	tensile
Flexural: X Direction			
Max. Flexural Strength (MPa) {ksi}	171 {24.8}	132 {19}	-
Flexural Modulus (GPa) {Msi}	71 {10.3}	44 {6.4}	-
Strain to Failure (%)	0.6	0.1	-
Proportional Limit (MPa) {ksi}	45 {6.6}	25 {3.6}	-
0.02% Offset Stress (MPa) {ksi}	81 {11.8}	54 {7.8}	-
Failure Mode			

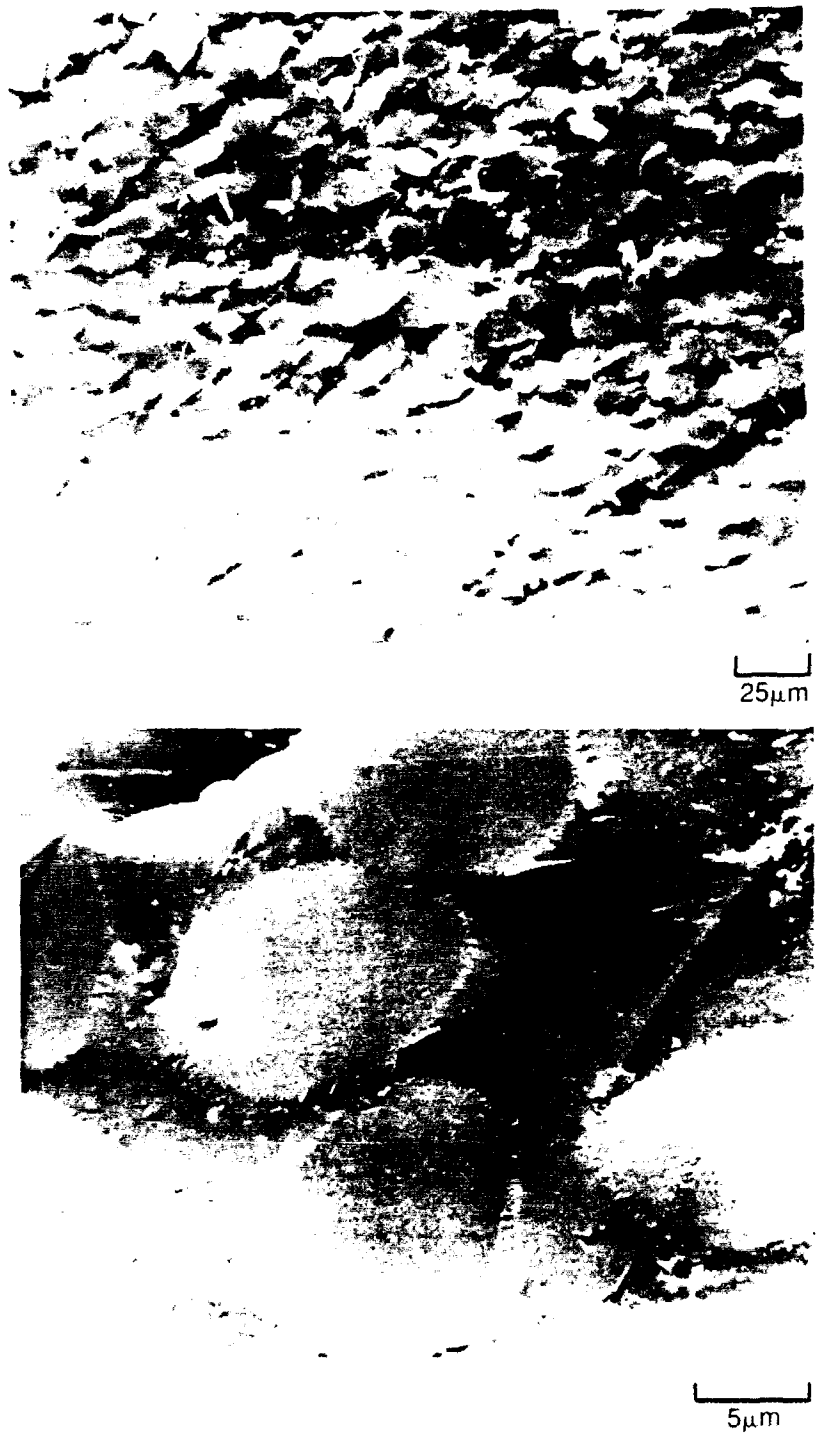

Fig. 1 Fracture Surface of LAS Matrix/HPZ Fiber Composite

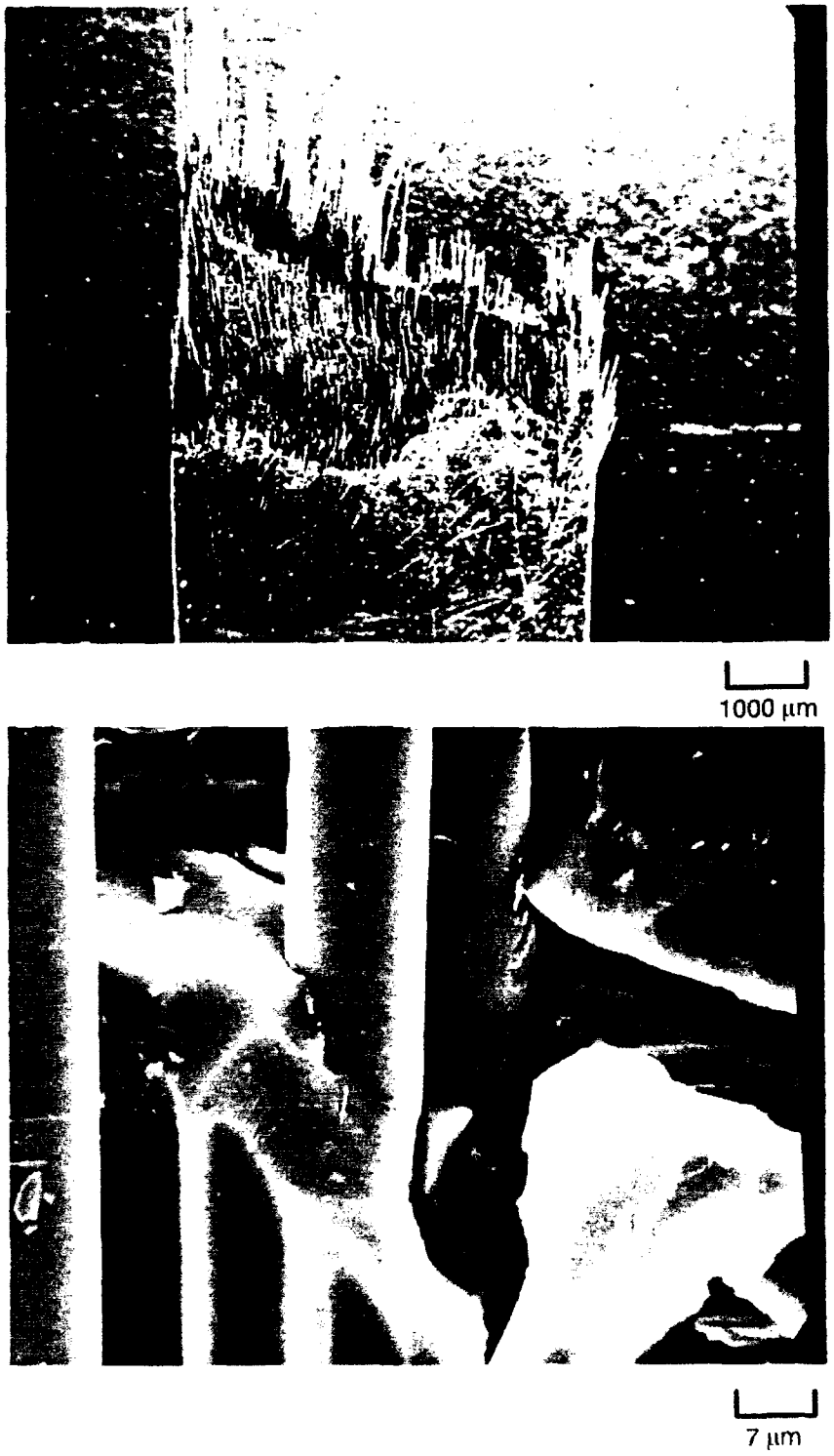

Fig. 2 Fracture Surface of UTRC-100 LAS Matrix/3000Å Carbon Coated HPZ Fiber Composite #78-87, As-pressed [σ=120 ksi (830 MPa)]

EP301-10-1

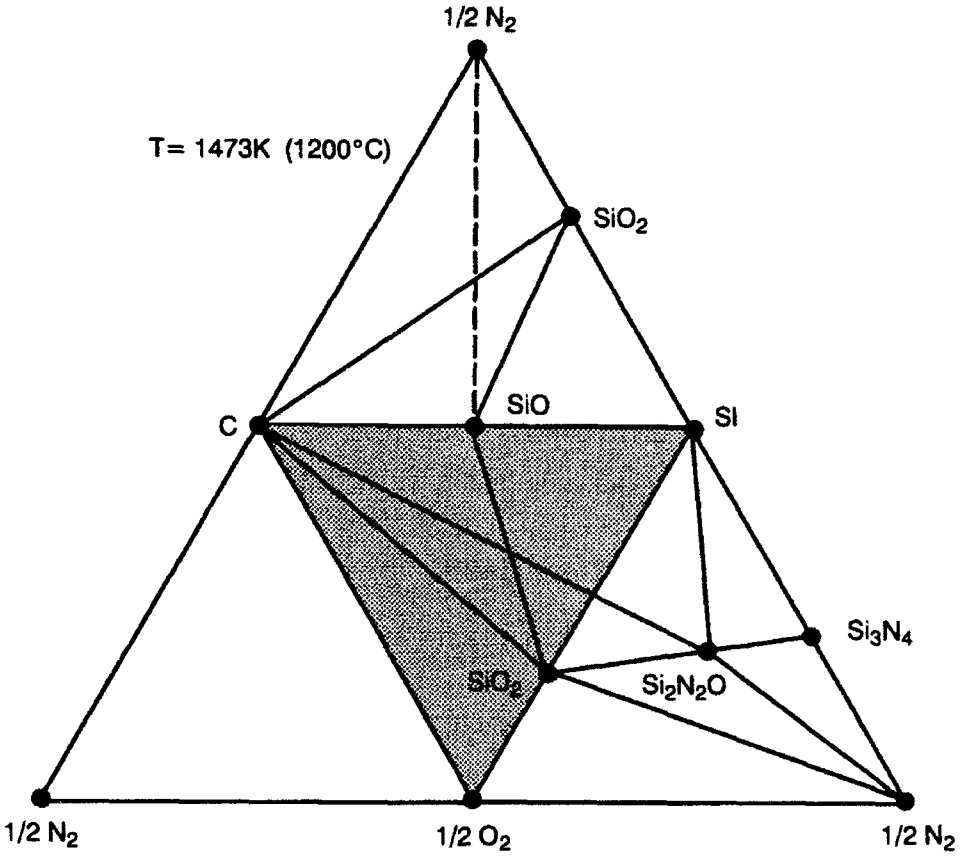

Fig. 3 Calculated Si-C-O-N System at 1473 K

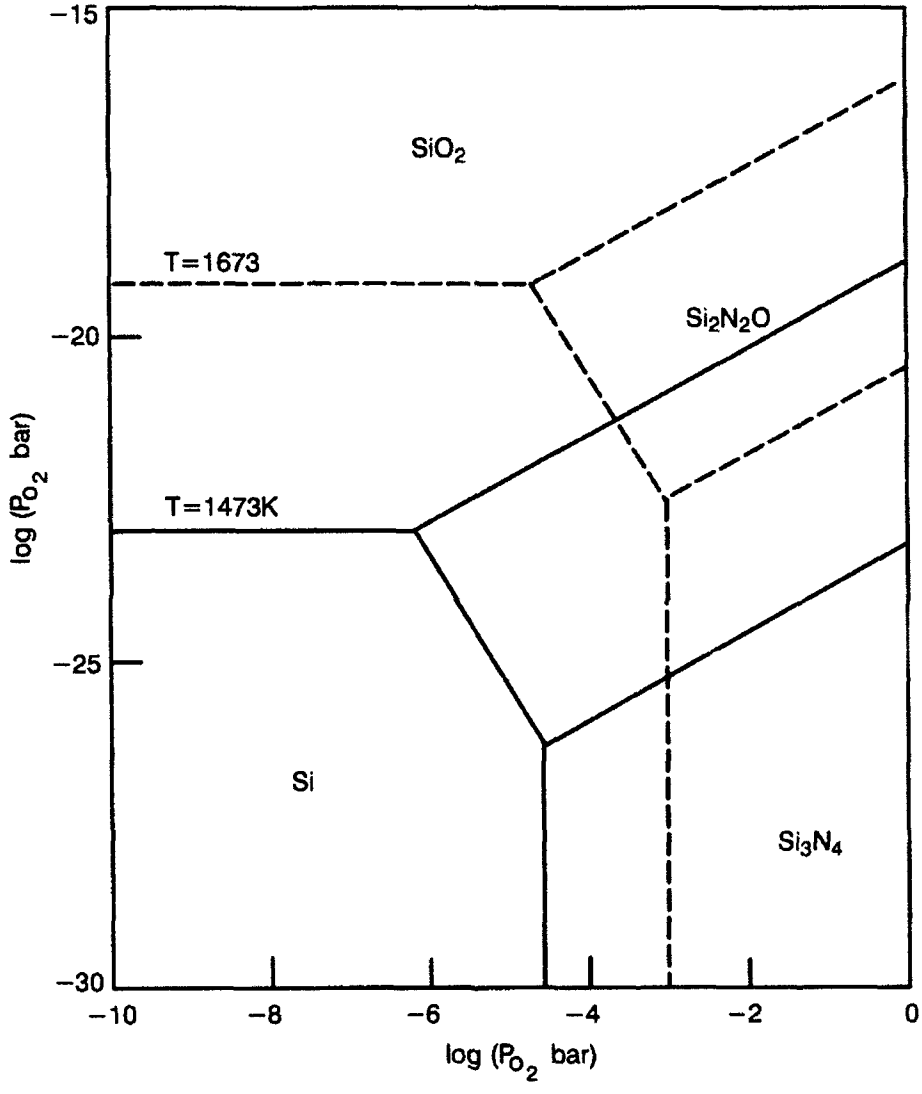

Fig. 4 Calculated Si-O-N Stability Diagrams at 1473K and 1673K

EP301-10-59

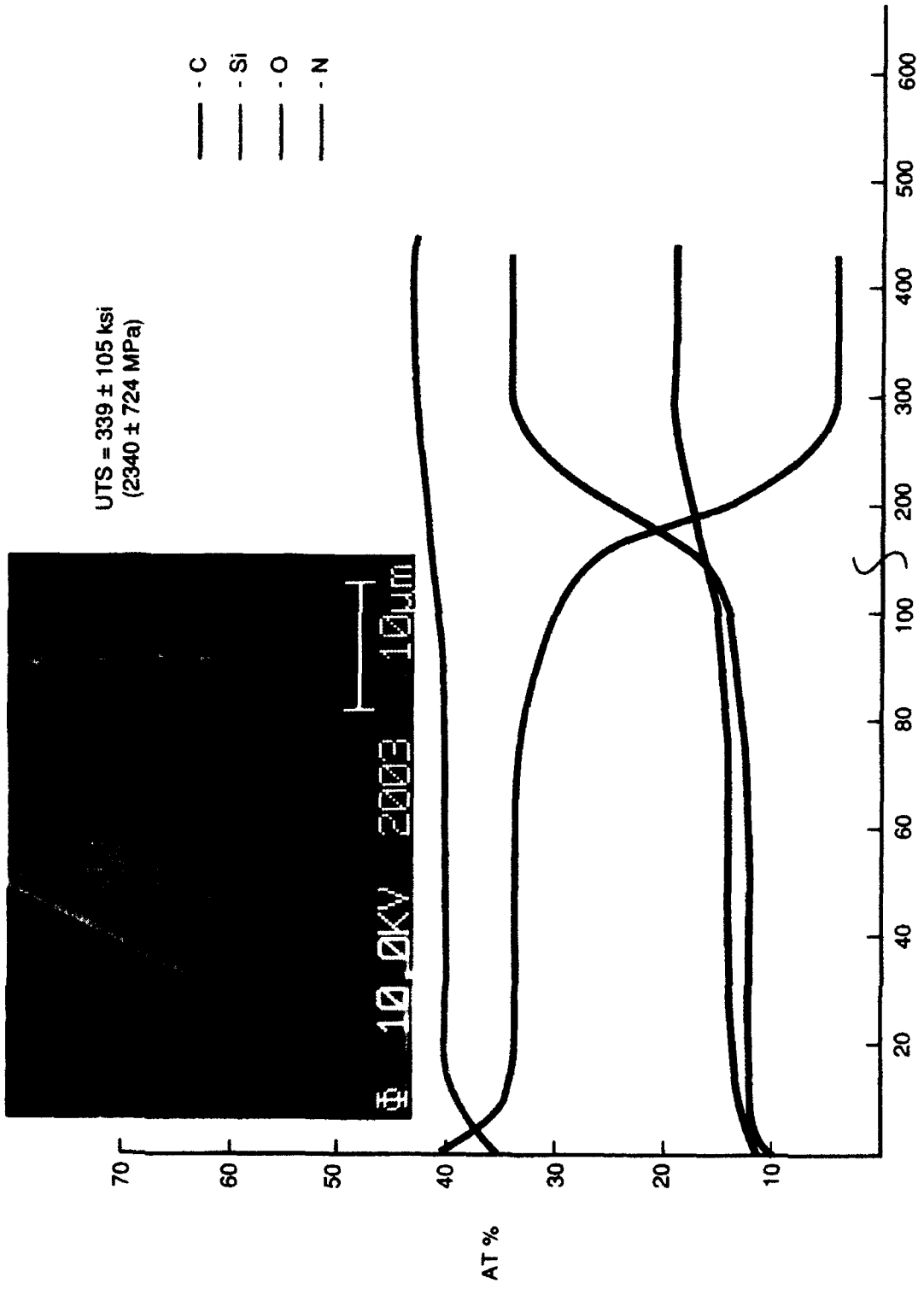

Fig. 5 SAM Depth Profile — Dow Corning HPZ Fiber - Lot #100173 - 1 As-Received

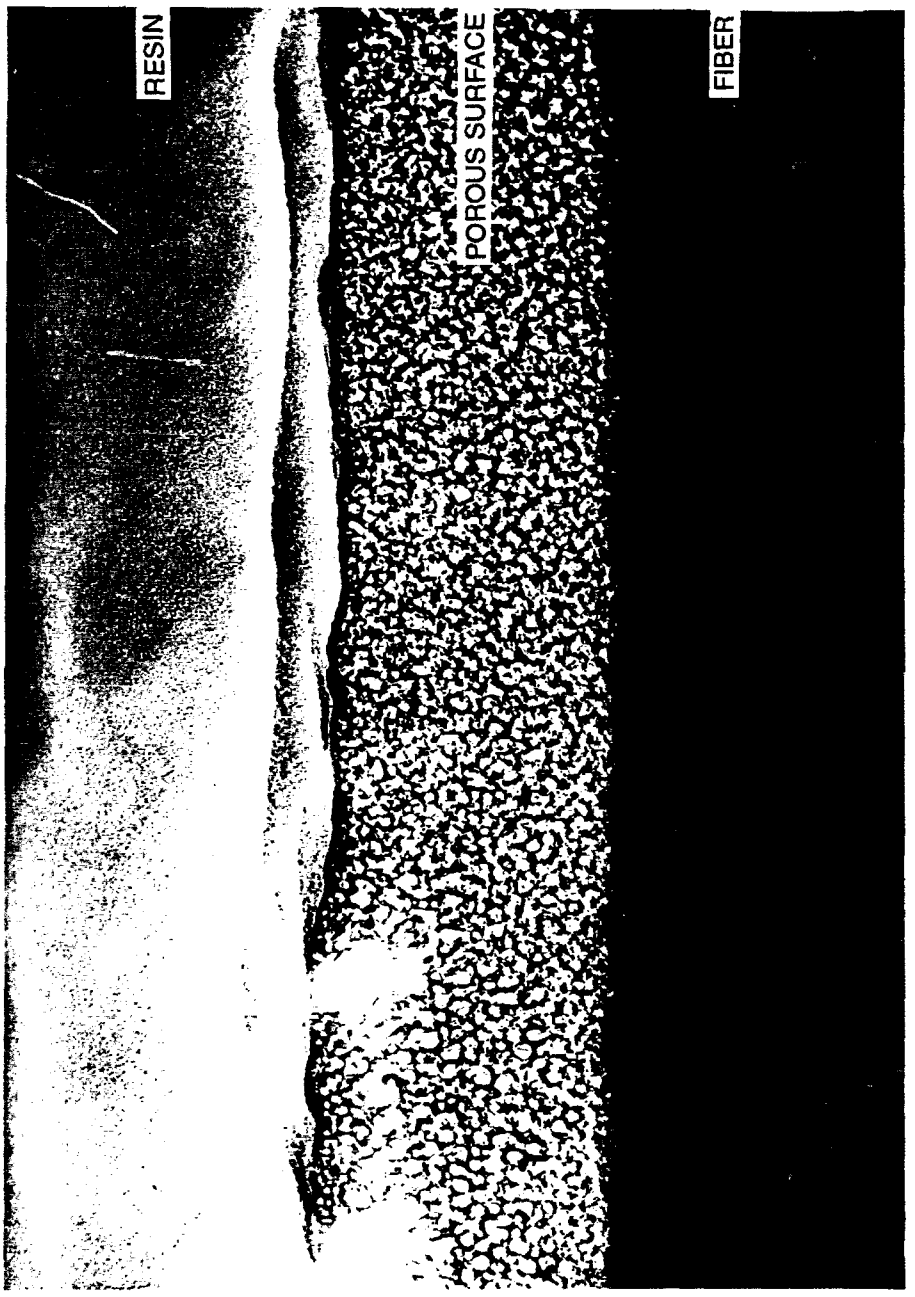

Fig. 6 TEM Thin Foil Characterization of Longitudinally Thinned Dow Corning HPZ Fiber-#100173-1

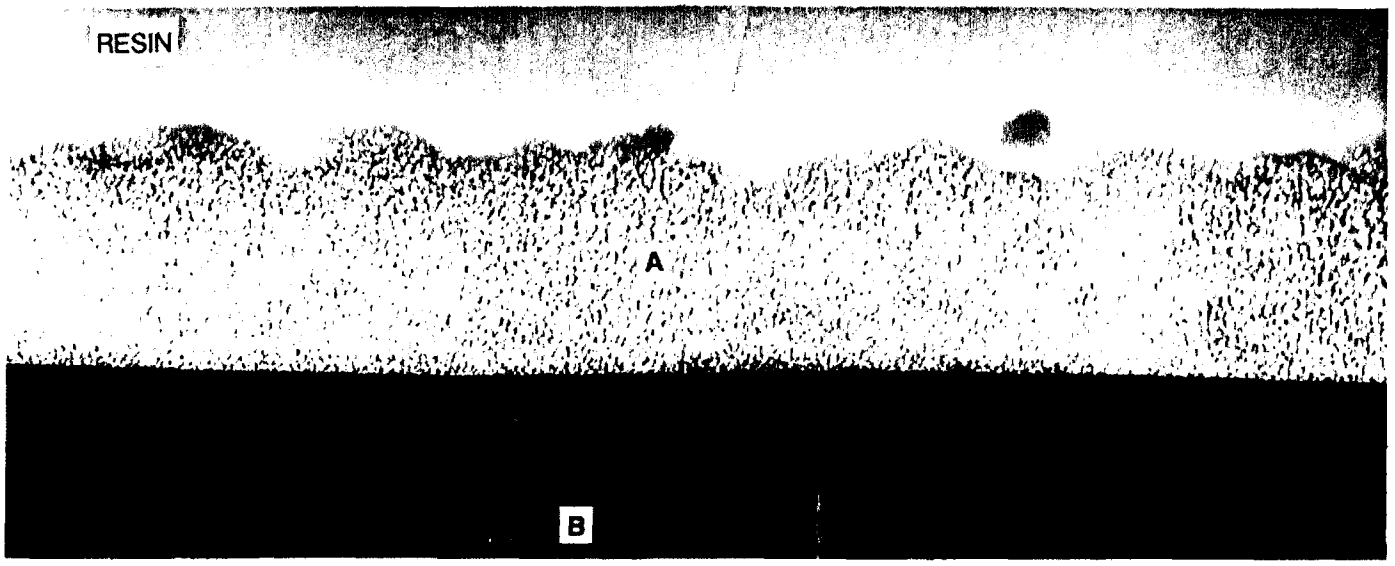

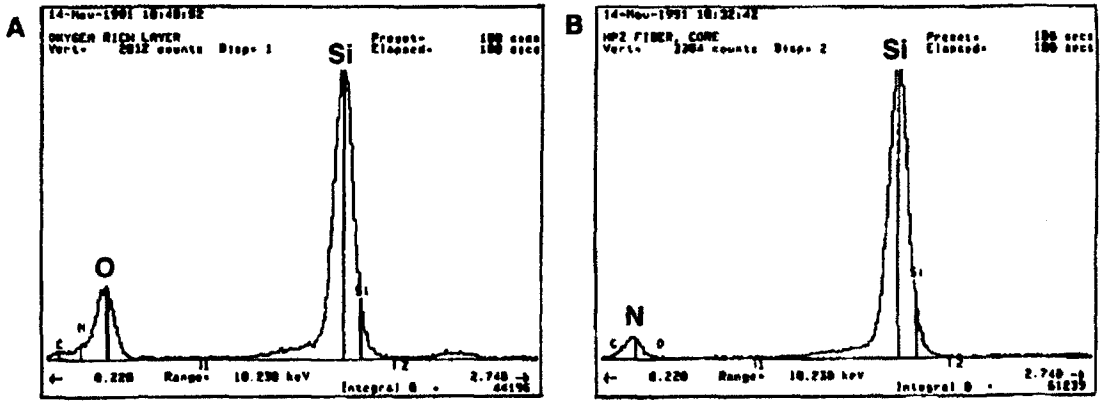

Fig. 7 TEM/EDX Thin Foil Characterization of Longitudinally Thinned Dow Corning HPZ Fiber #92372–16 (As–Received)

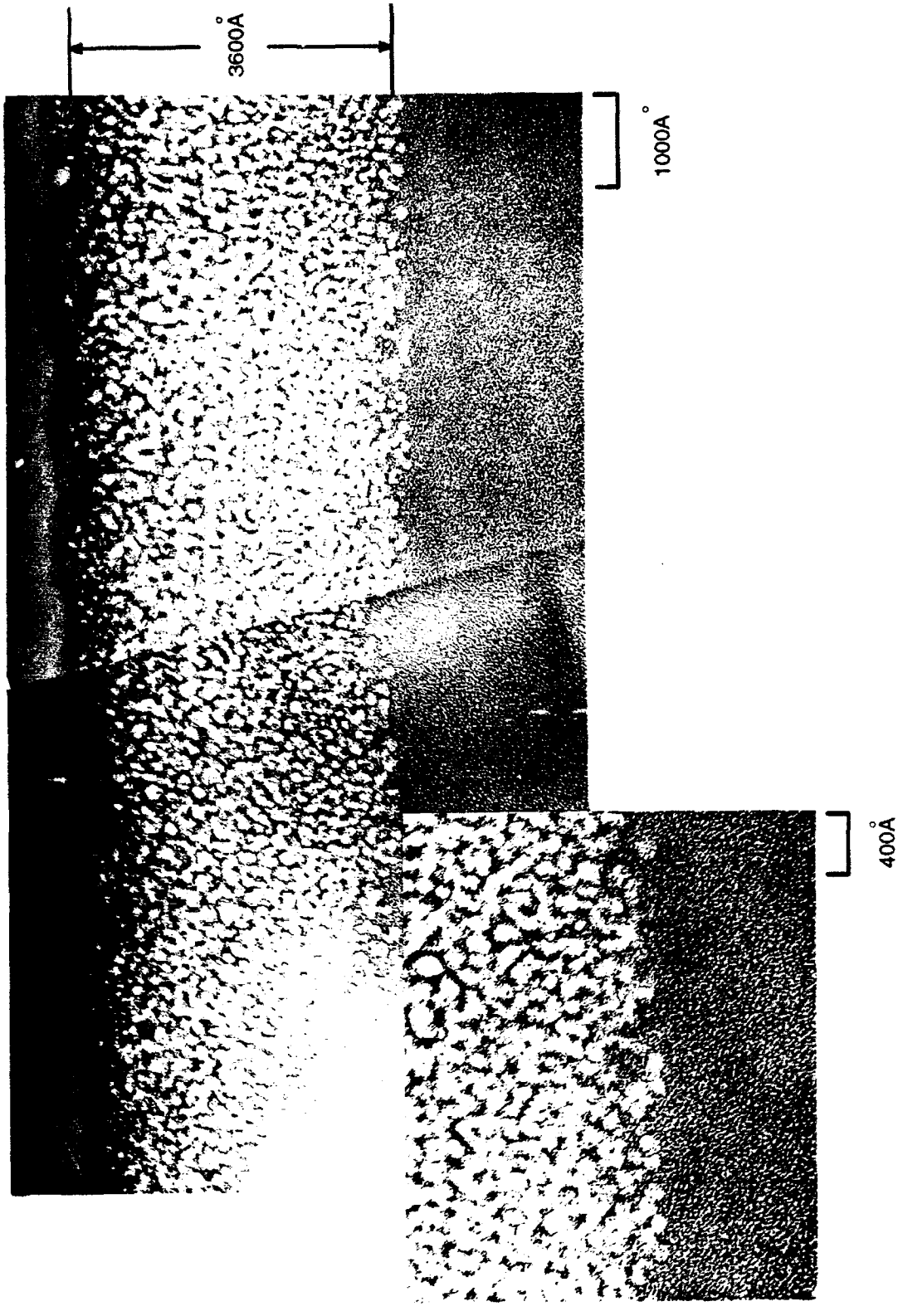

Fig. 8 TEM Thin Foil Characterization of Longitudinally Thinned Dow Corning HPZ Fiber #92372-16 (As Recieved)

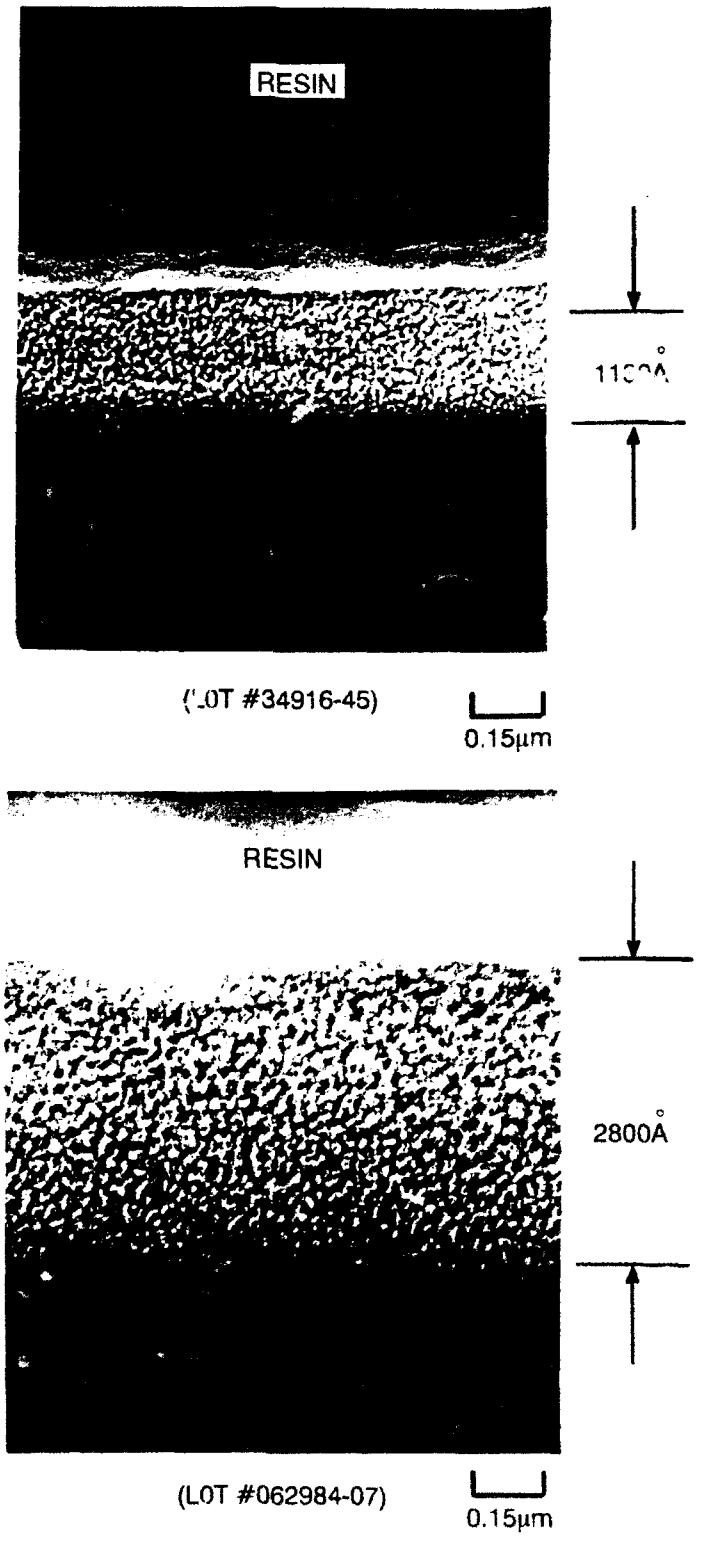

Fig. 9 **TEM Thin Foil Characterization of "Old" (Lot #34916-45) and "New " (Lot #062984-07) HPZ Fiber**

EP301-10-6

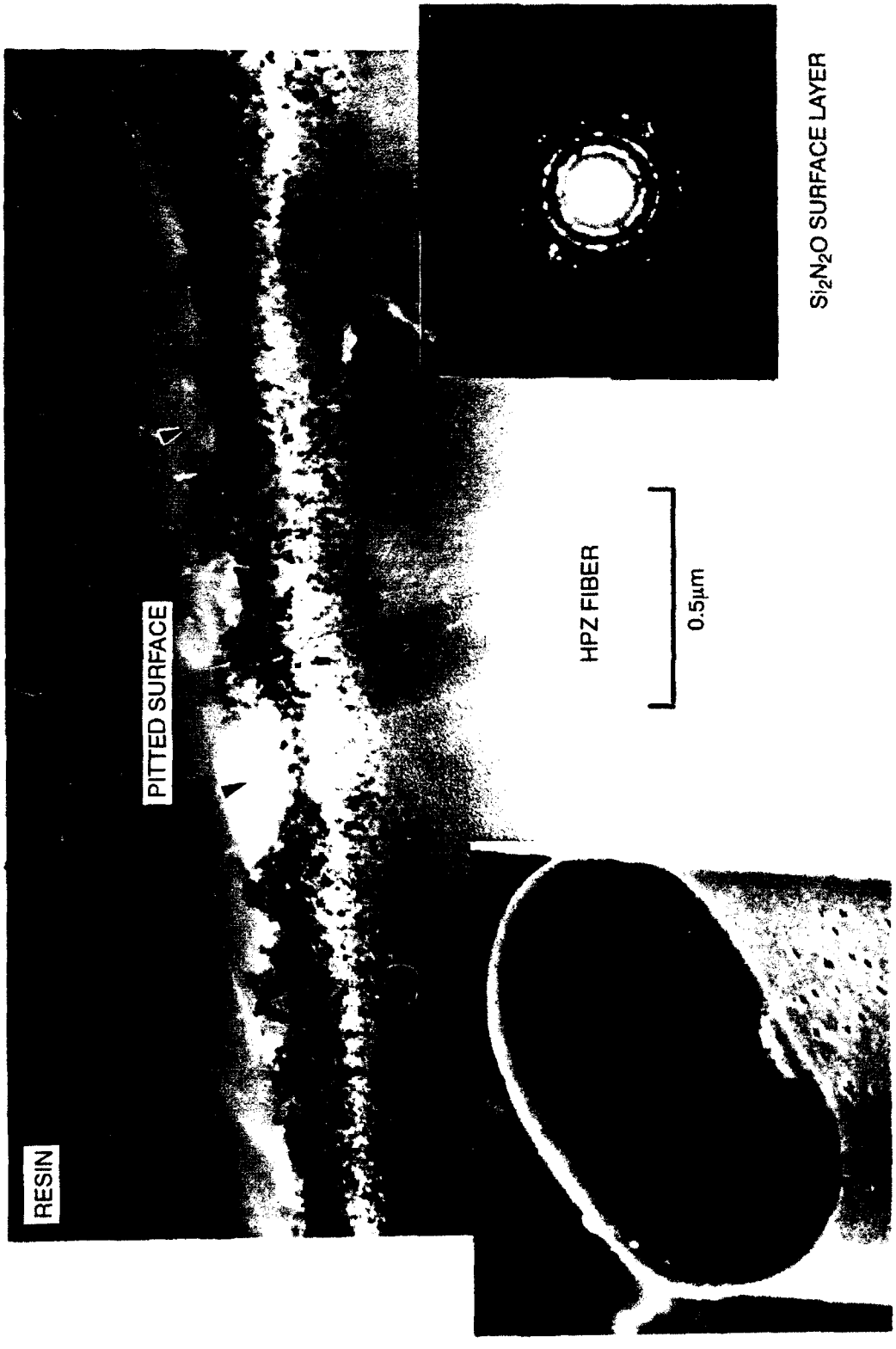

Fig. 10 TEM/SEM/SAED Analysis of HPZ Fiber (Si-C-O-N) Lot #03028013 (1430°C/10 min, N_2)

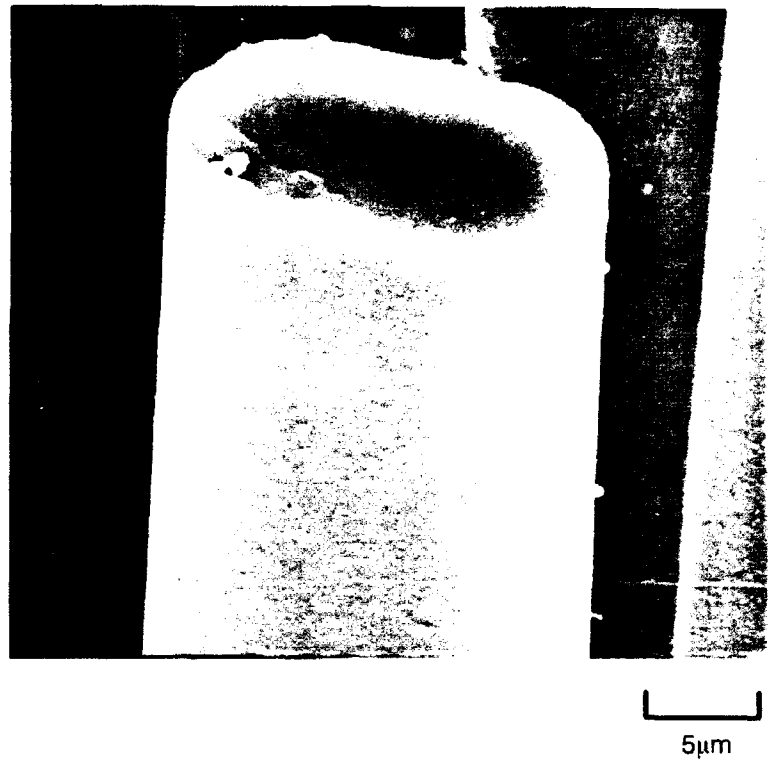

5μm

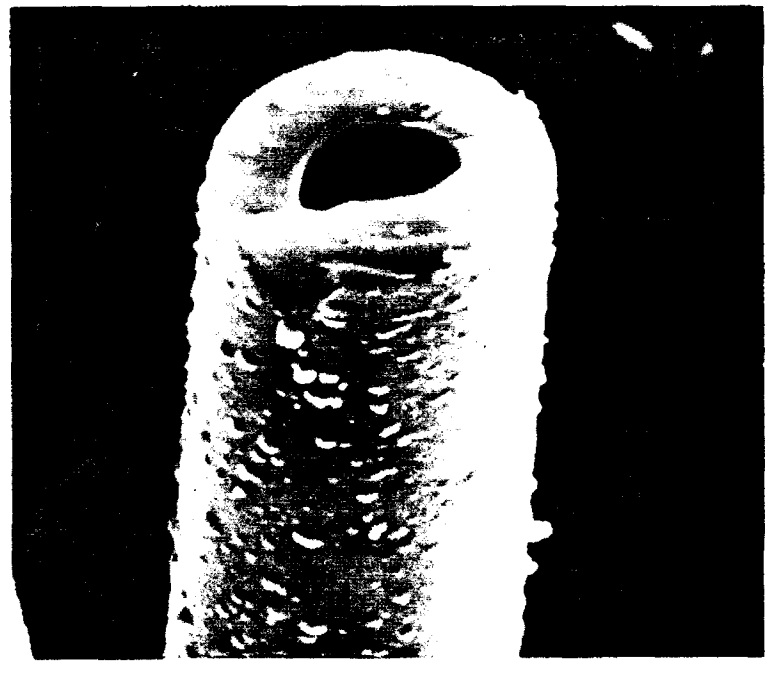

5μm

Fig. 11 3M SiC/BN Coated HPZ Fibers (Run #92172:57)

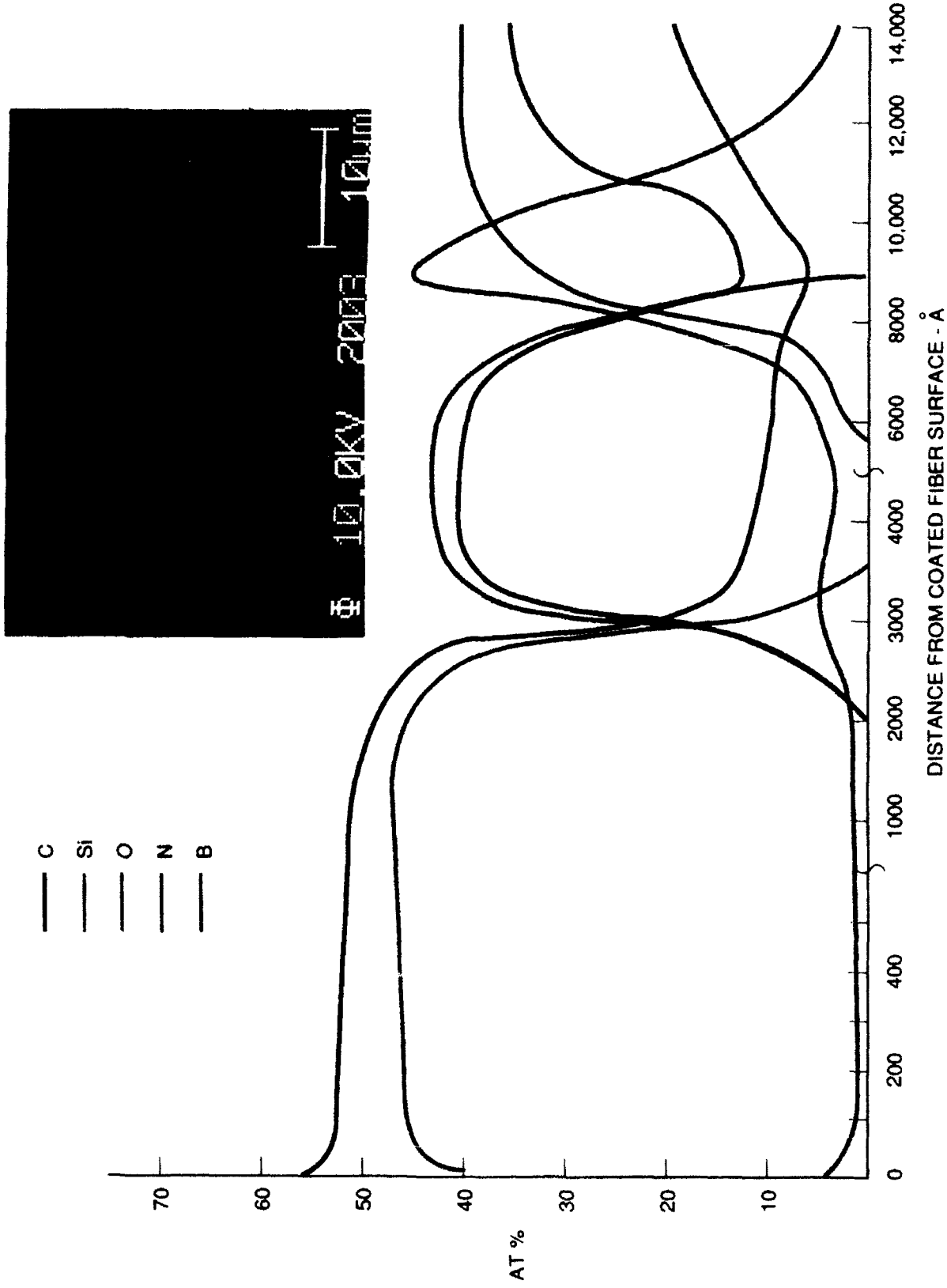

Fig. 12 SAM Depth Profile – SiC/BN Coated HPZ Fiber (9545-20-12) - Run #92172:57
UTS = 137 ± 47ksi (945 ± 324 MPa)

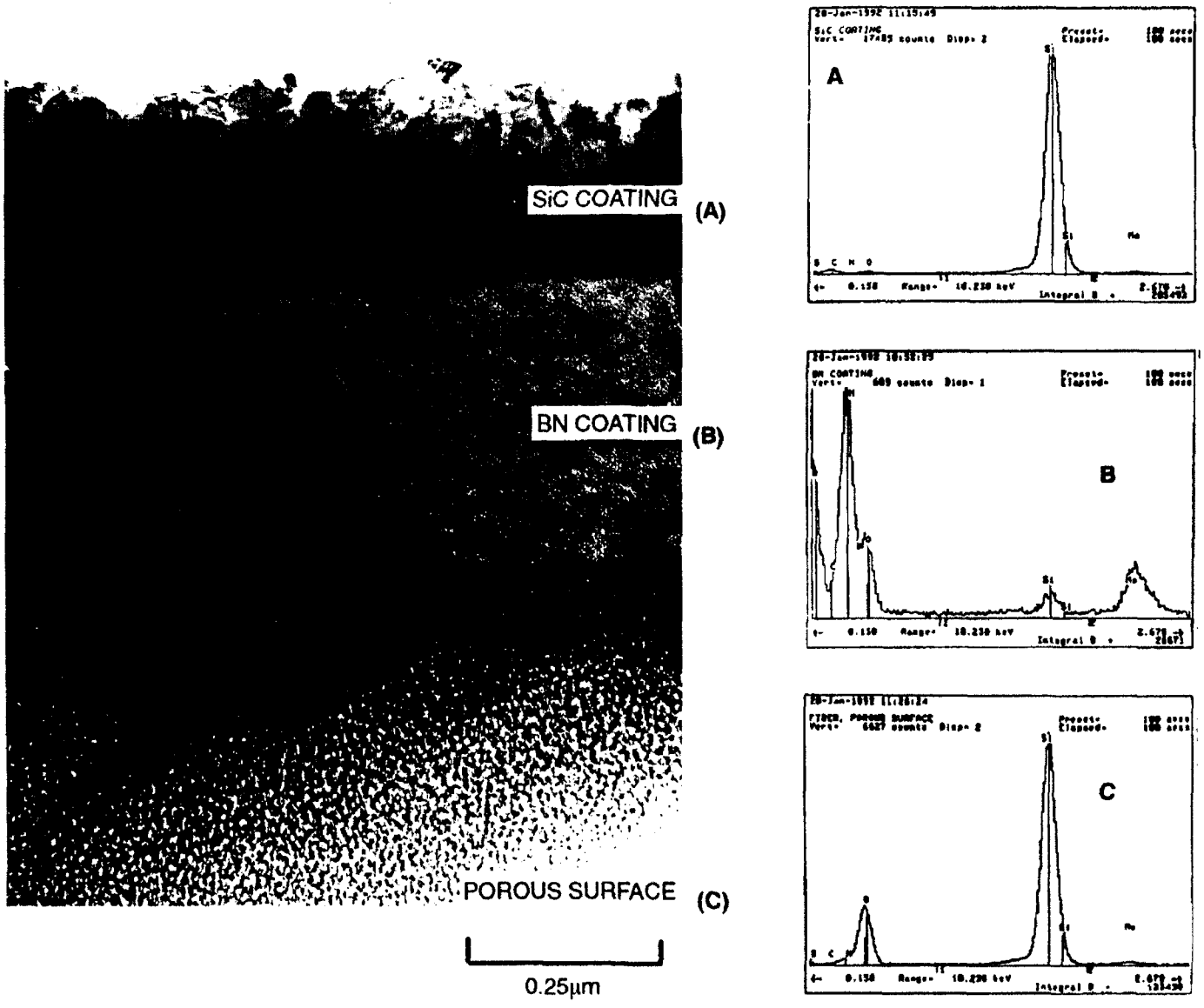

Fig. 13 TEM/EDX Thin Foil Characterization of Longitudinally Thinned SiC/BN Coated HPZ Fiber–#92172:57

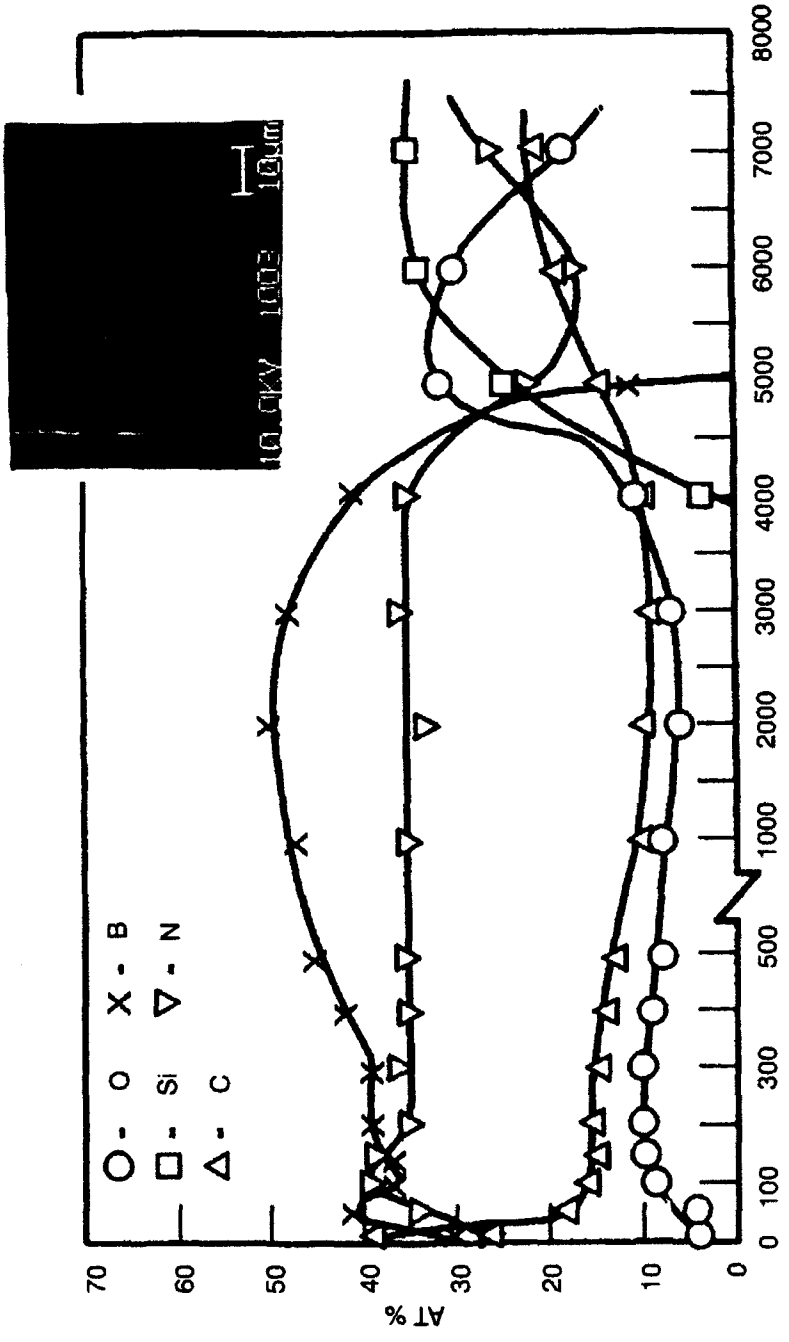

Fig. 14 SAM Depth Profile-BN COATED HPZ (9545-20-5A) FIBER (RUN #92171:56)
UTS = 286±142KSI (1989±850MPa)

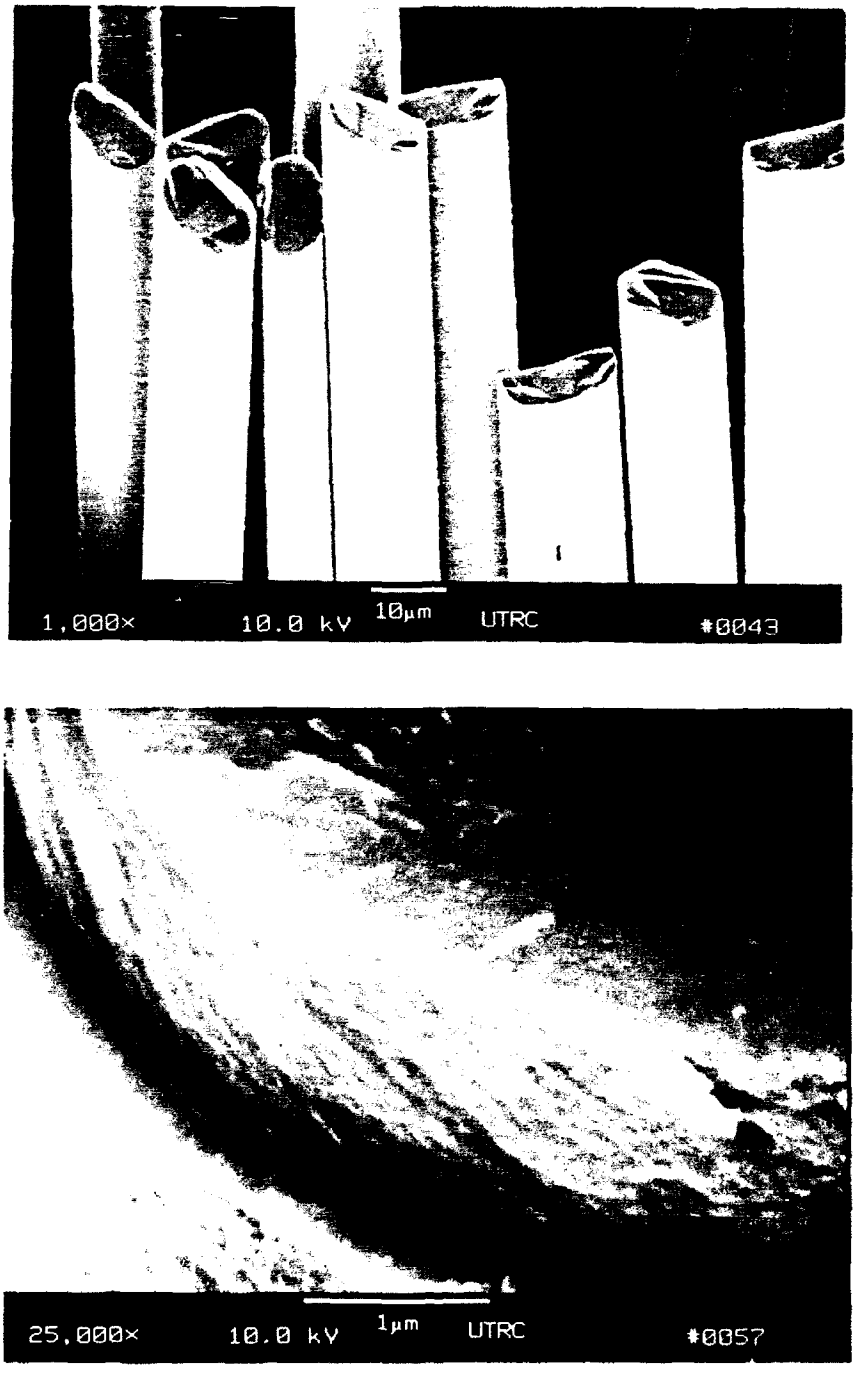

Fig. 15 3M SiC/BN Coated HPZ Fiber (Lot 92172:74)

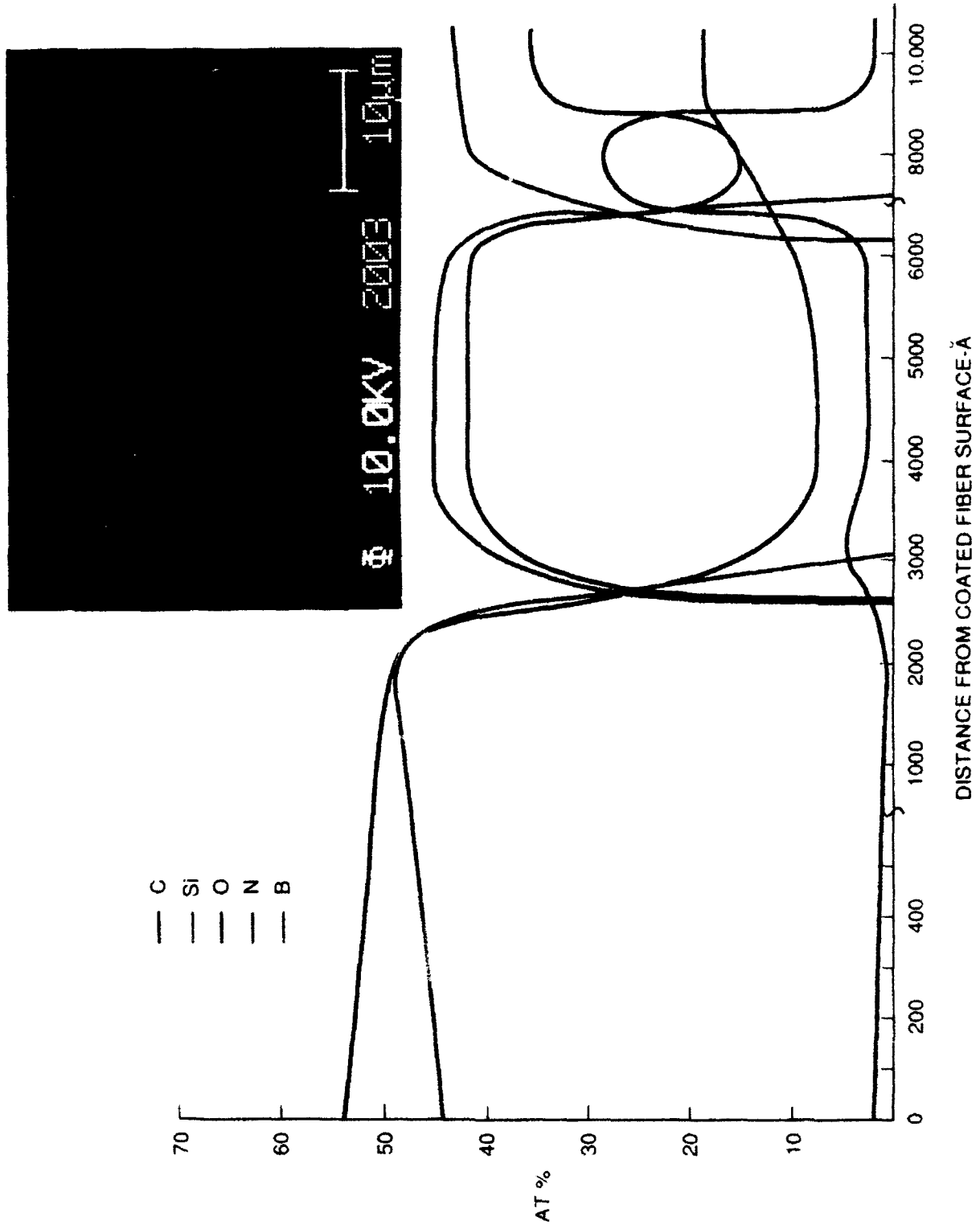

Fig. 16 SAM Depth Profile – SiC/BN/HPZ Fiber #92172:74 UTS = 244 ± 57ksi (1680 ± 394 MPa)

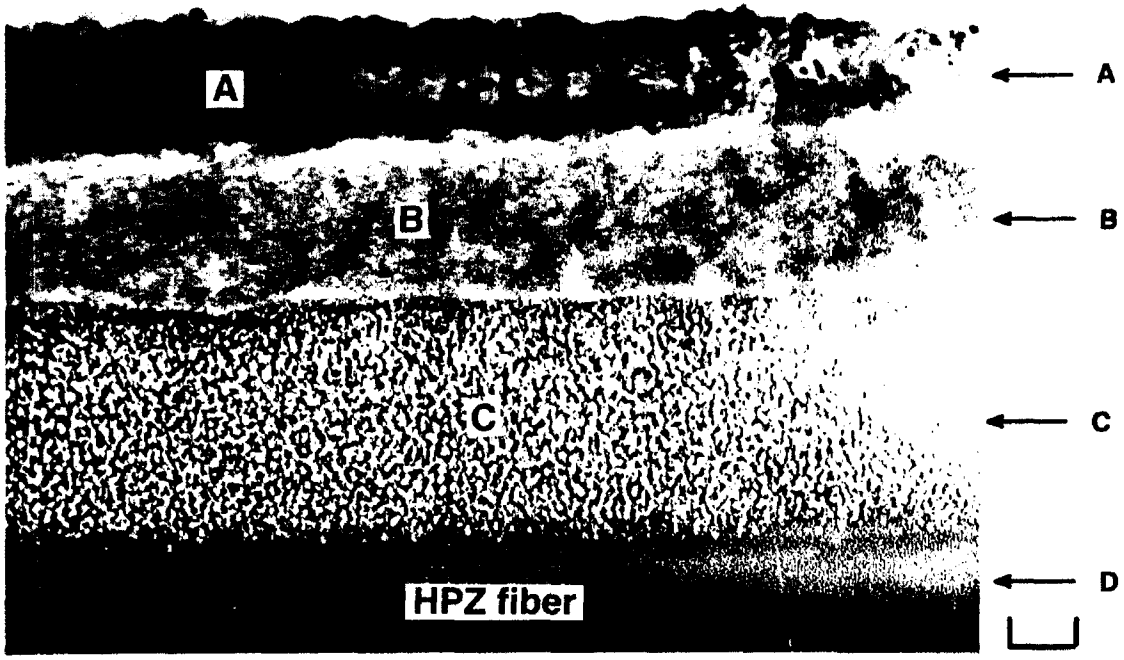

COATING THICKNESS (Å):

SiC	1956
BN	2174
POROUS ZONE	3043

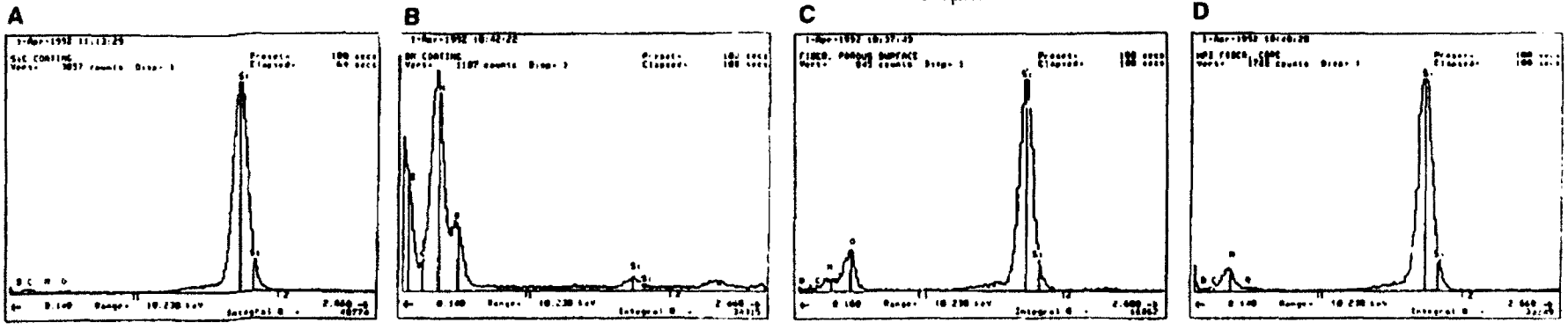

Fig. 17 TEM/EDX Thin Foil Characterization of SiC-BN Coated/HPZ Fiber (#92172:74)

(MOUNTED IN RESIN)

1μm

COATING THICKNESS:
SiC – 130 nm
BN – 155 nm

1μm

COATING THICKNESS
SiC –180 nm
BN – 670 nm

Fig. 18 TEM Replica Micrographs of SiC/BN Coated HPZ Fibers-Lot 92172:74

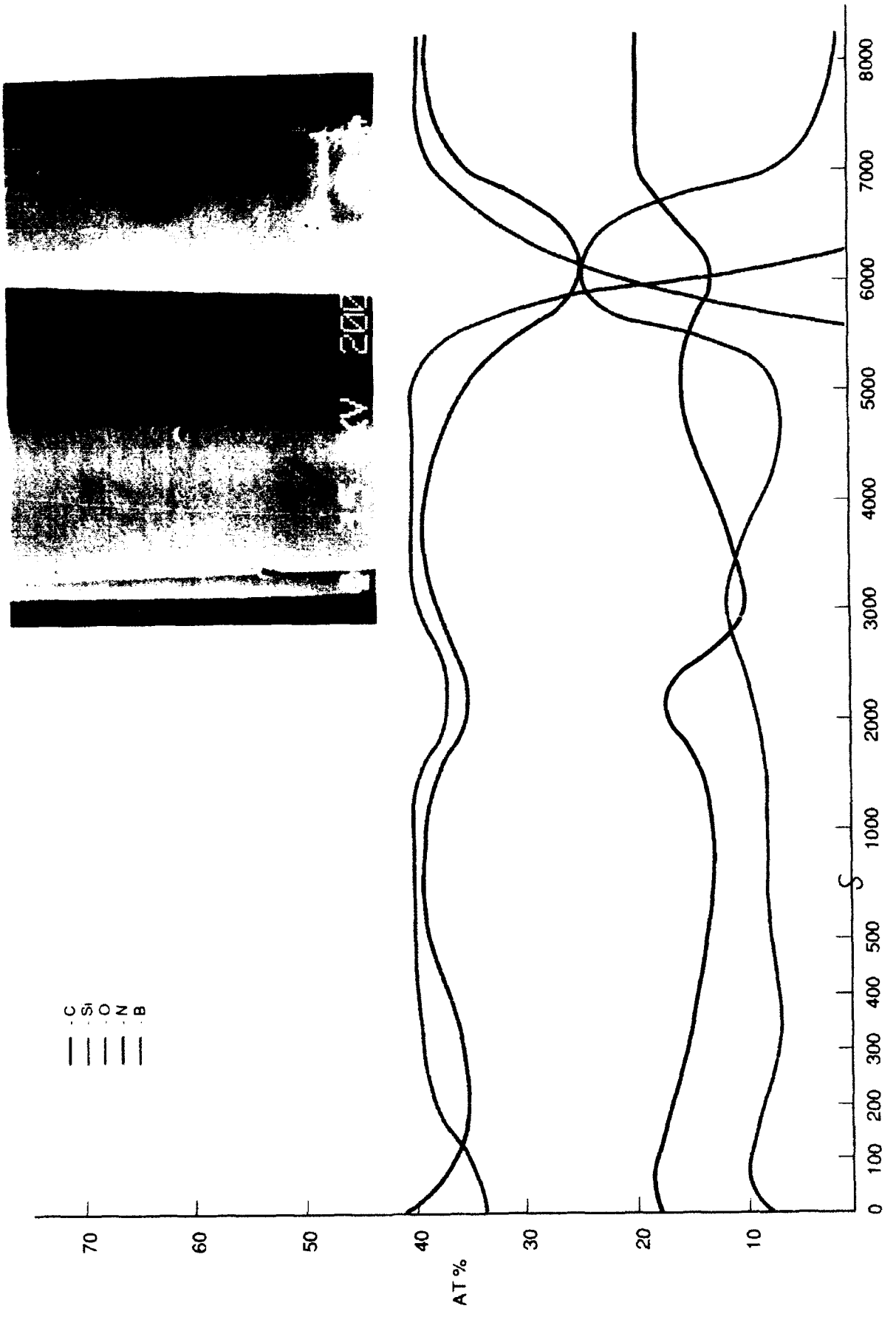

Fig. 19 SAM Depth Profile — 3M BN/HPZ Fiber (Lot 062984-07) #97037:23 UTS = 229 ± 101ksi (1578 ± 699 MPa)

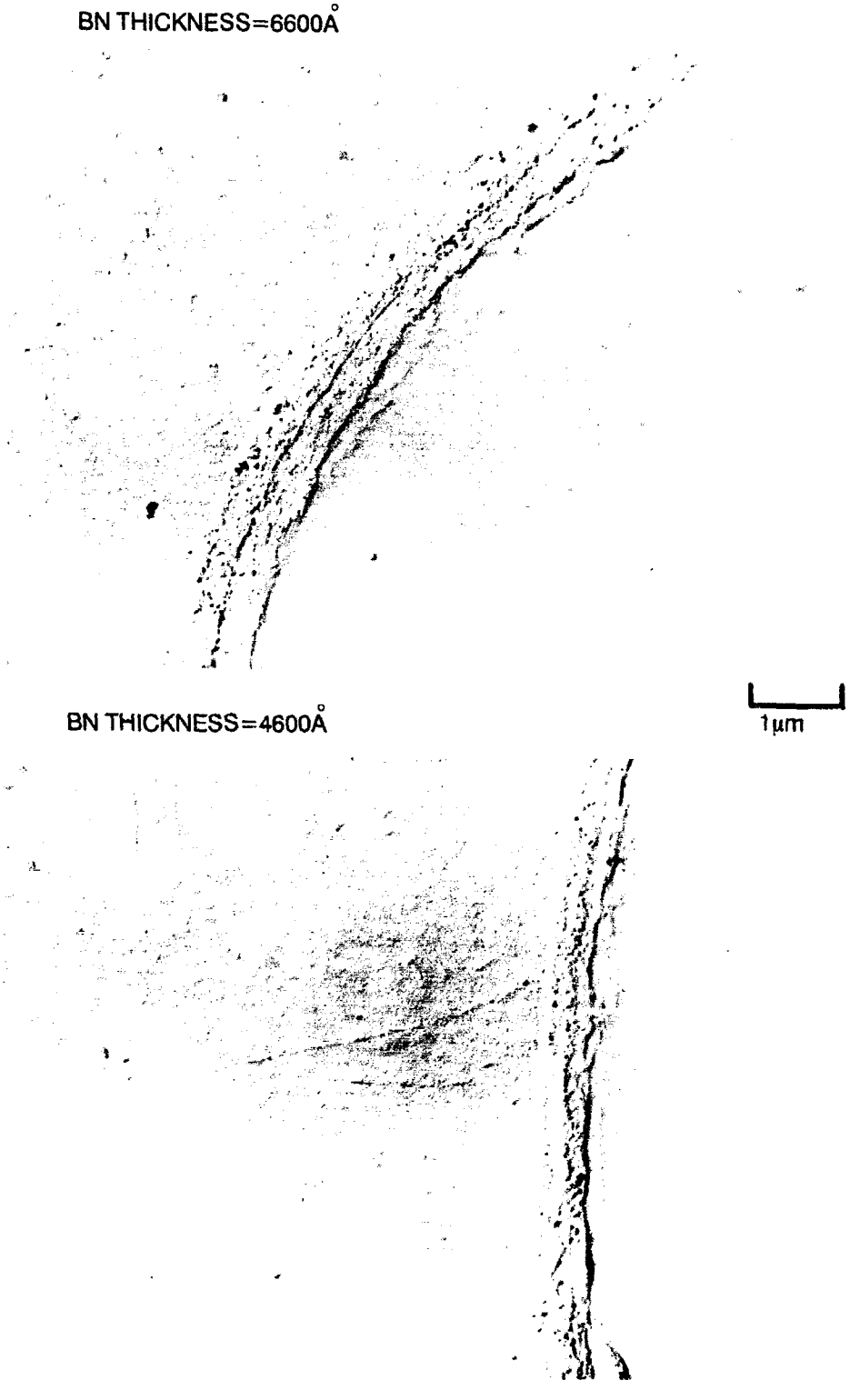

Fig. 20 TEM Micrographs of Transversely Sectioned BN Coated/HPZ Fibers Mounted in Resin-Lot#97037:23

EP301-10-33

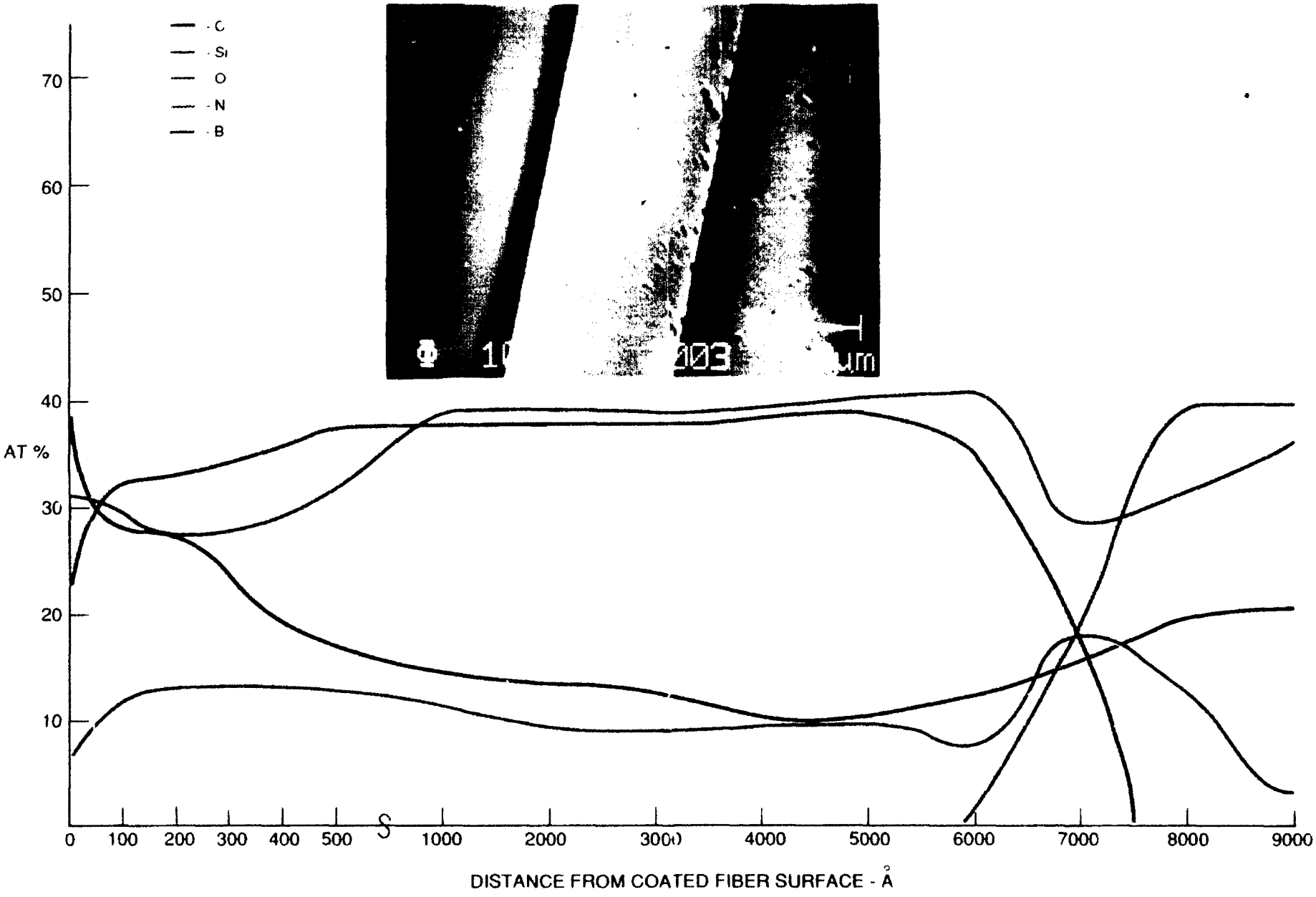

Fig. 21 SAM Depth Profile — 3M BN Coated HPZ Fiber (062984-07) - Lot #97037:69-1 UTS = 248 ± 60ksi (1710 ± 413 MPa)

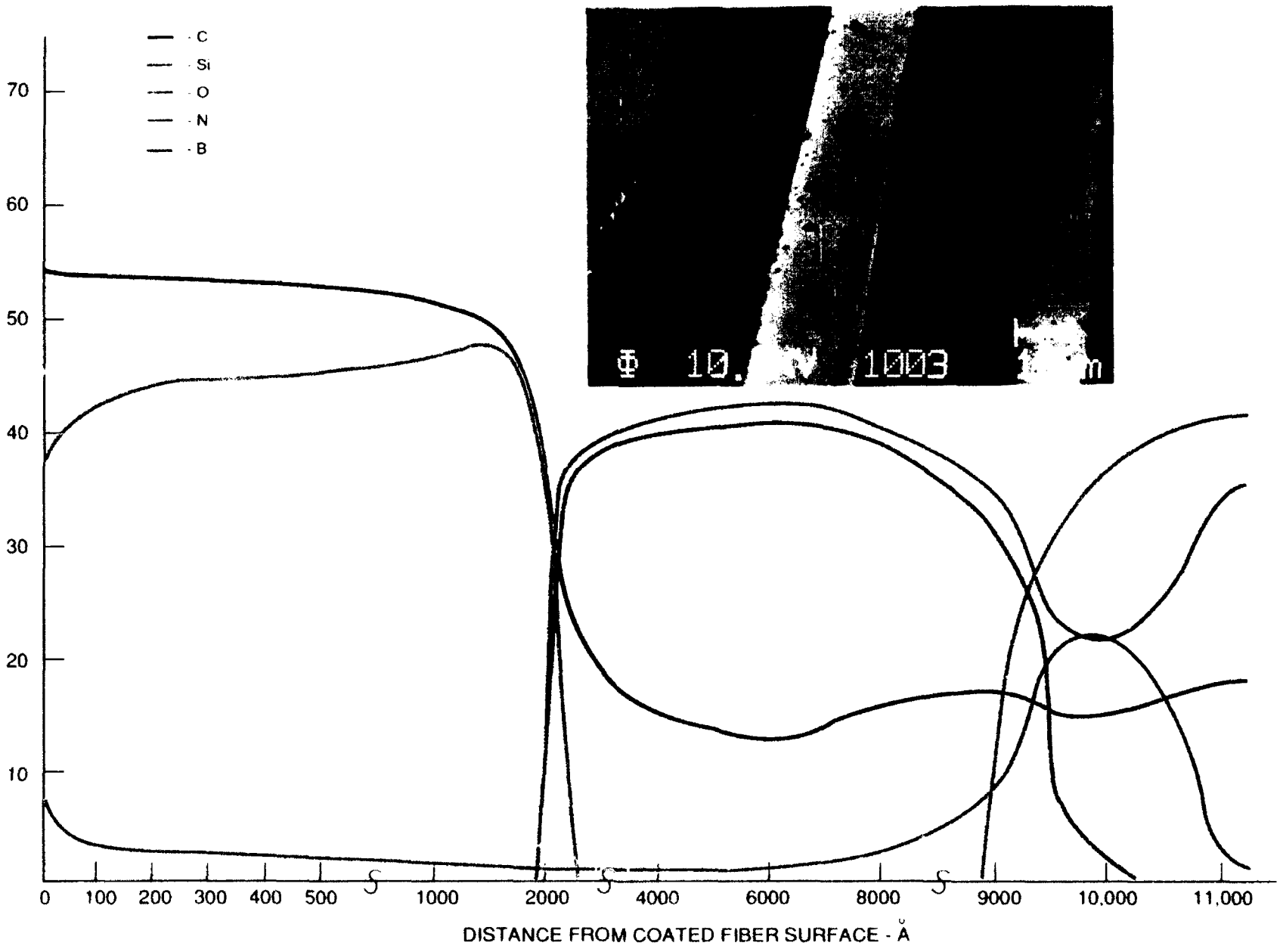

Fig. 22 SAM Depth Profile – 3M SIC over BN Coated HPZ Fiber (062984-07) - Lot #97037:69-2 UTS = 172 ± 40ksi (1185±278 MPa)

1000μm

10μm

Fig. 23 RT Fracture Surface of BMAS Matrix/HPZ Fiber Composite #349-91

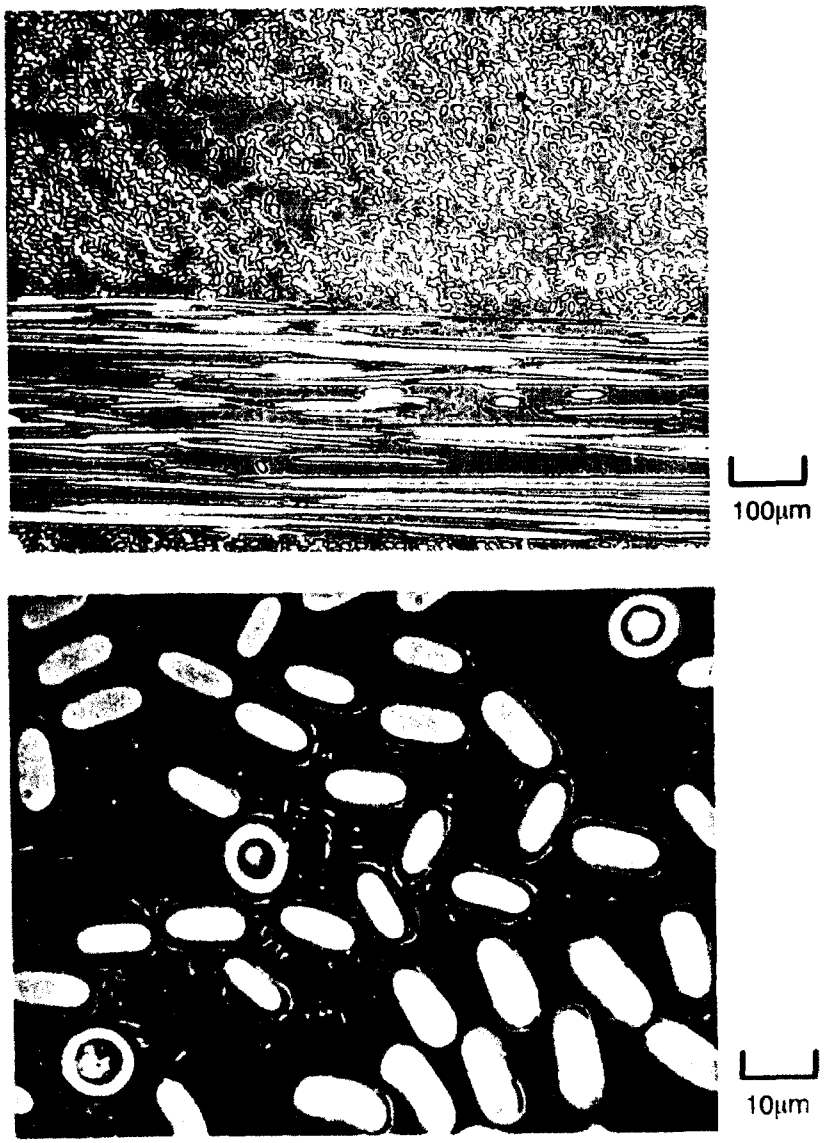

R93-970104-2

Fig. 24 Optical/TEM Replica Characterization of Transverse Sections of BMAS/HPZ (#9545-20-12) Composite #349-91, As-Pressed

EP301-10-9

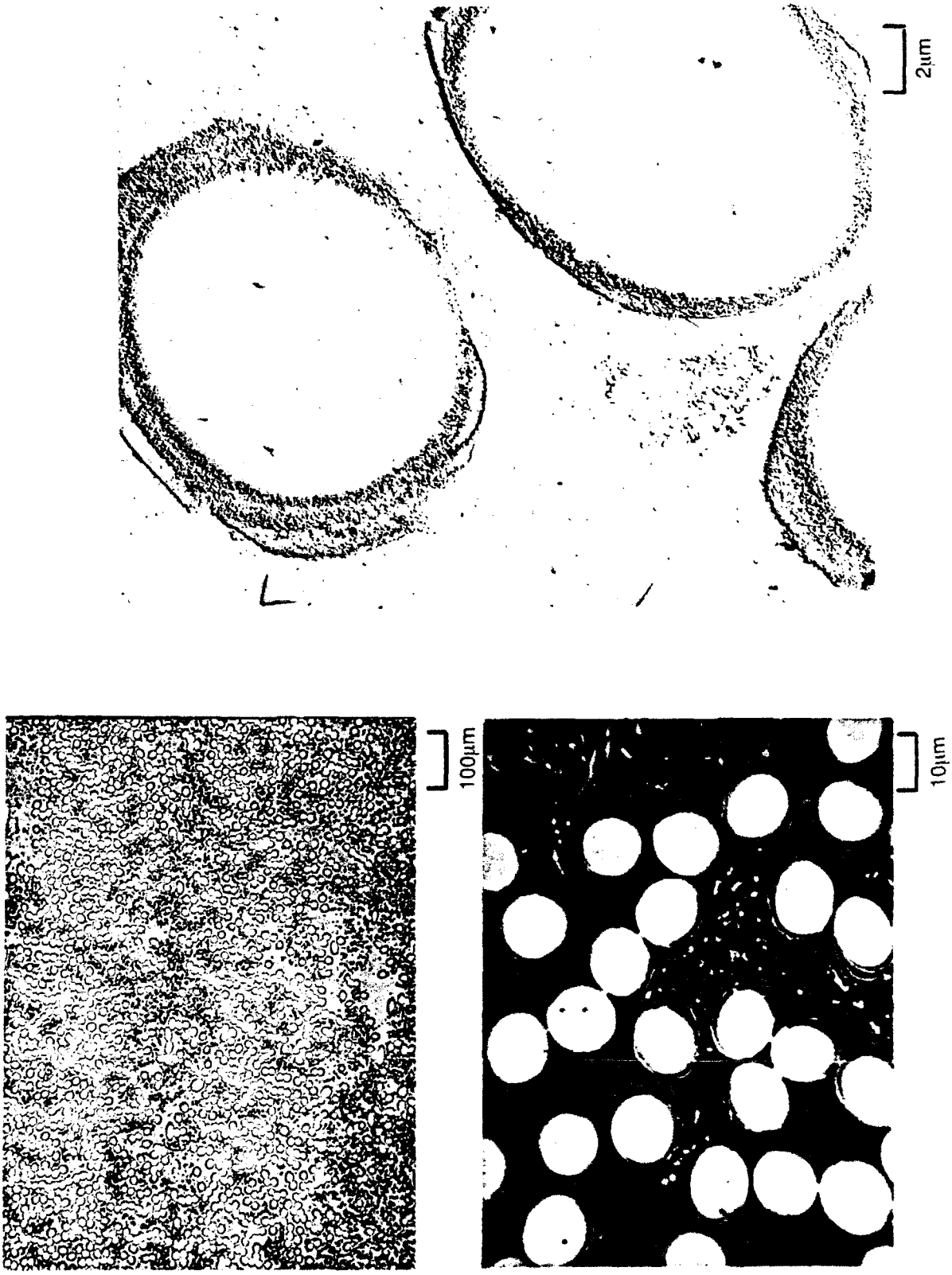

Fig. 25 Optical/TEM Replica Micrographs of Transversely Sectioned BMAS/HPZ "Old Vintage" Fiber (Lot#34916-45-3) Composite-#245-92-2 (As-Pressed)

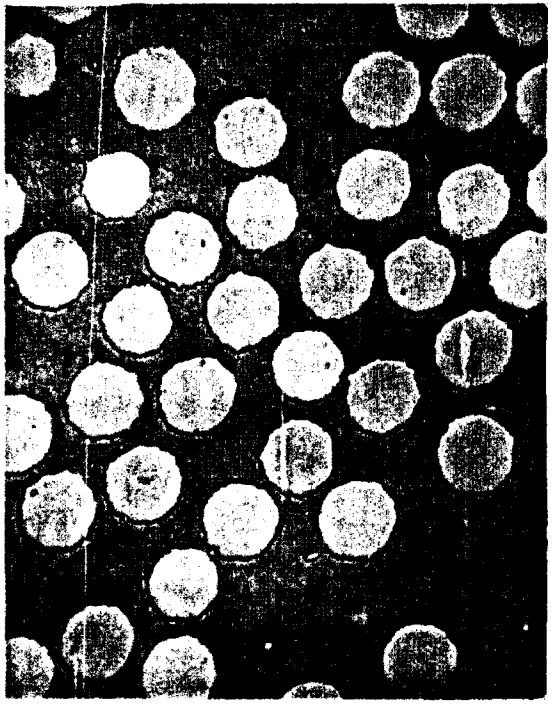

Fig. 26 Optical/TEM Replica Micrographs of Transversely Sectioned BMAS/TONEN Si_3N_4 Fiber Composite-#269-92 (As-Pressed)

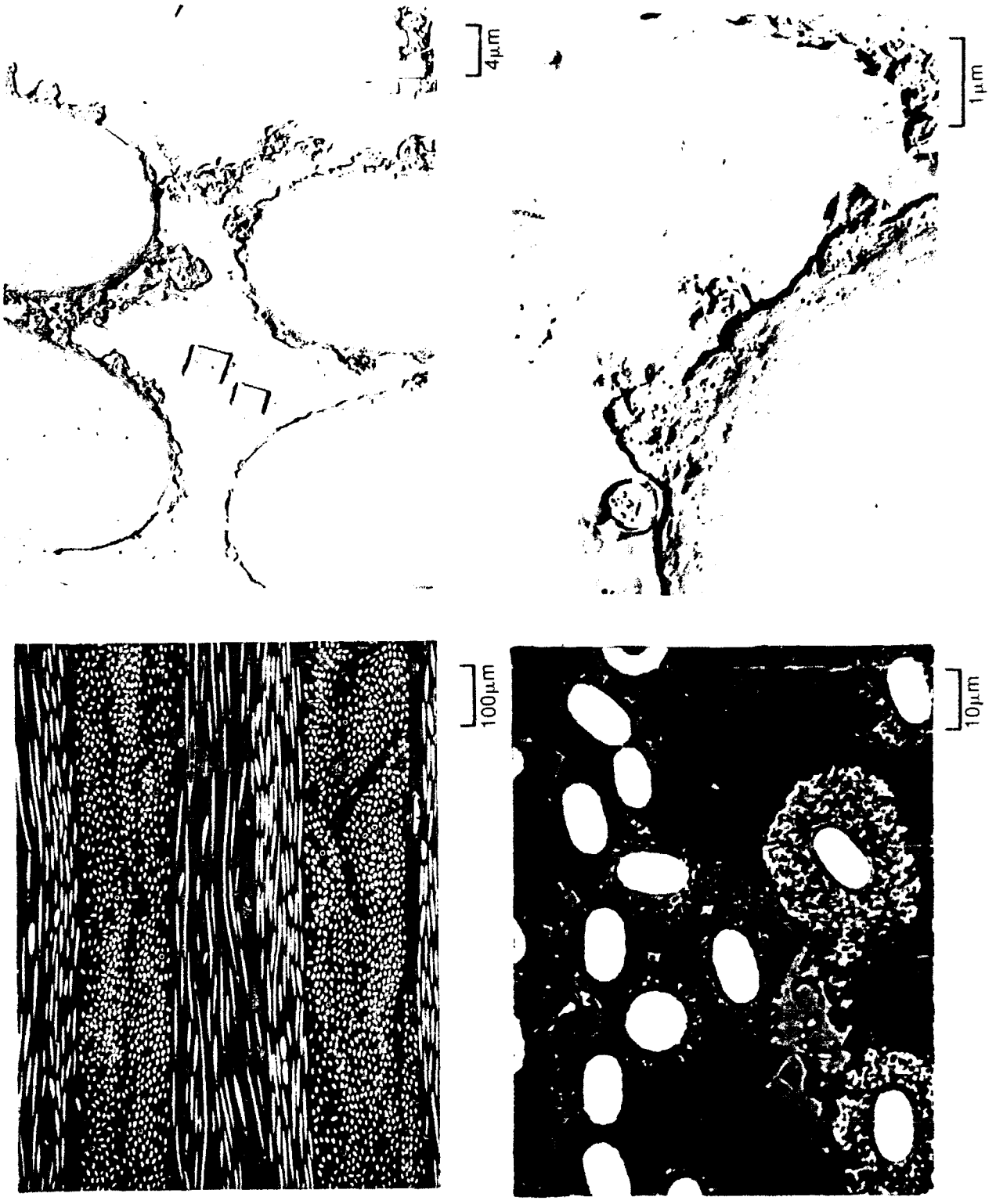

Fig. 27 Optical/TEM Characterization of BMAS Matrix BN Coated HPZ Si-N-C) Dow Corning Fiber - (As-Pressed) Composite #5-91

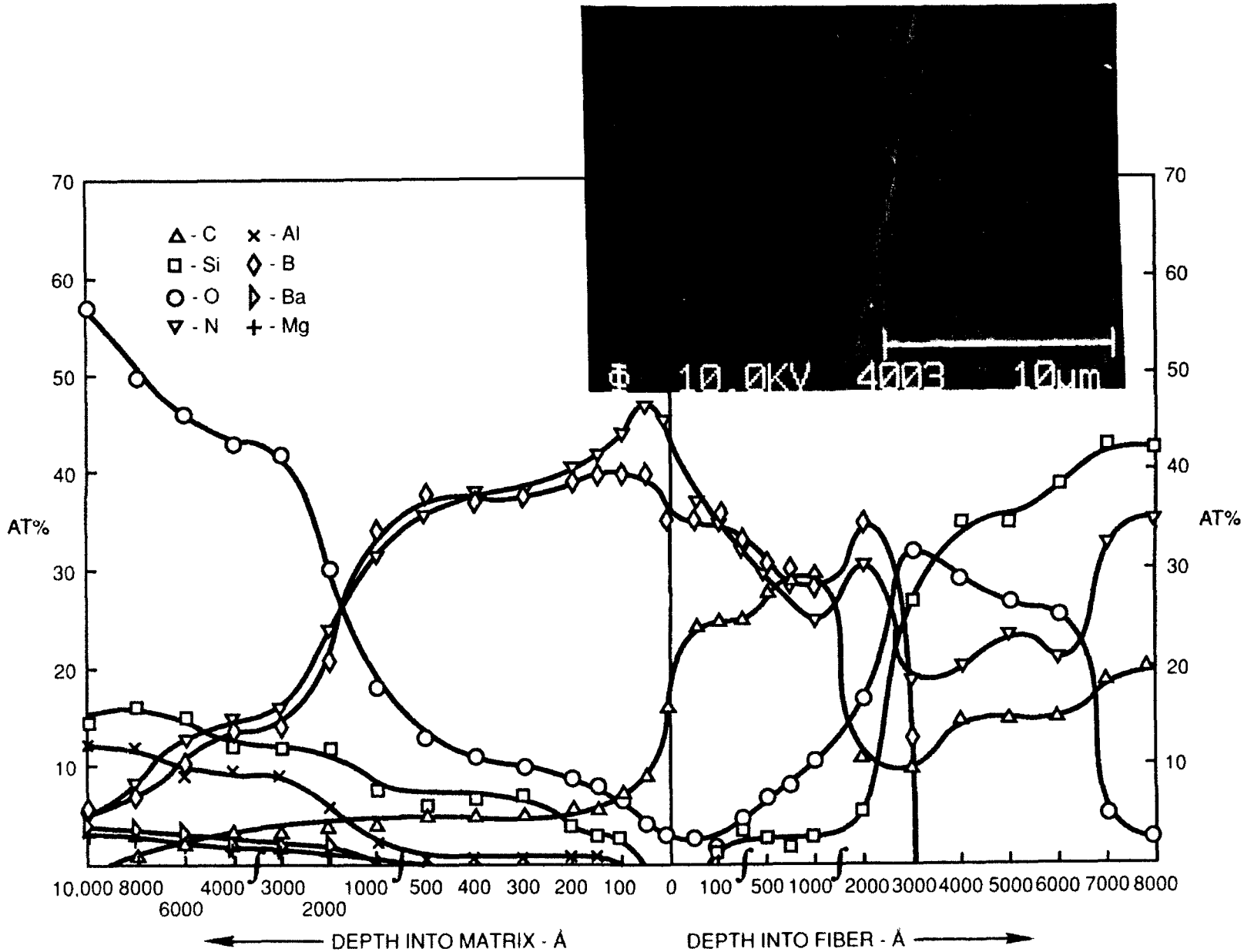

Fig. 28 SAM Depth Proofile – Interfacial Chemistry of BMAS Matrix/3M BN Over HPZ Fiber Composite #5-91

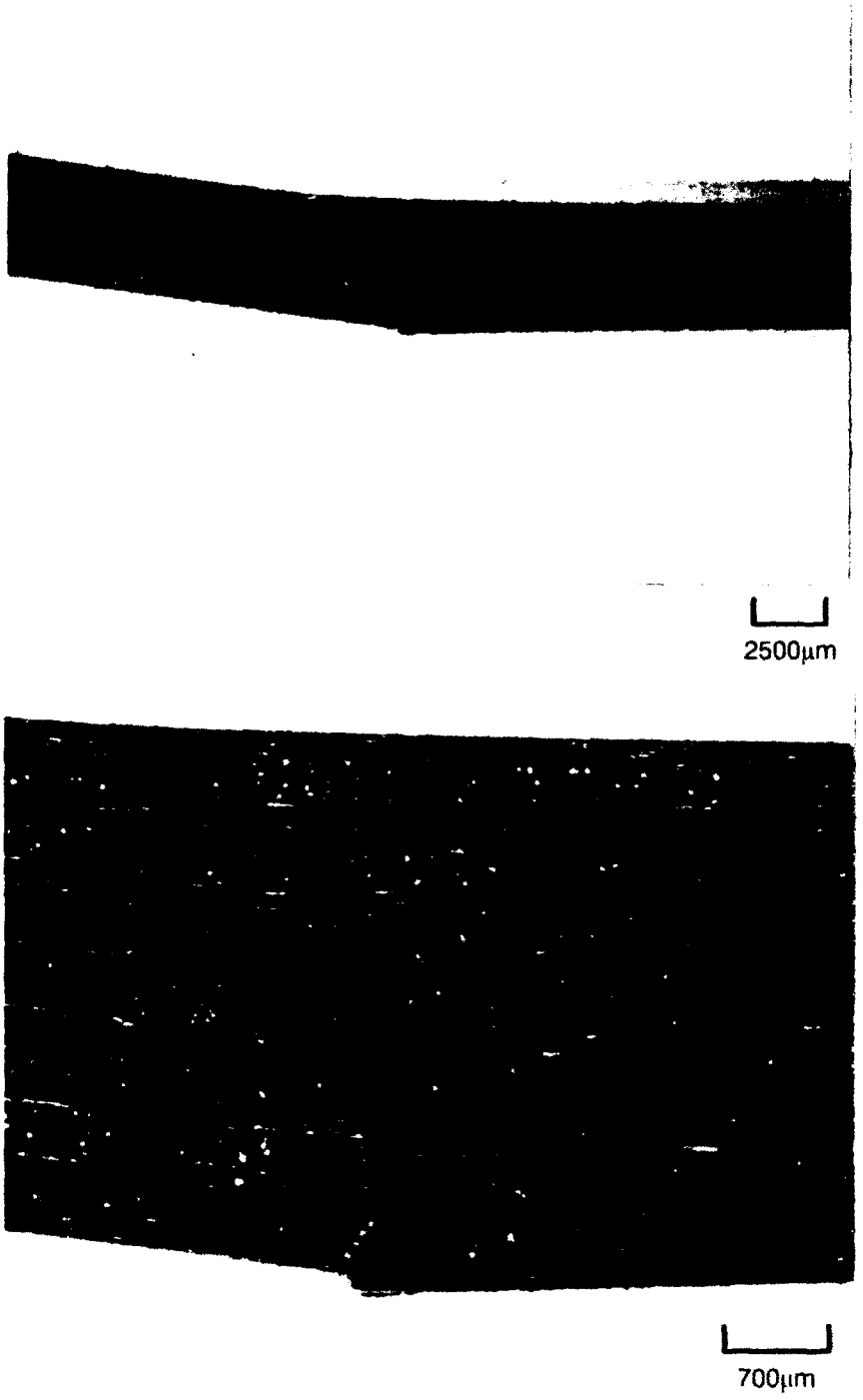

Fig. 29 RT 3-PT Flexural Fracture Mode of BMAS Matrix/BN Coated HPZ Fiber Composite #415-91 (Ceramed)

EP301-10-17

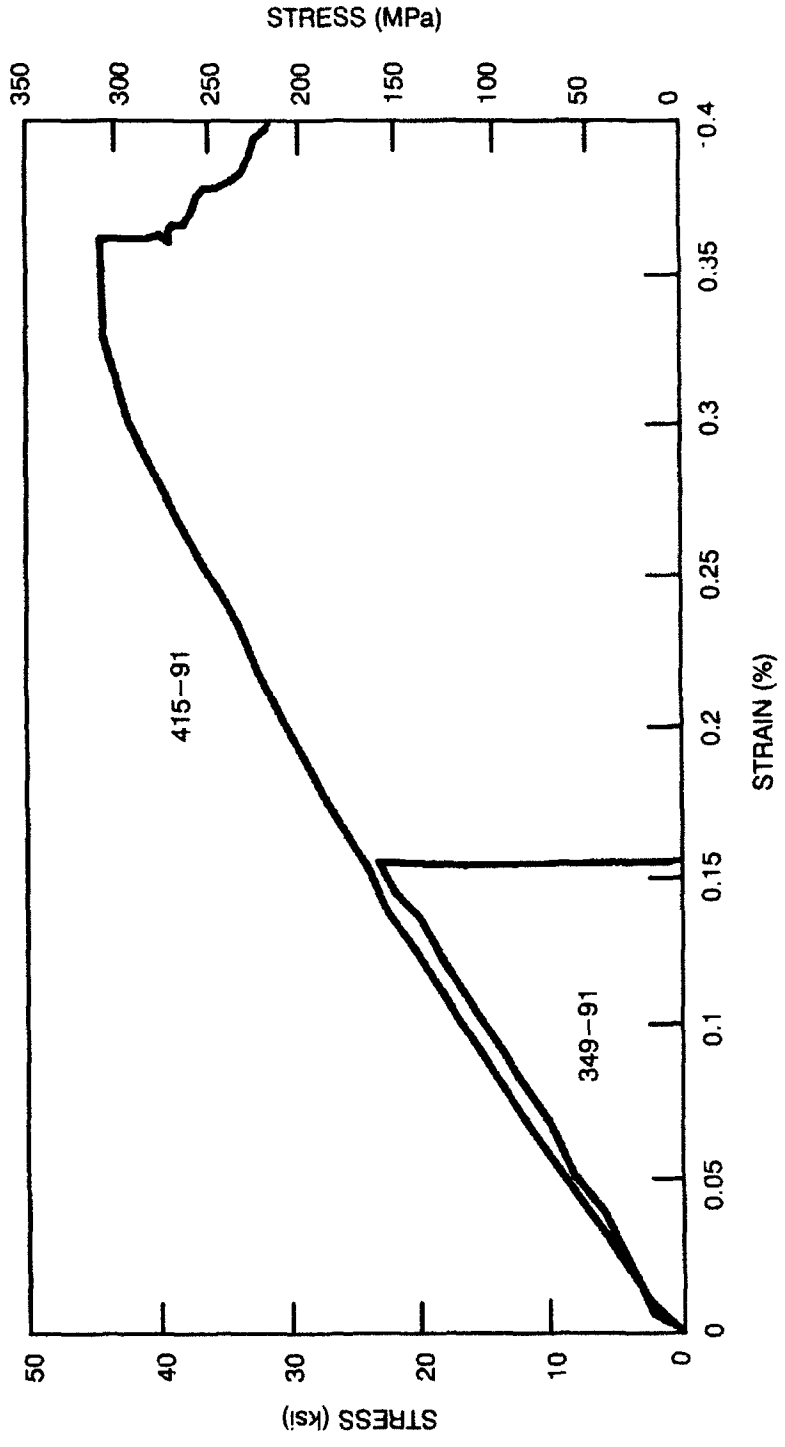

Fig. 30 RT3-pt Flexural Calculated Stress vs. Strain Curves for BMAS/HPZ Fiber Composites (With (#415-91) and without (#349-91) BN Fiber/Matrix Interfacial Layers)

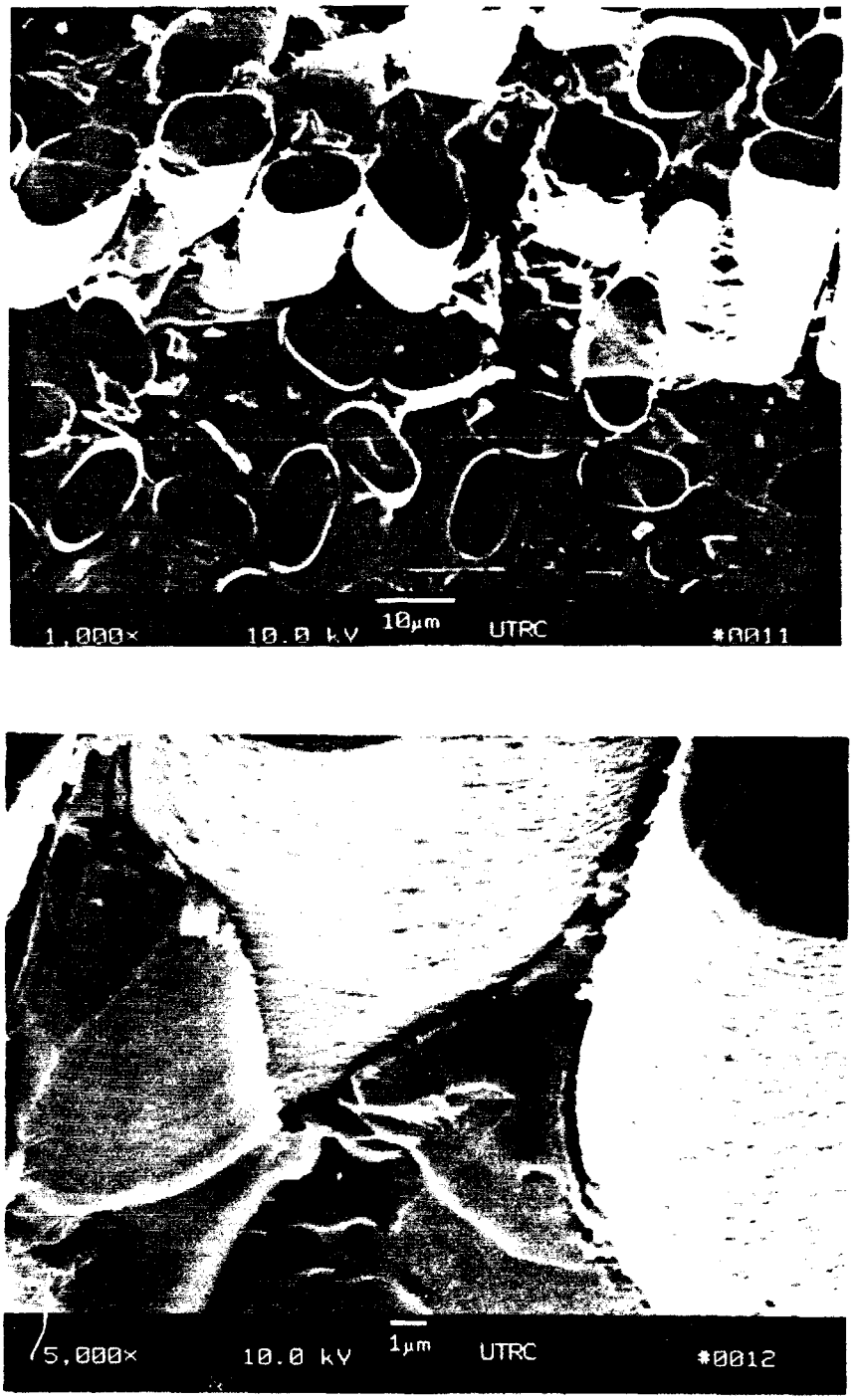

Fig. 31 Fracture Surface of BMAS Matrix/Si/BN Coated HPZ Fiber (92172:74) Composite #53-92

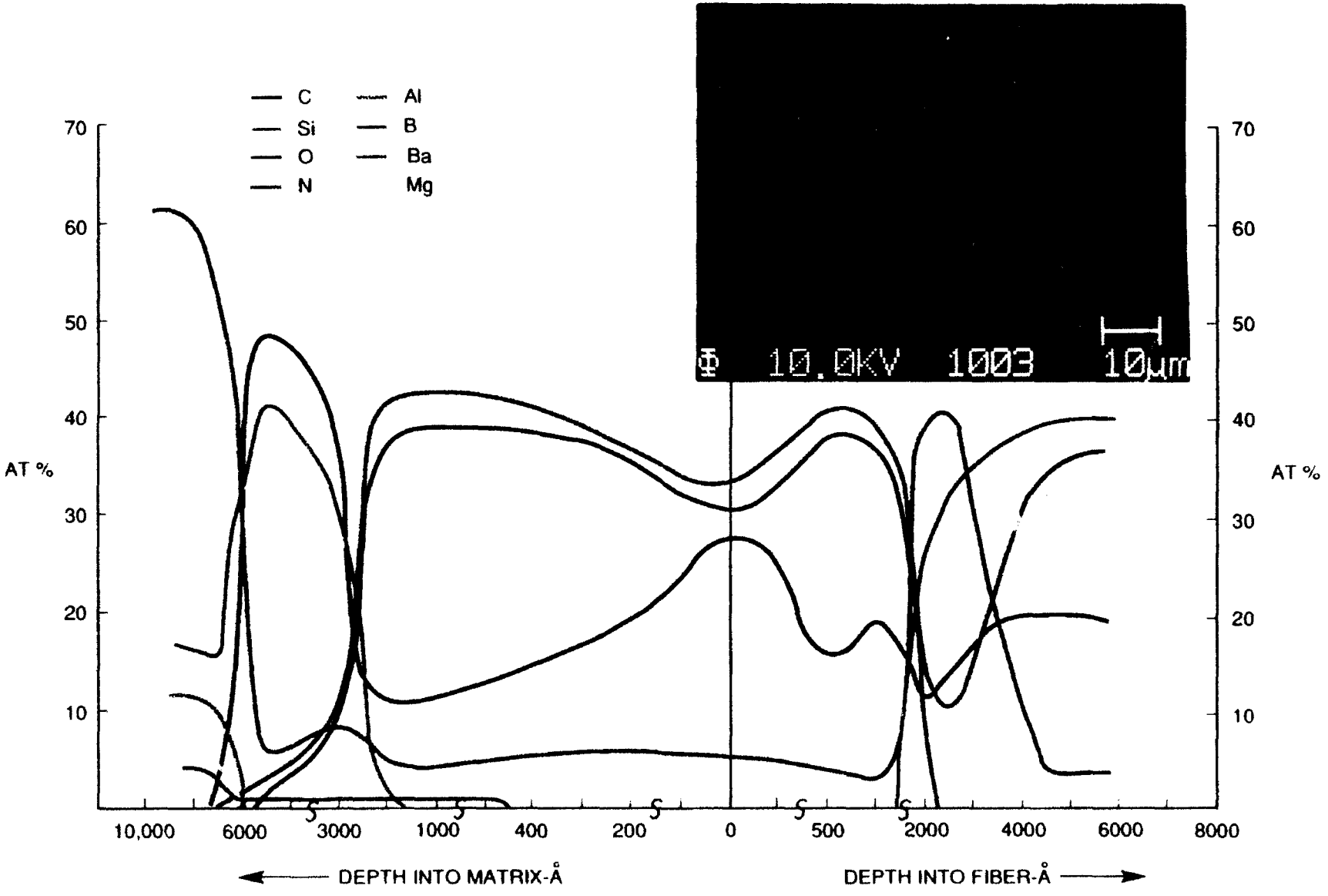

Fig. 32 SAM Depth Profile —Interfacial Chemistry of BMAS Matrix/SIC/BN/HPZ (#92172:74) Composite #53-92 (As-Pressed)

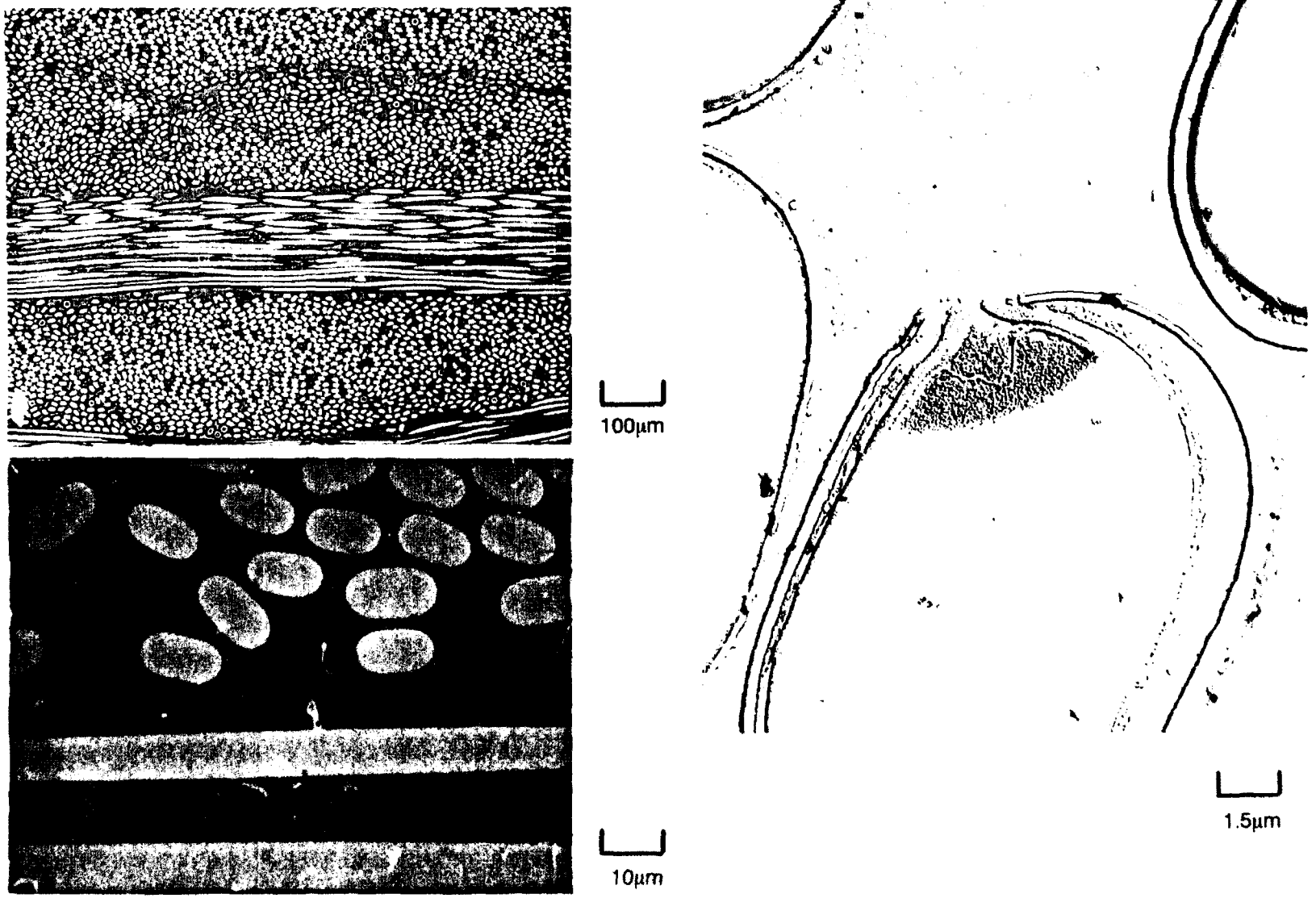

Fig. 33 Optical/TEM Micrographs of BMAS/SiC-BN Coated/HPZ Fiber (#92172:78) Composite #88-92-5 (As-Pressed)

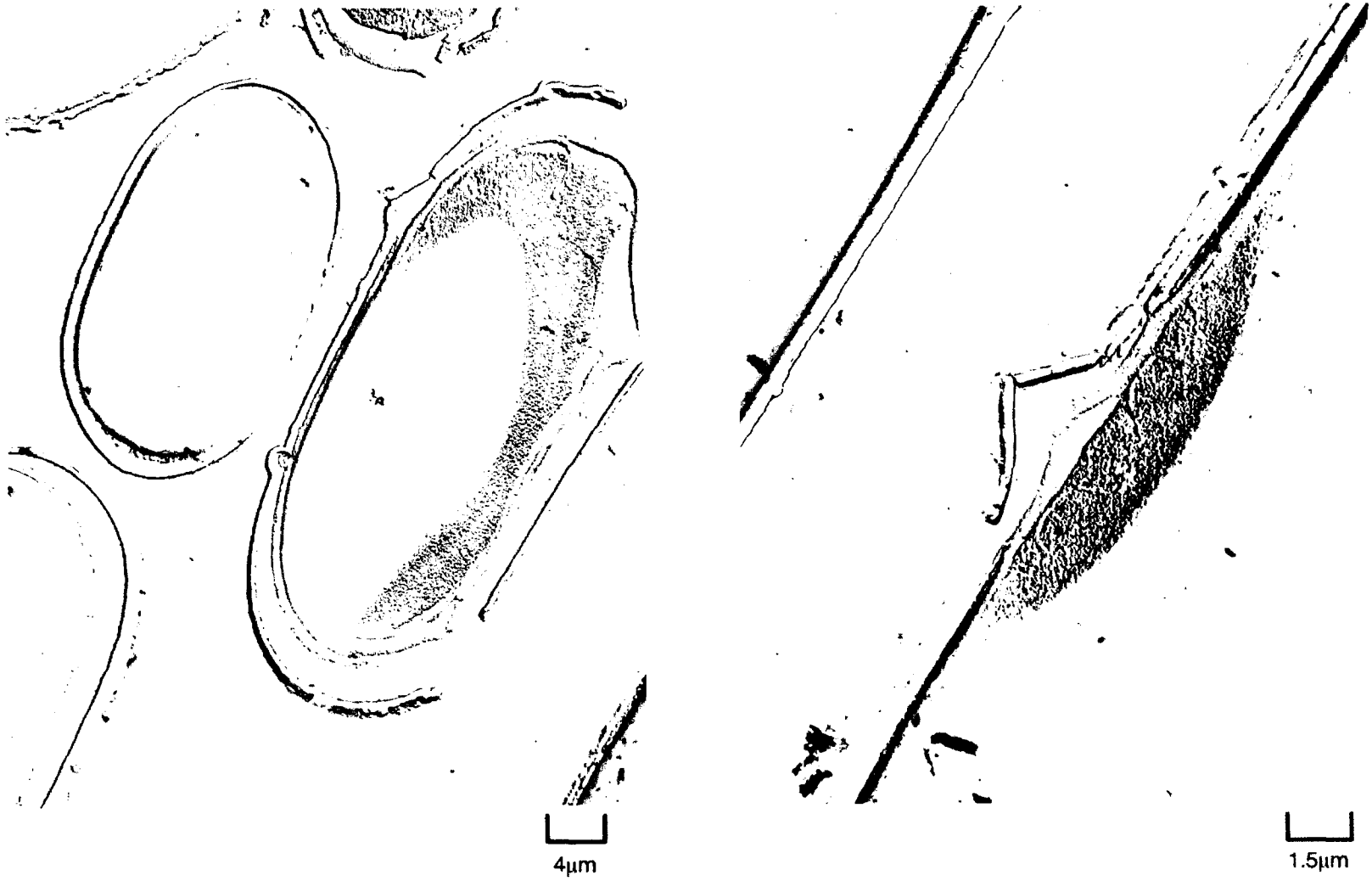

Fig. 34 TEM Replica Micrographs of Transverse and Longitudinal Sections of BMAS/SiC-BN Coated/HPZ Fiber (#92172:78) Composite #88-92-5 (As-Pressed)

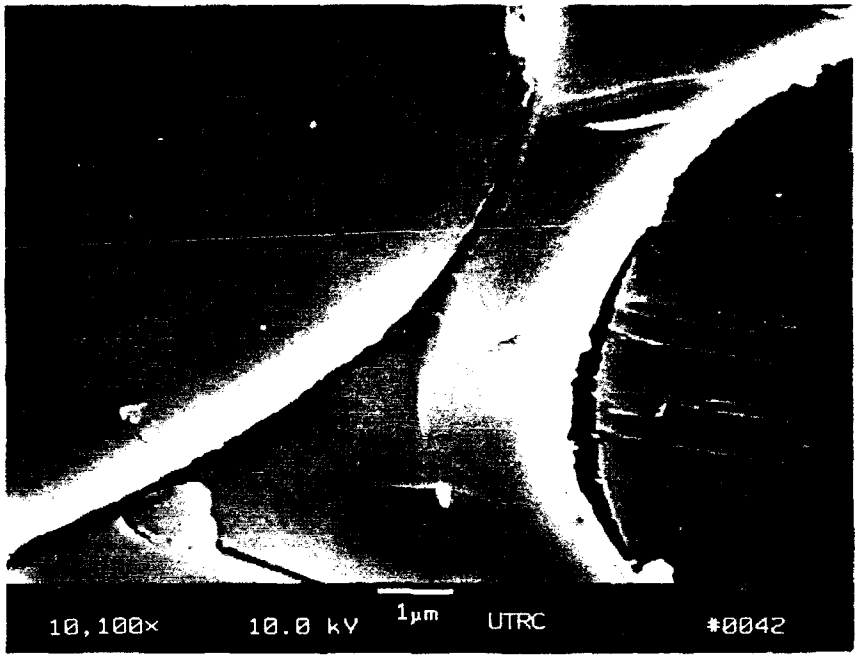

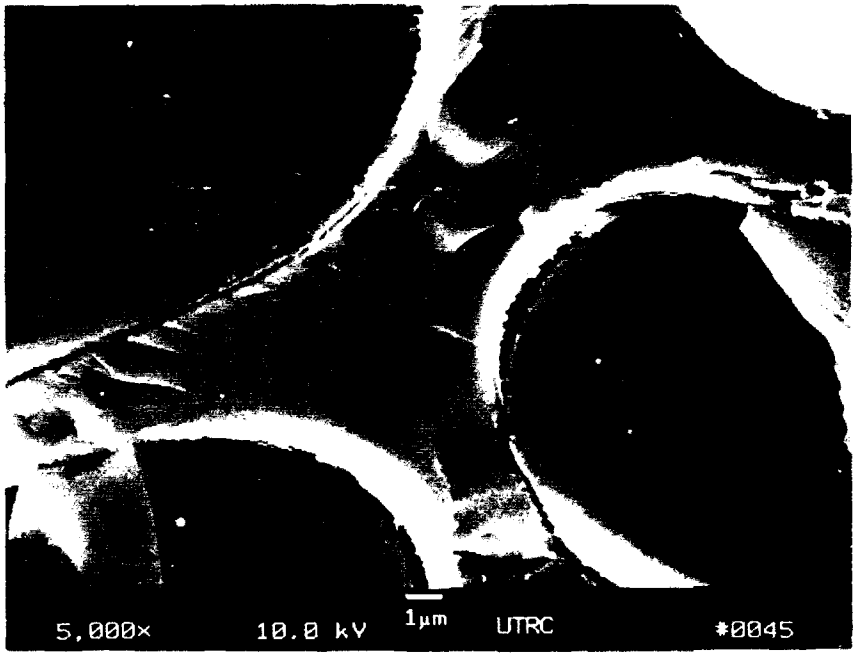

Fig. 35 Fracture Surface of BMAS Matrix/SiC/BN Coated HPZ Fiber (92172:74) Composite #53-92

EP301-10-22

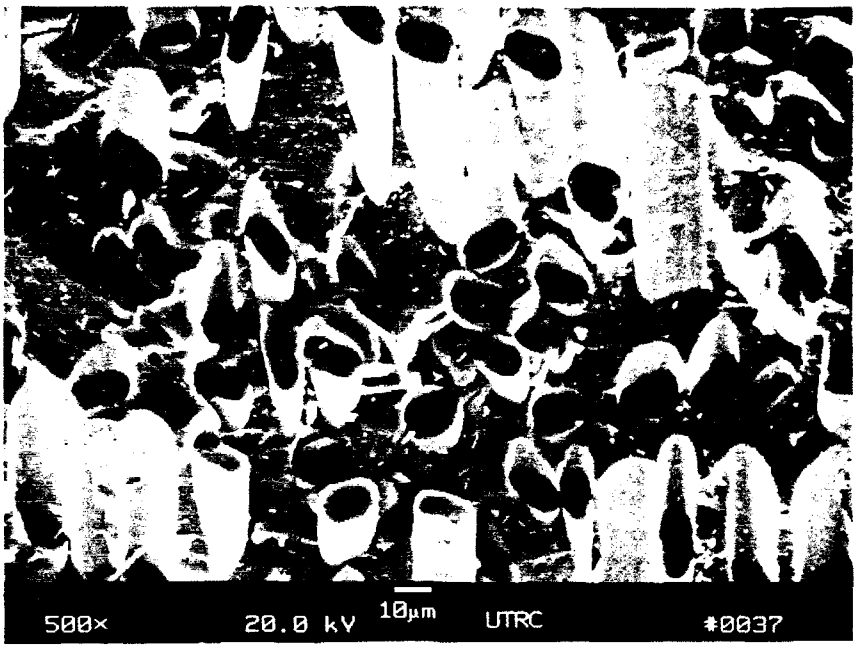

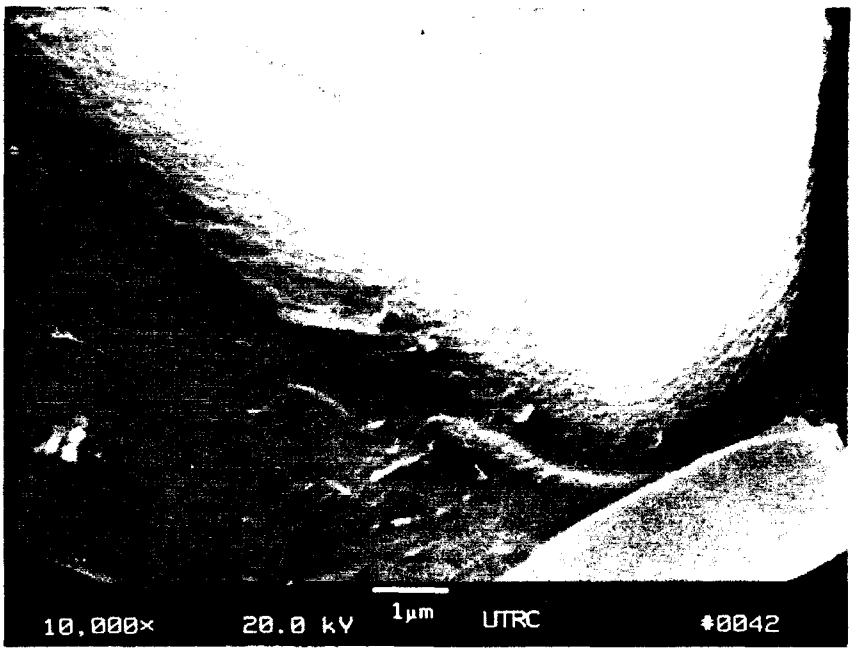

Fig. 36 Fracture Surface of BMAS Matrix/SiC-BN Coated HPZ Fiber (#92172:74) Composite #213-92 (1050°C Press)

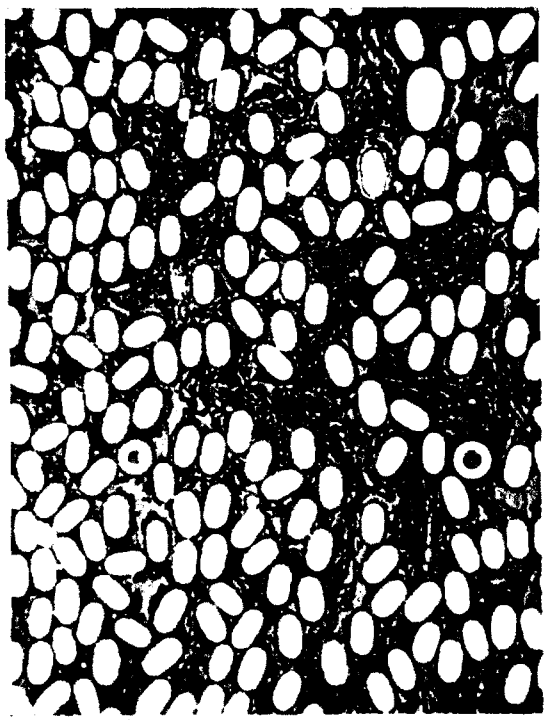

40μm

COATINGS THICKNESS
SiC = 256nm
BN = 364nm

1μm

Fig. 37 Optical/TEM Characterization of BMAS Matrix/SiC-BN Coated HPZ (#92172:74) Fiber Composite #213-92-1 (Pressed at 1050° C/2Ksi, As-Pressed)

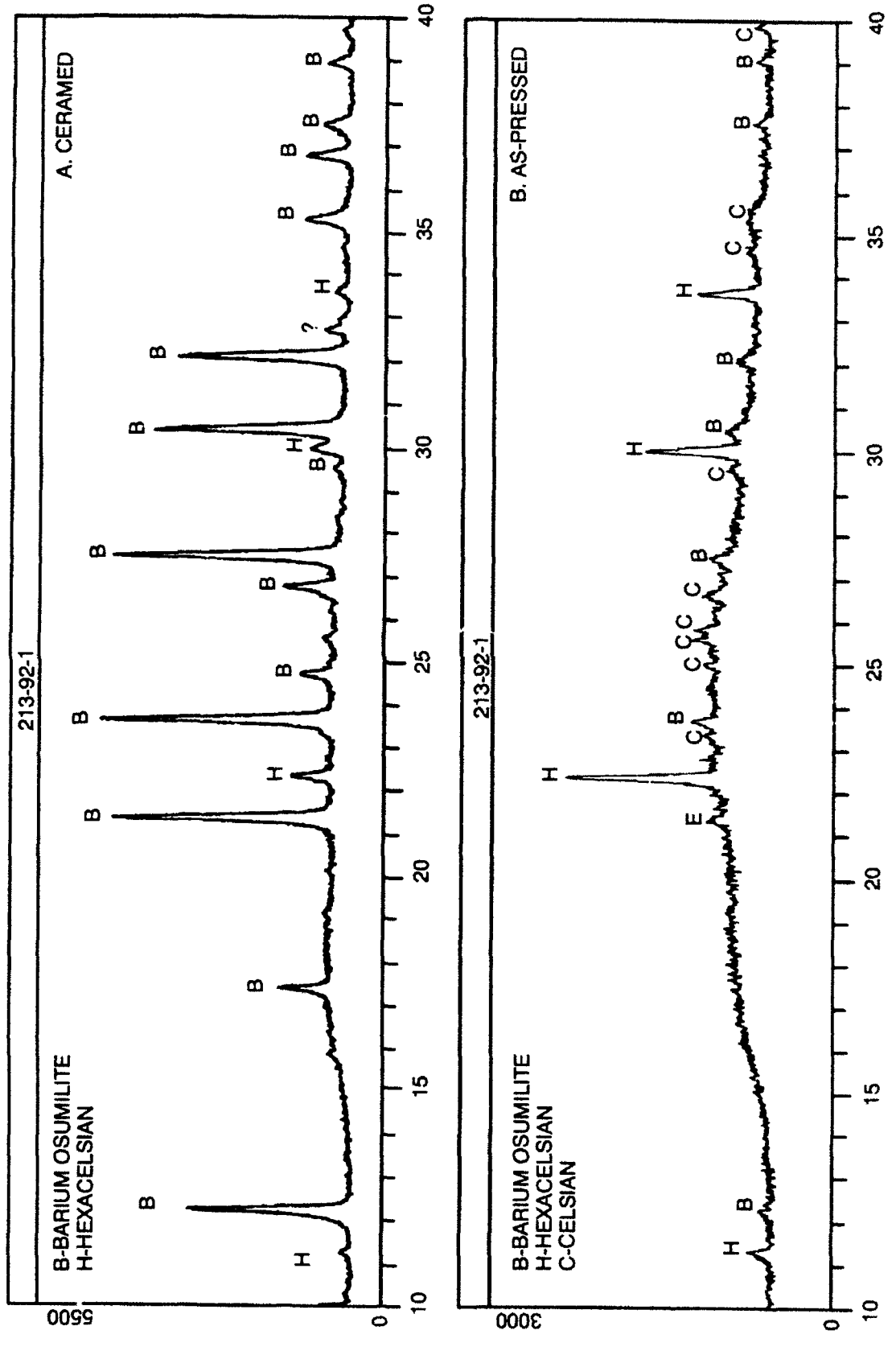

Fig. 38 X-Ray Diffraction Patterns for BMAS Matrix/SiC Over BN Coated HPZ Fiber Composite #213-92

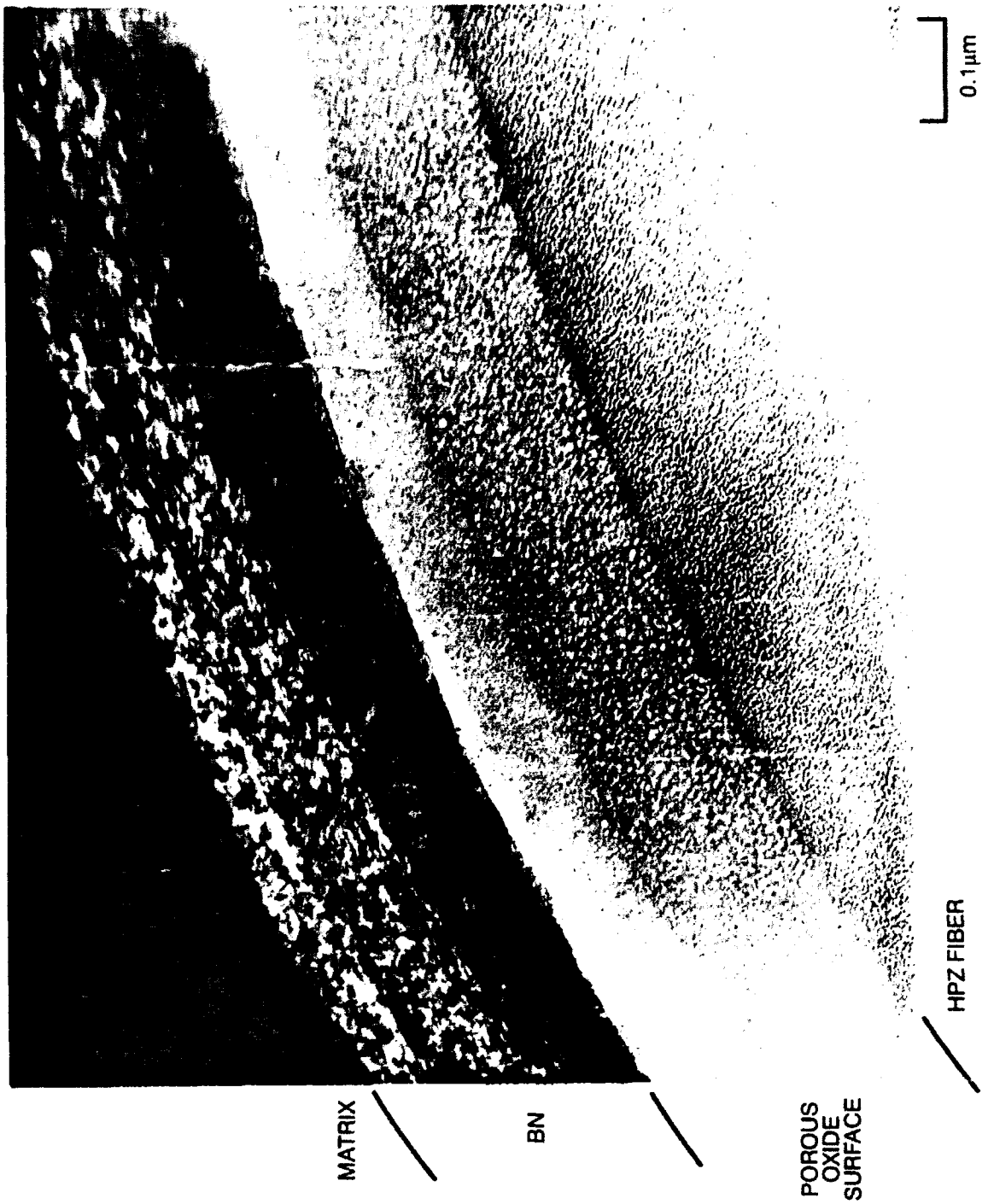

Fig. 39 TEM Thin Foil Characterization of Transversely Sectioned BMAS/BN Coated HPZ Fiber Composite-#5-91 (As-Pressed)

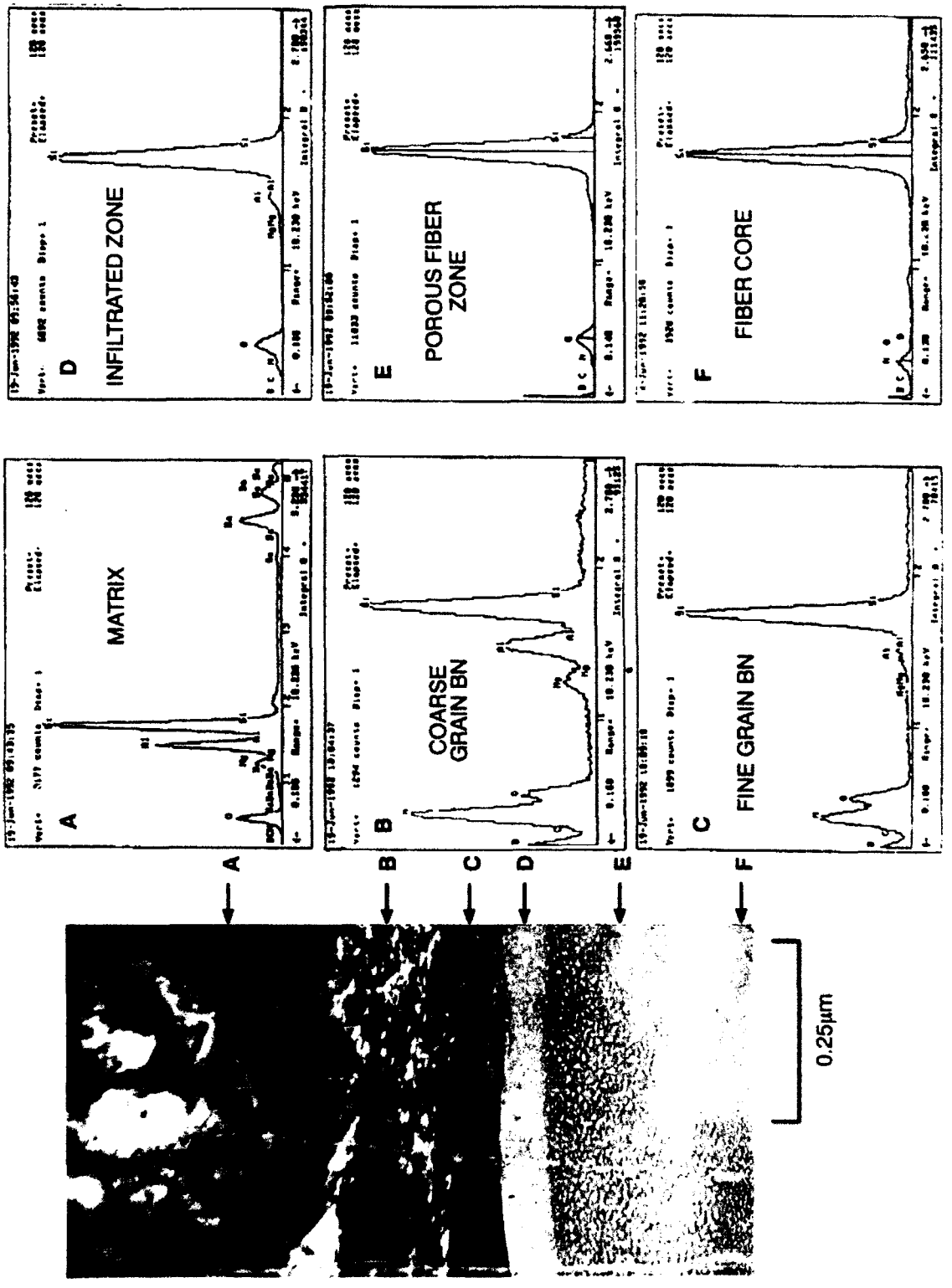

Fig. 40 TEM/EDX Thin Foil Characterization of Transversely Sectioned BMAS Matrix BN/HPZ Fiber Composite-#5-91 (As-Pressed)

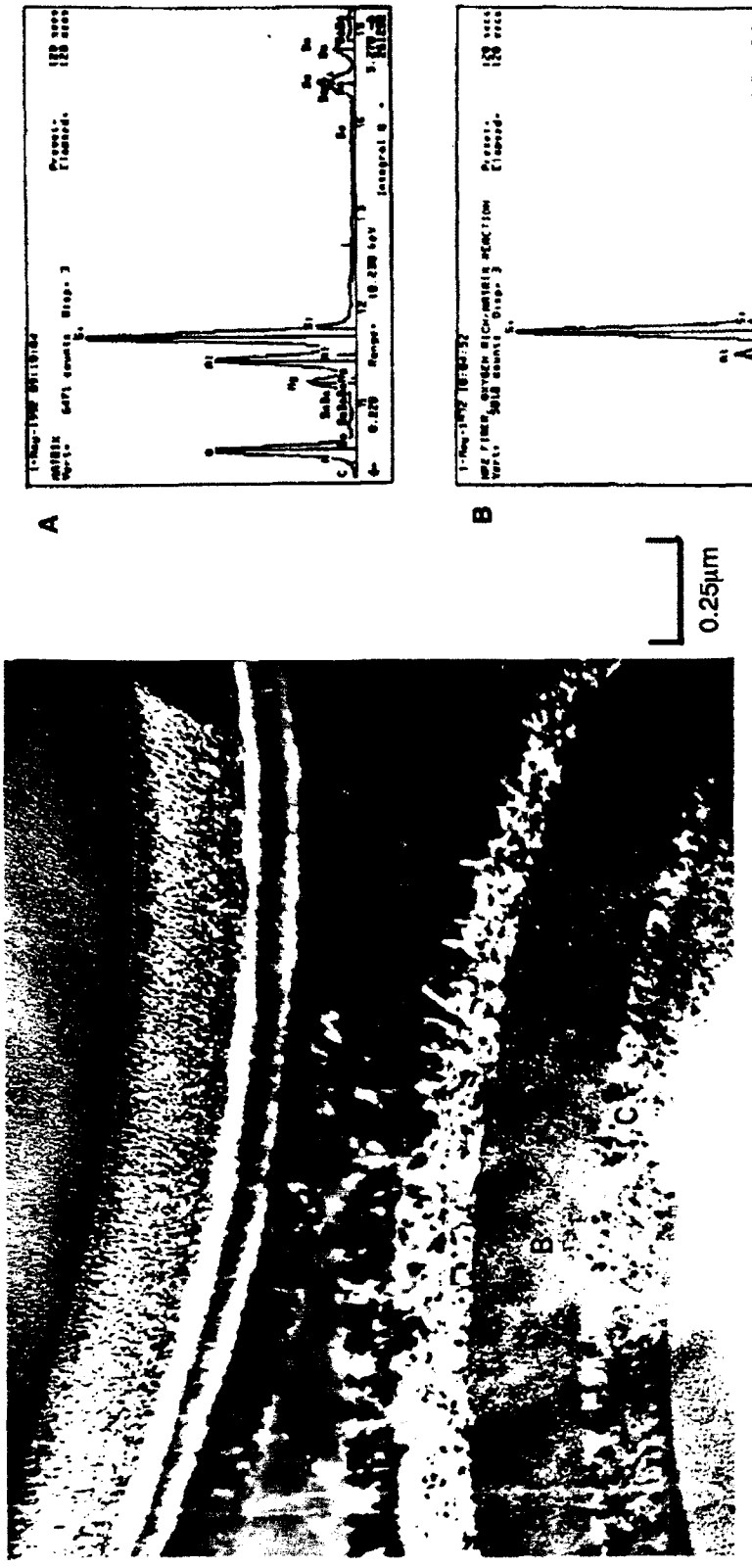

Fig. 41 TEM/EDX Thin Foil Microgrphs of Transversely Sectioned BMAS/SiC-BN Coated/HPZ Fiber (#92172:78) Composite #88-92-5 (As-Pressed)

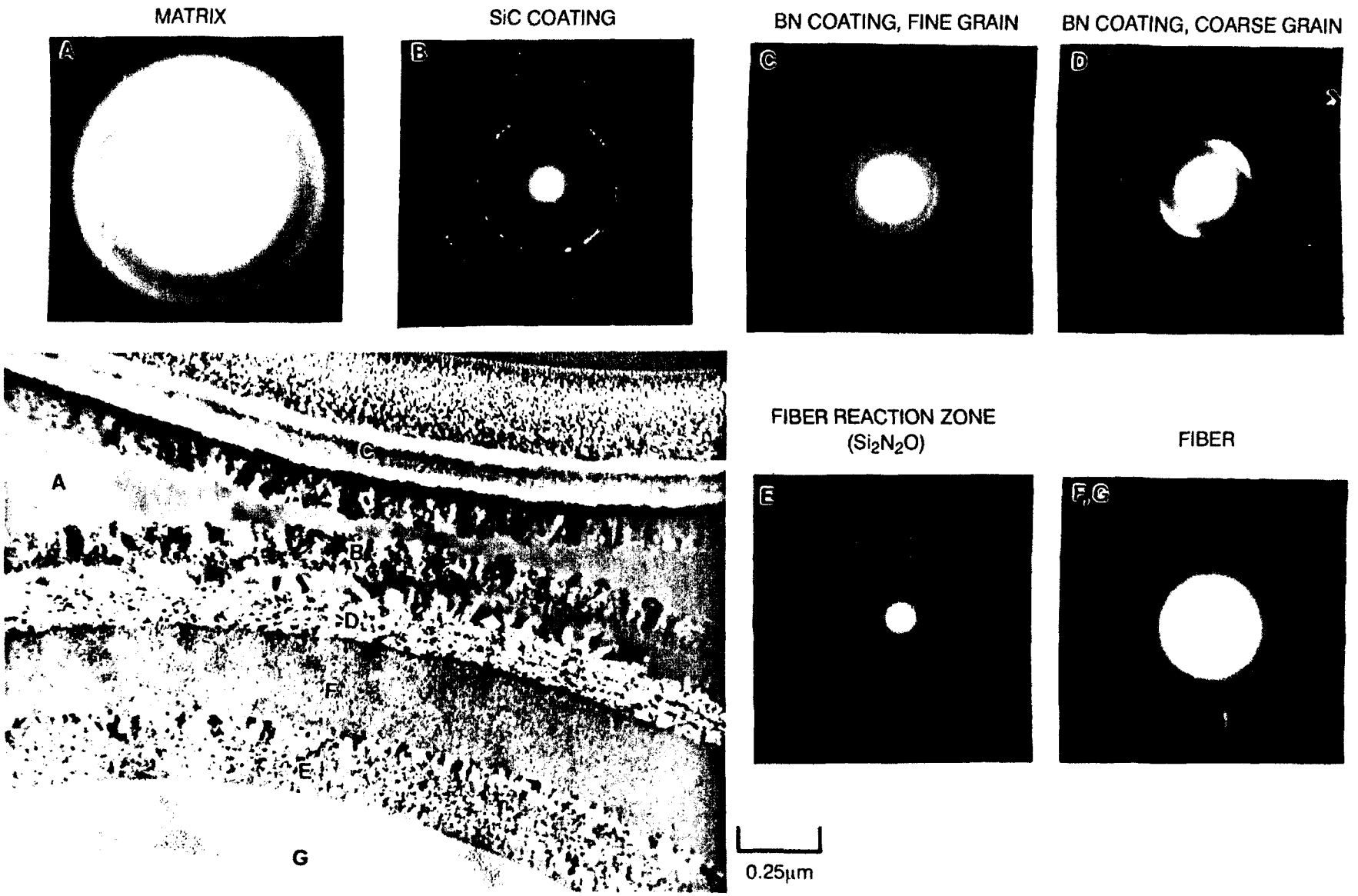

R93-970104-2

Fig. 42 TEM/SAED Thin Foil Micrographs of Transversely Sectioned BMAS/SiC-BN Coated/HPZ Fiber (#92172:78) Composite #88-92-5 (As-Pressed)

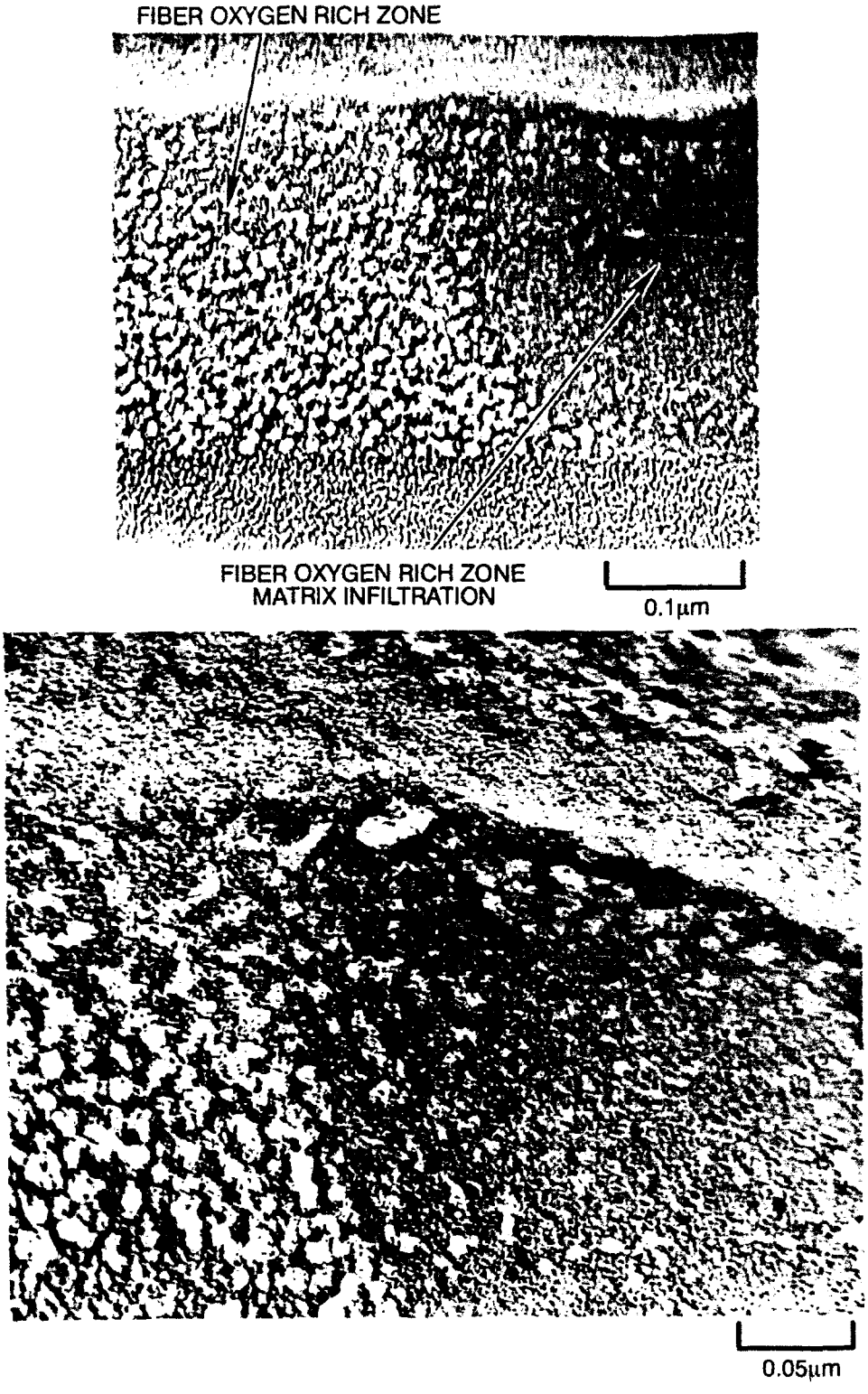

Fig. 43 TEM Thin Micrographs of Transversely Sectioned BMAS/SiC-BN Coated/HPZ Fiber (#92172:78) Composite #88-92-5 (As-Pressed)

EP301-10-27

(SiC OVERCOAT DETACHMENT IN BOTH COMPOSITES)

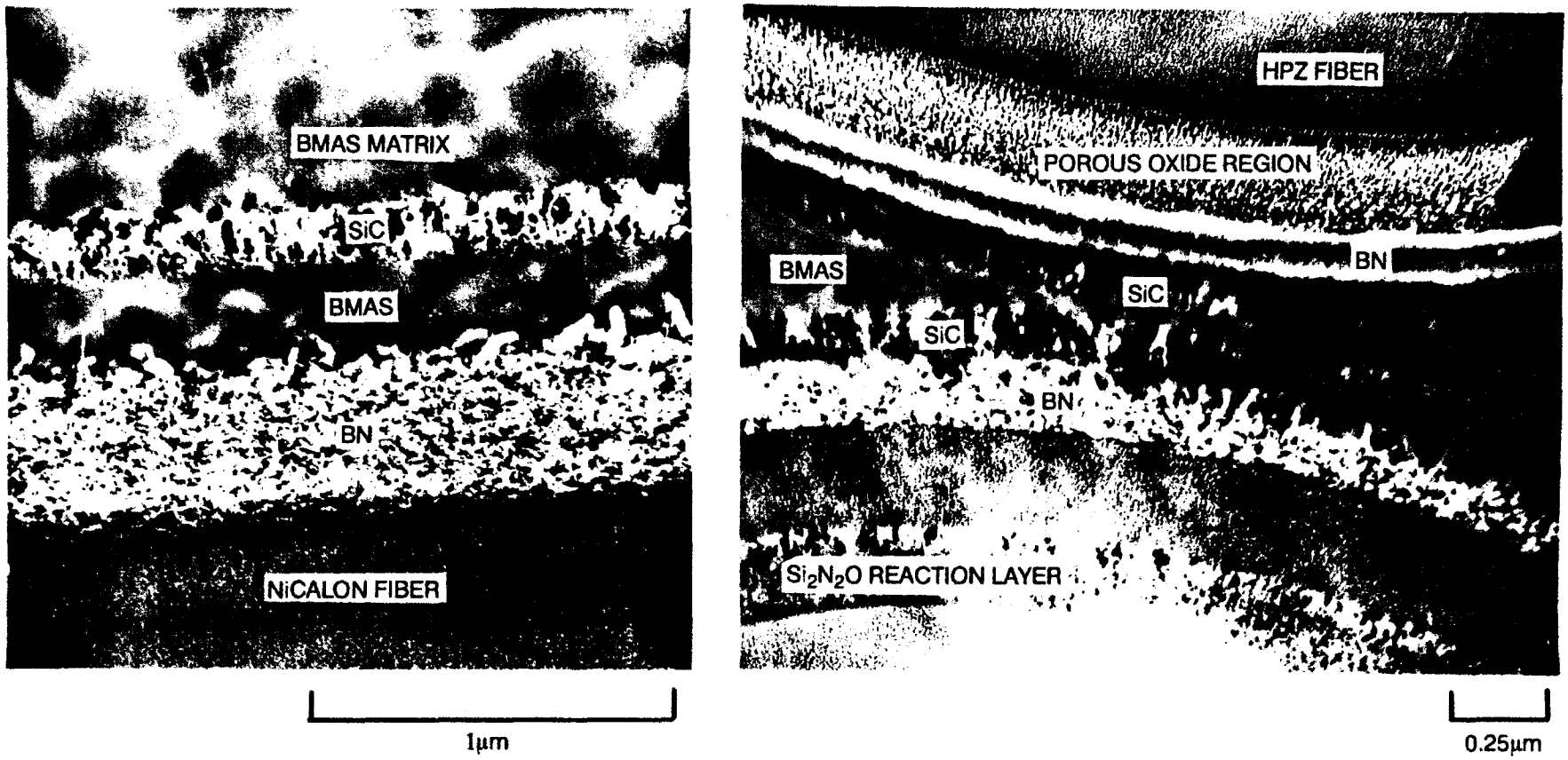

A. BN HAS CRYSTALLIZED BUT NO REACTION WITH NICALON FIBER

B. NO SiC DETACHMENT ON UPPER FIBER, NO REACTION, SiC LAYER DETACHMENT ON LOWER FIBER, Si_2N_2O REACTION LAYER FORMED, HPZ FIBER STRENGTH DEGRADED

Fig. 44 TEM Thin Foil Characterization of BMAS Matrix/SiC over BN Coated Nicalon (A) and HPZ (B) Fiber Composite Interfaces

A. BMAS/SiC/BN/Nicalon, RTσ = 90 ksi (620 MPa)

10μm

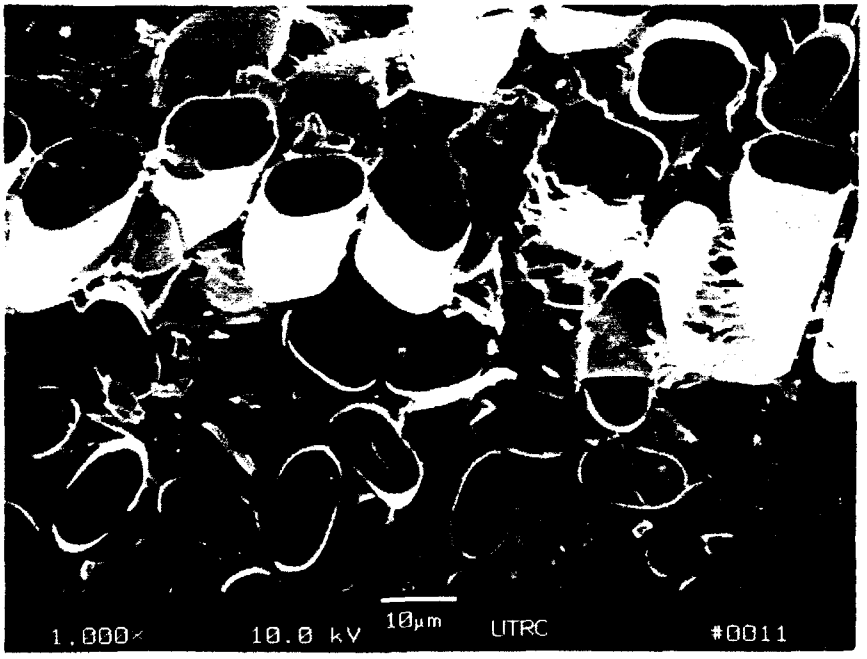

B. BMAS/SiC/BN/HPZ, RTσ = 31 ksi (214 MPa)

10μm

Fig. 45 Fracture Surfaces of Typical BMAS Matrix/SiC Over BN Coated Nicalon (A) and HPZ (B) Fiber Composites (0°/90°)

EP301-10-29

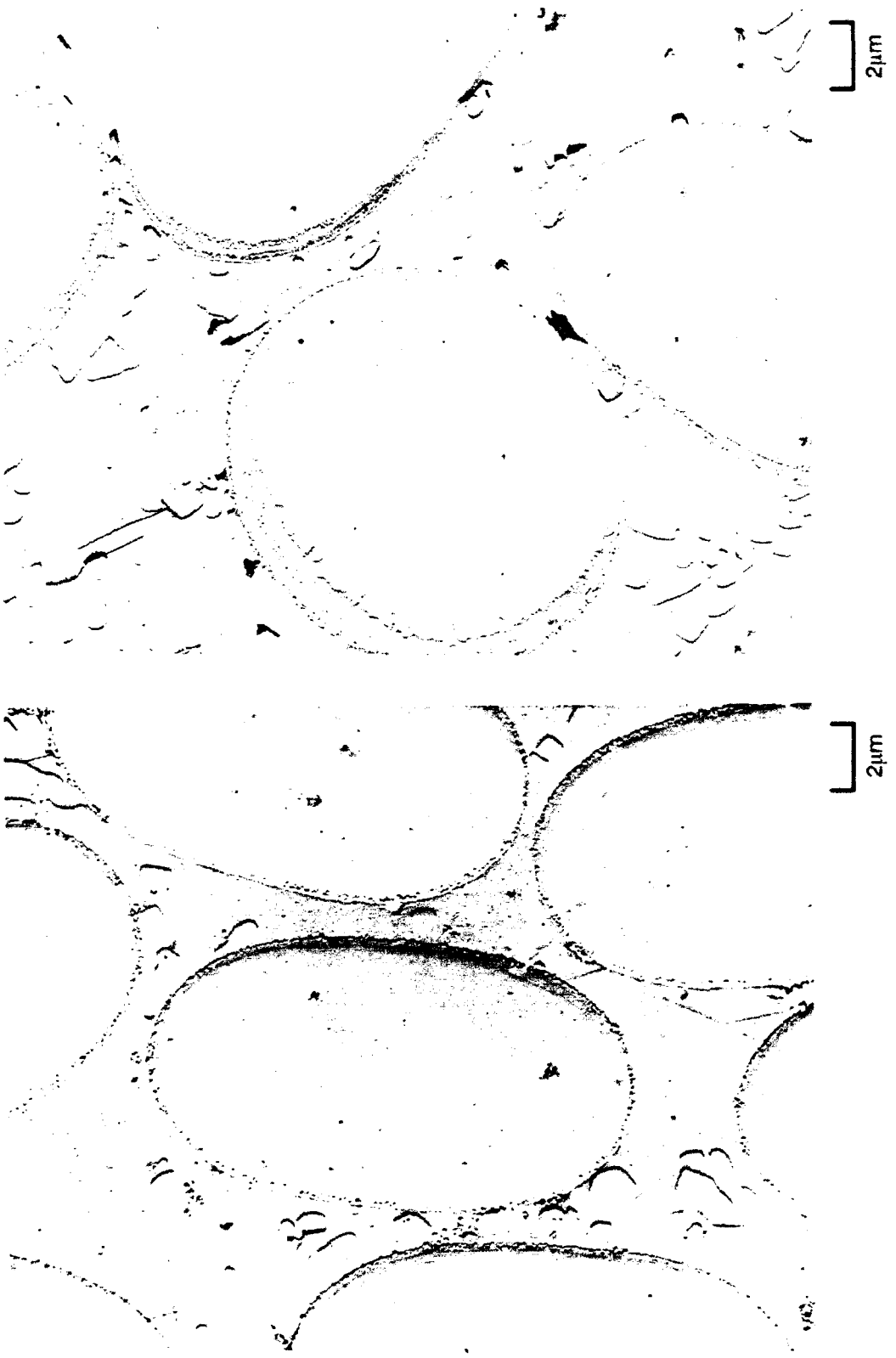

Fig. 46 TEM Replica Characterization of 0°/90° BMAS/BN Coated/HPZ Fiber Composite - #334-92-6 (Ceramed) RT σ = 61 ksi (420MPa)

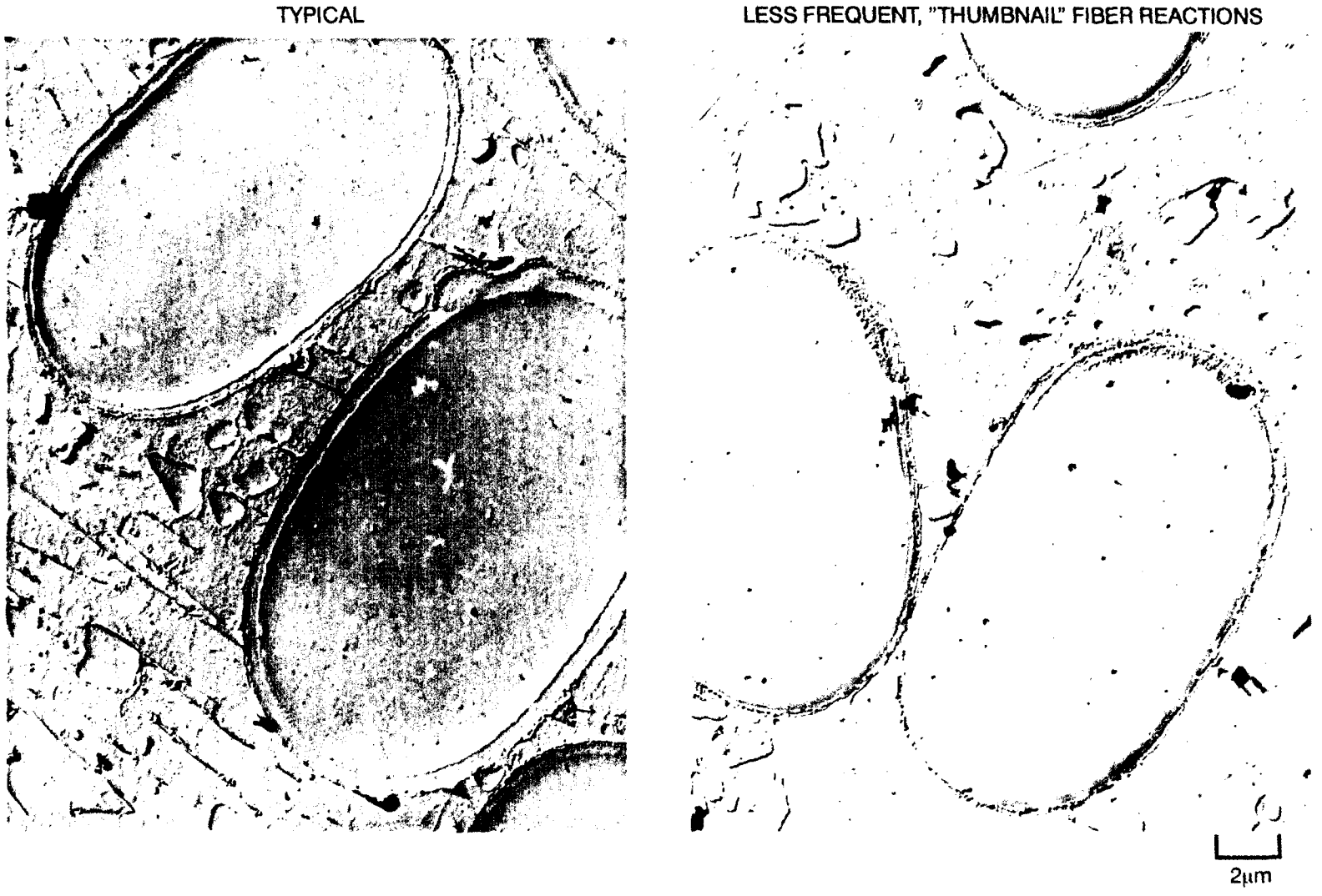

Fig. 47 TEM Characterization of BMAS/BN Coated/HPZ Fiber Composite-#392-92 (Ceramed)

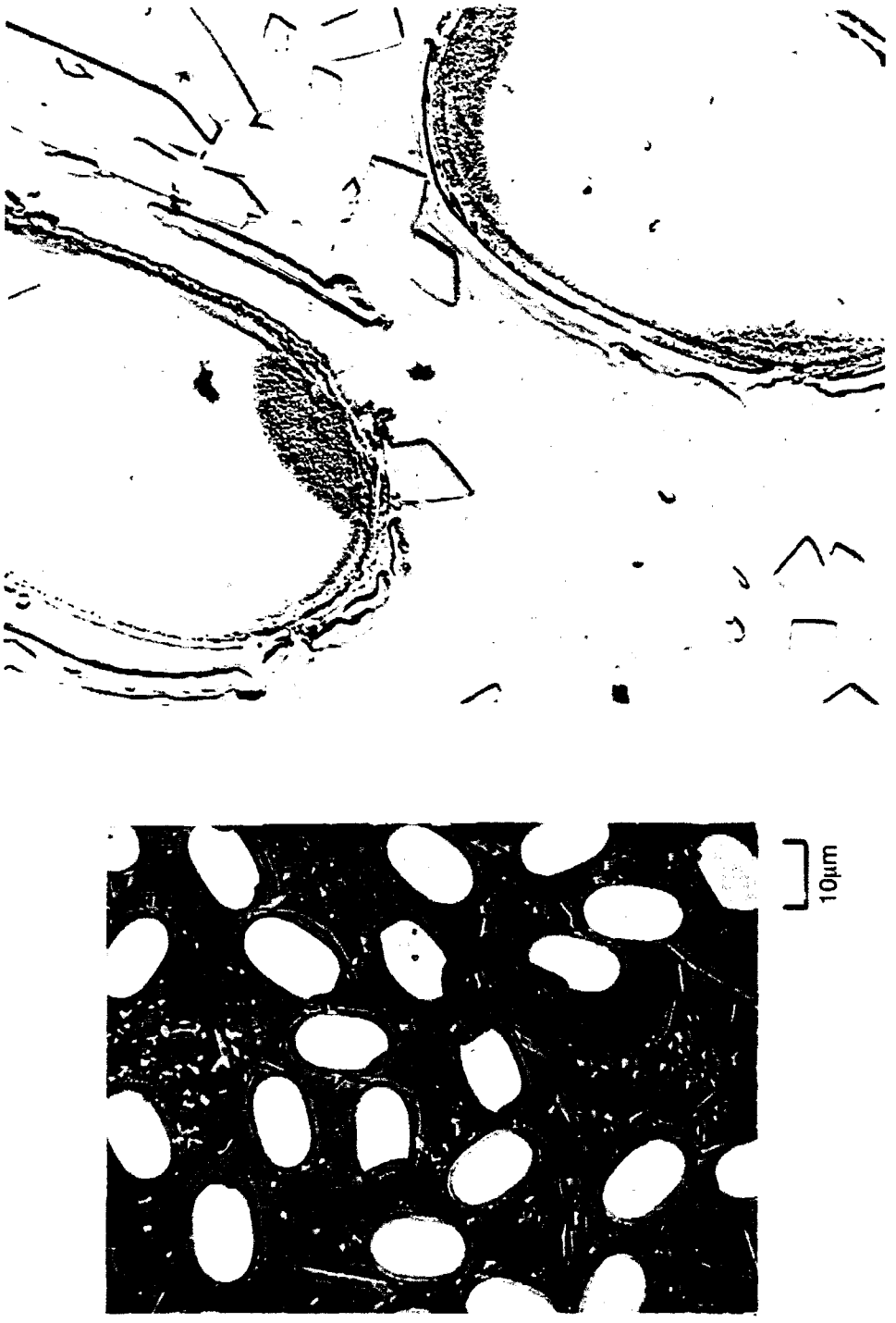

Fig. 48 Optical/TEM Characterization of BMAS/SiC-BN Coated/HPZ Fiber Composite - #393-92 (As-Pressed)

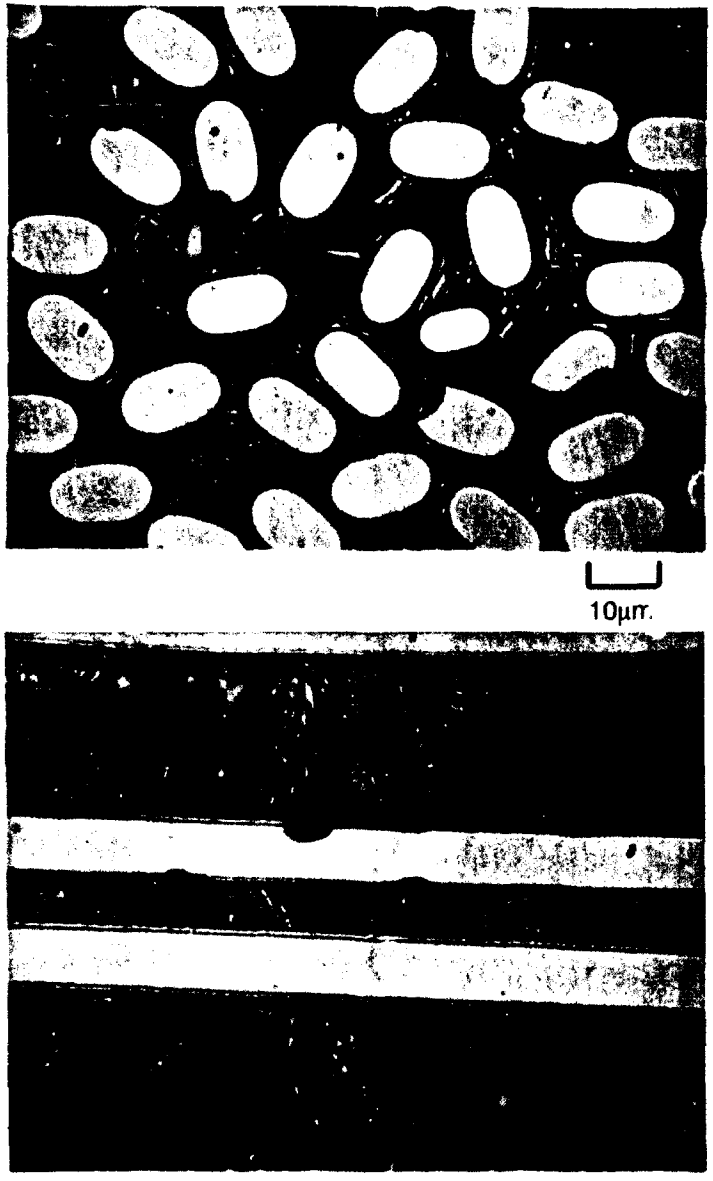

Fig. 49 Optical/TEM Replica Micrographs of Transversely Sectioned BMAS/SiC-BN Coated/HPZ Fiber Composite – #19-93-5

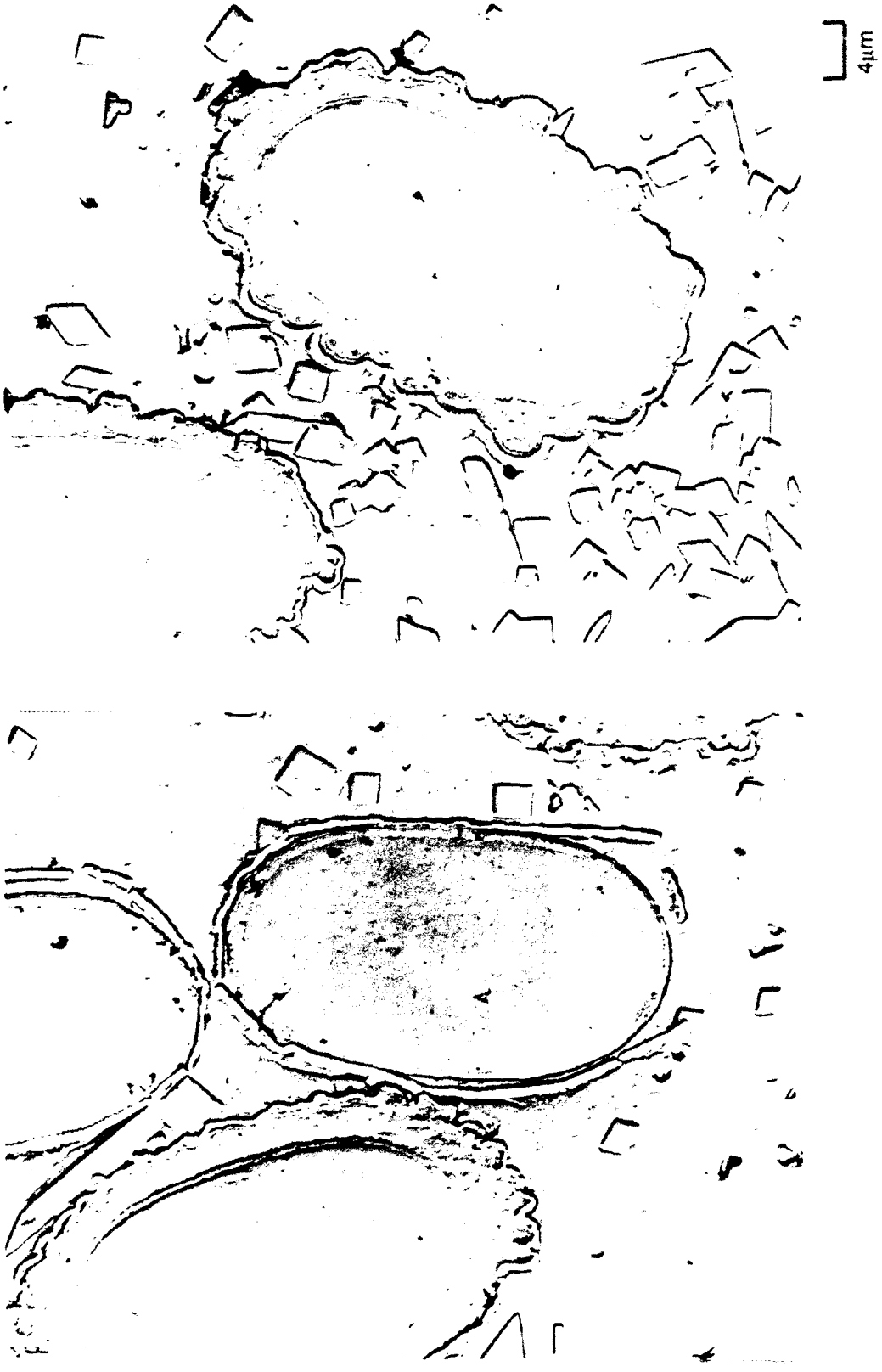

Fig. 50 TEM Replica Micrographs of Transversely Sectioned BMAS/SiC-BN Coated/HPZ Fiber Composite – #19-93-5

A.

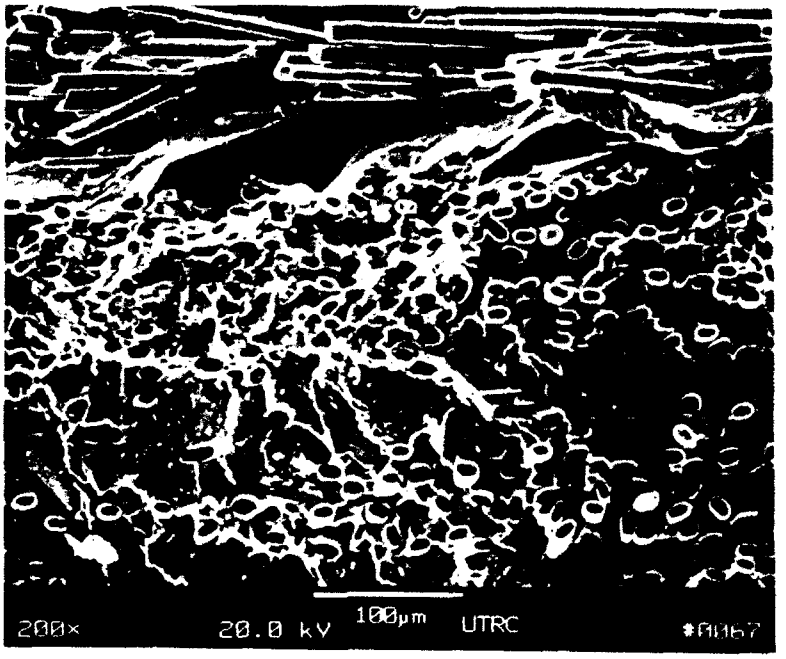

B.

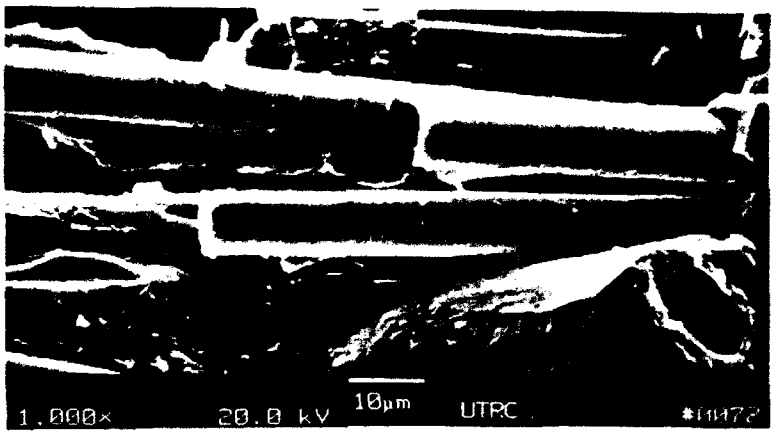

C.

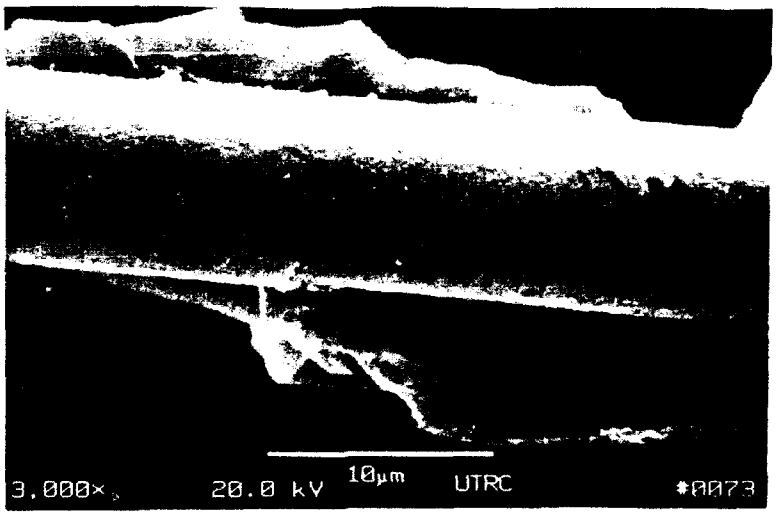

Fig. 51 Fracture surface of BMAS Matrix/SiC Over BN Coated HPZ Fiber Composite #19-93 (As-Pressed)

EP301-10-55

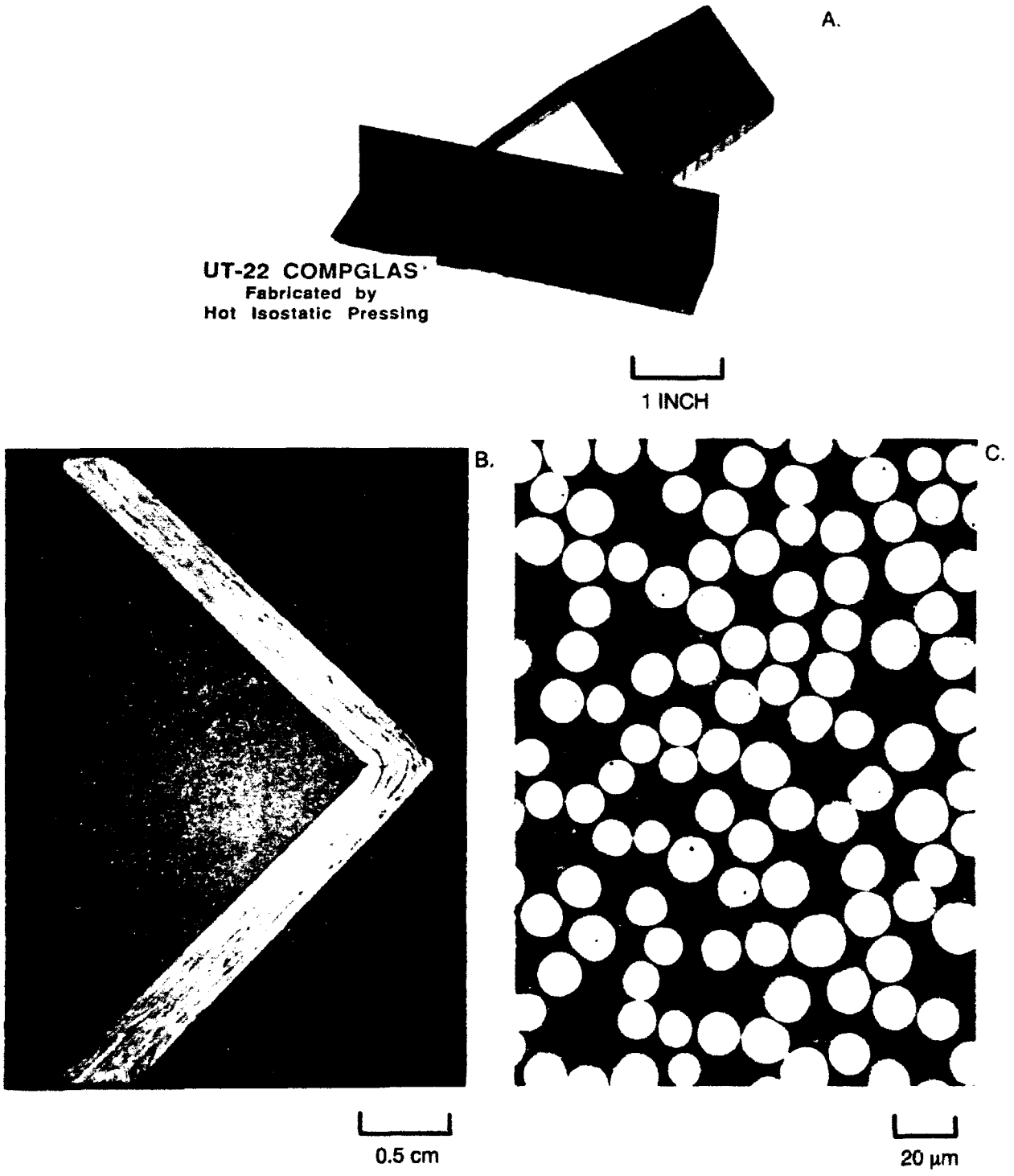

Fig. 52 BMAS Matrix/SIC Over BN Coated Nicalon Fiber Composite L-Brackets Processed by HIP Consolidation

EP301-10-32

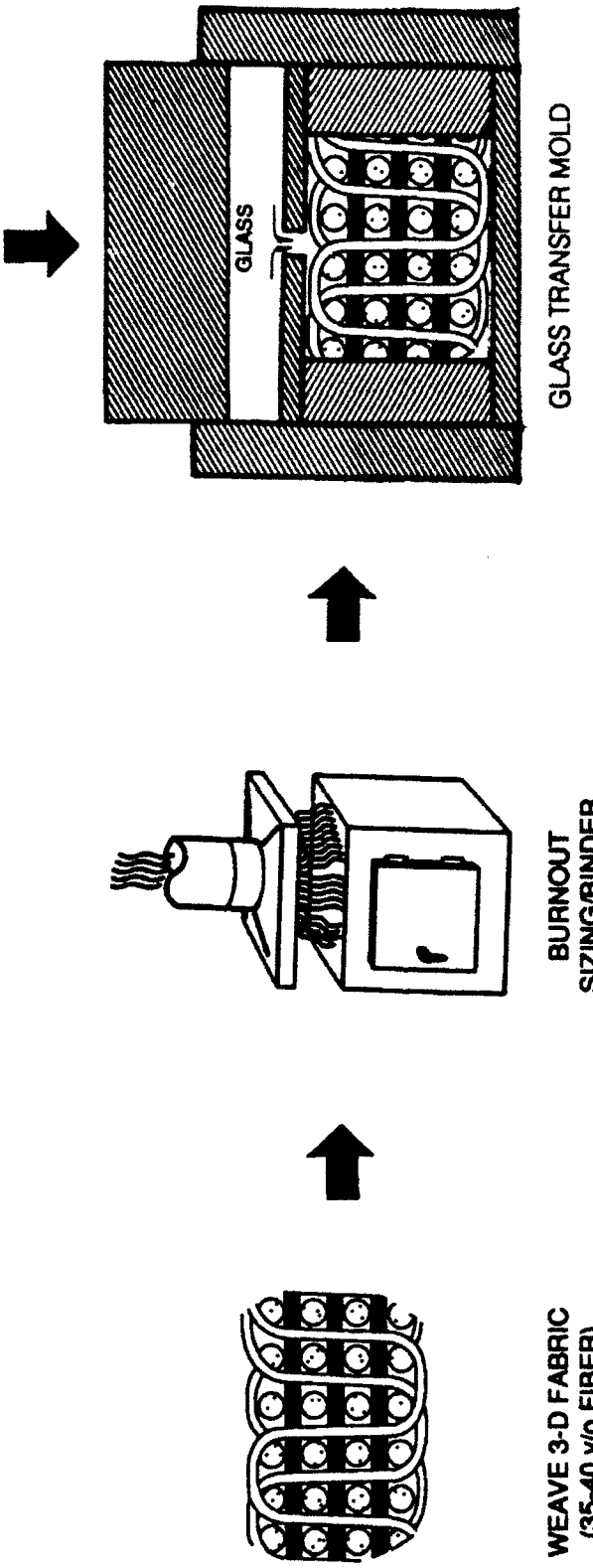

Fig. 53 Processing of a 3-D Fiber Reinforced Glass Composited by Glass Transfer Molding

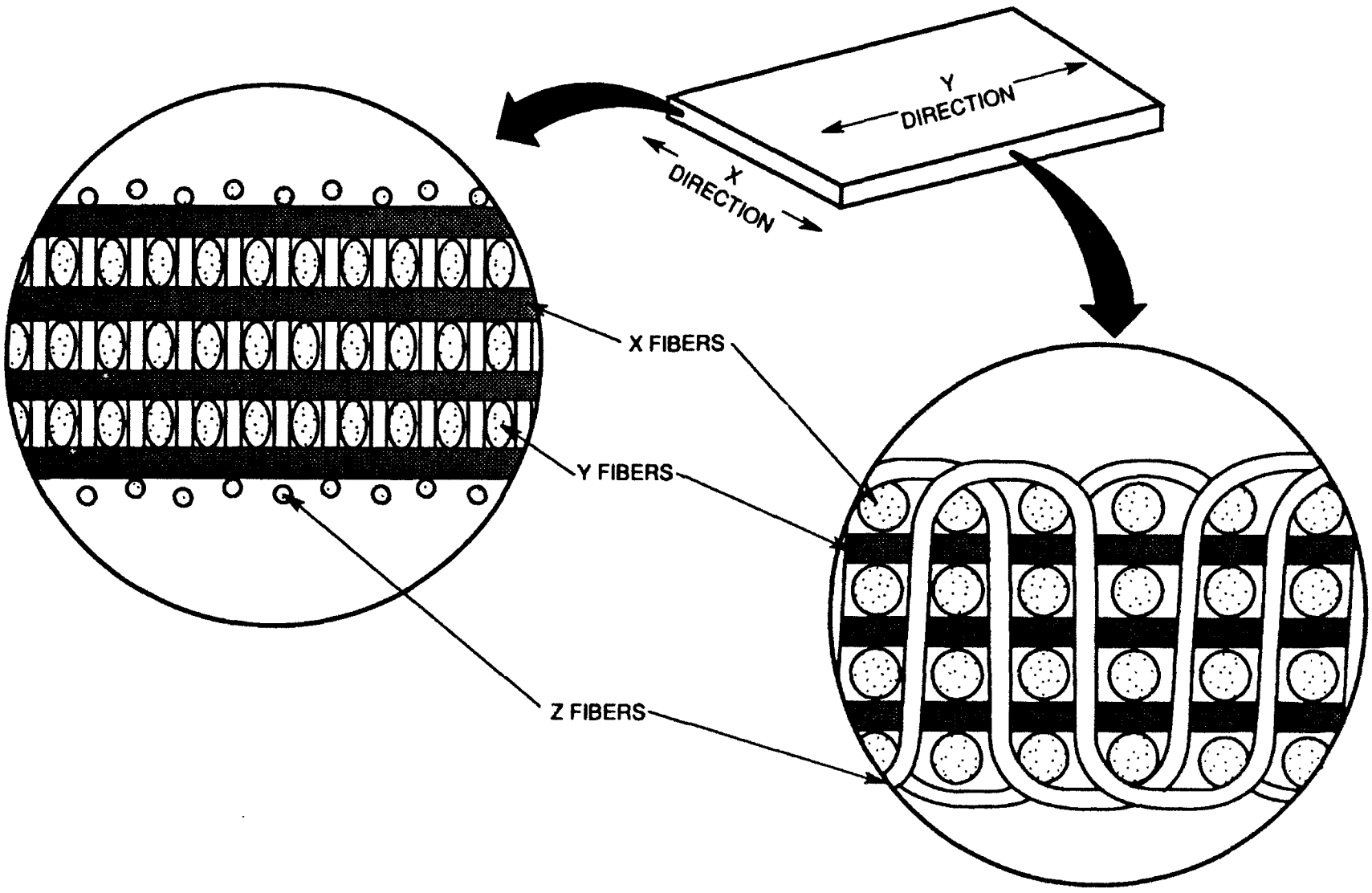

Fig. 54 Nomanclature and Orientation of Orthogonal Weave
(Warp and Fill Terminology is not Used Because Fabrics Made on this Program were Hand Woven)

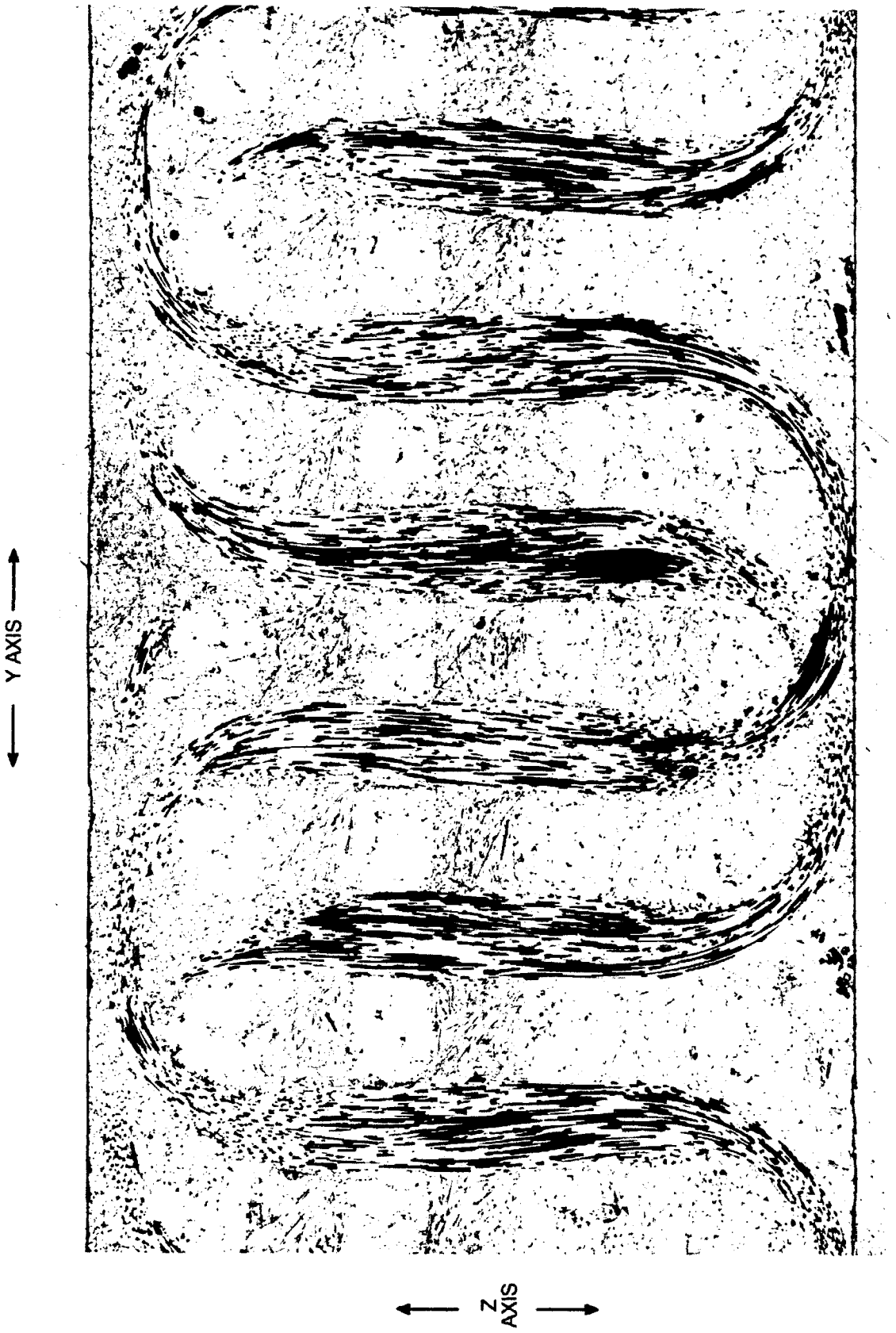

Fig. 55 Y-Z Cross Section of a Nicalon/MAS Composite Reinforced with an Orthogonal Weave and Fabricated by Glass Transfer Molding. (Composite No.102-92)

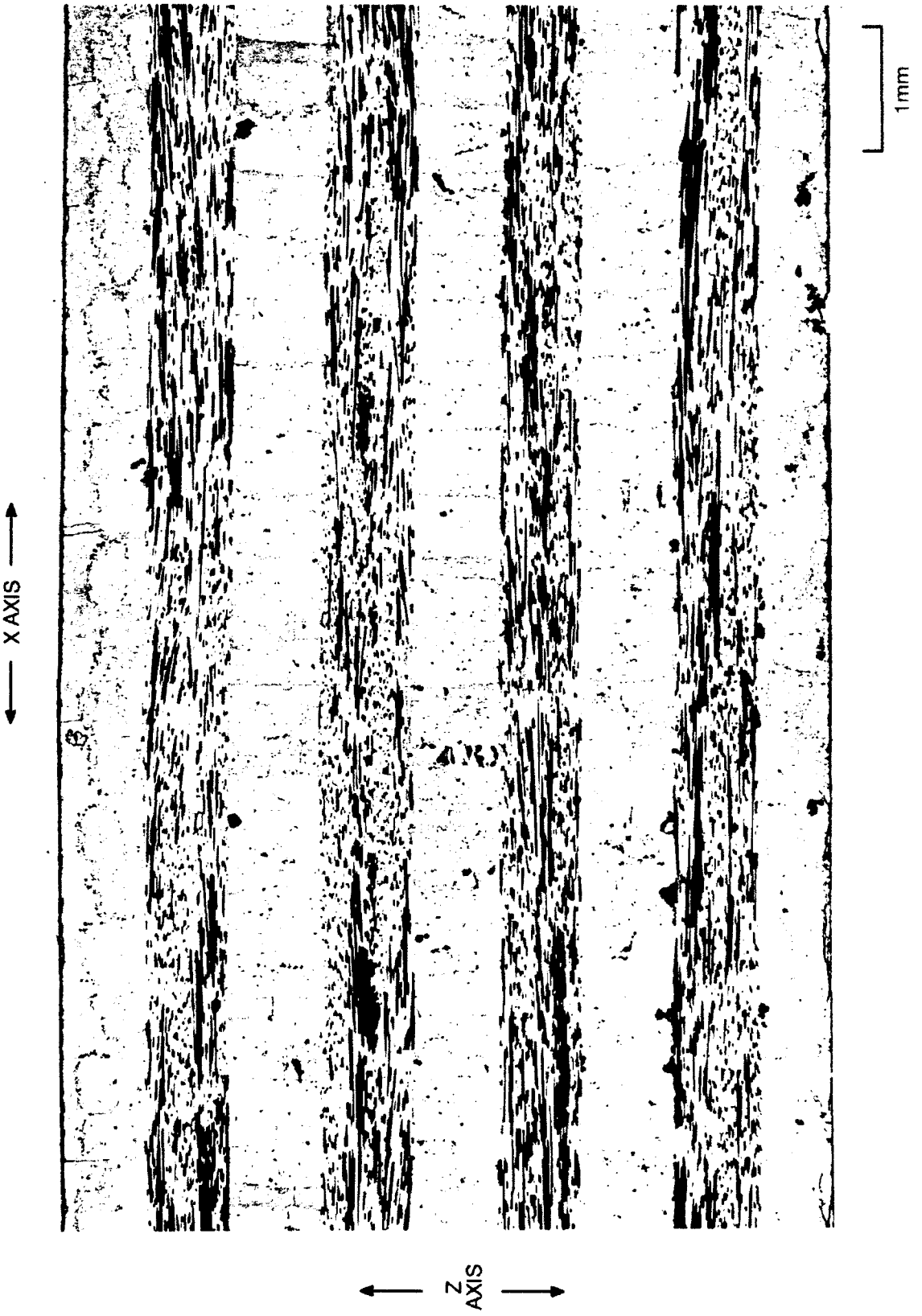

Fig. 56 X-Z Cross Section of a NICALON/MAS Composite Reinforced with an Orthogonal Weave and Fabricated by Glass Transfer Molding. (Composite No. 102-92)

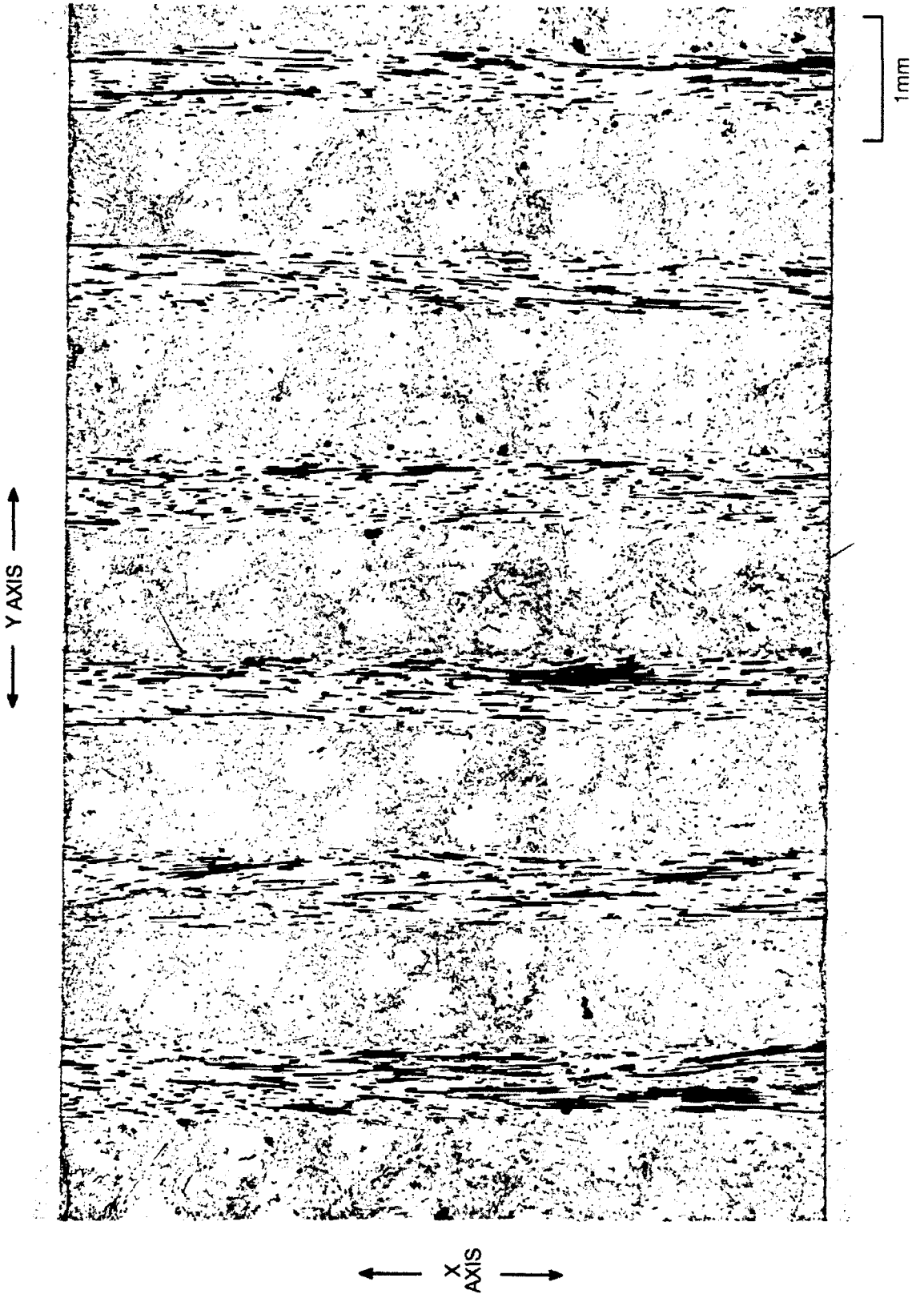

Fig. 57 X-Y Cross Section of a Nicalon/MAS Composite Reinforced with an Orthogonal Weave and Fabricated by Glass Transfer Molding (Composite No. 102-92)

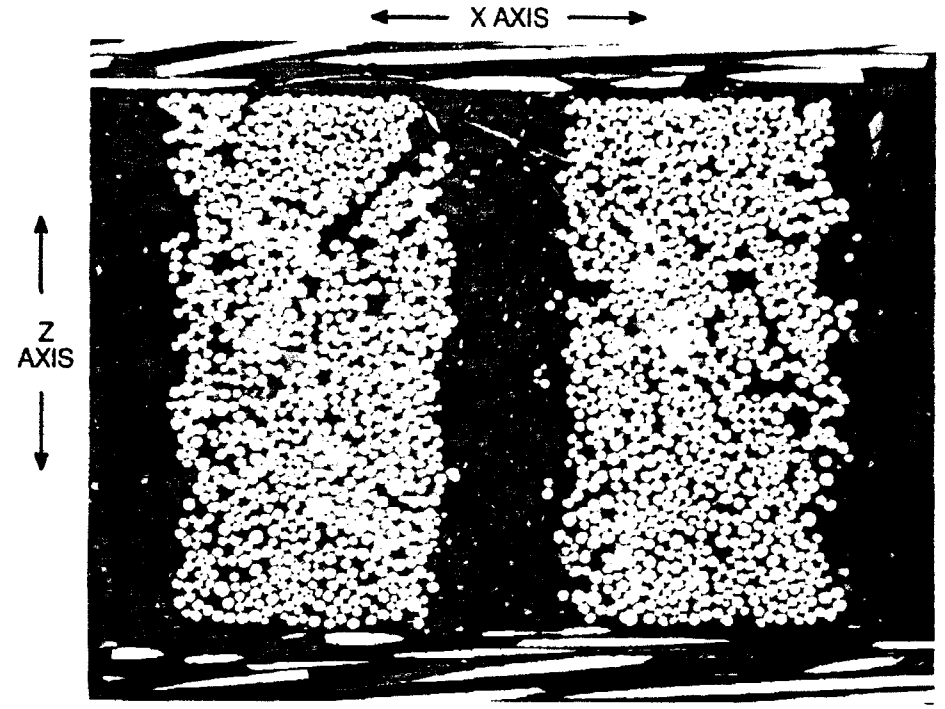

(A) TOWS ARE UNCOMPACTED

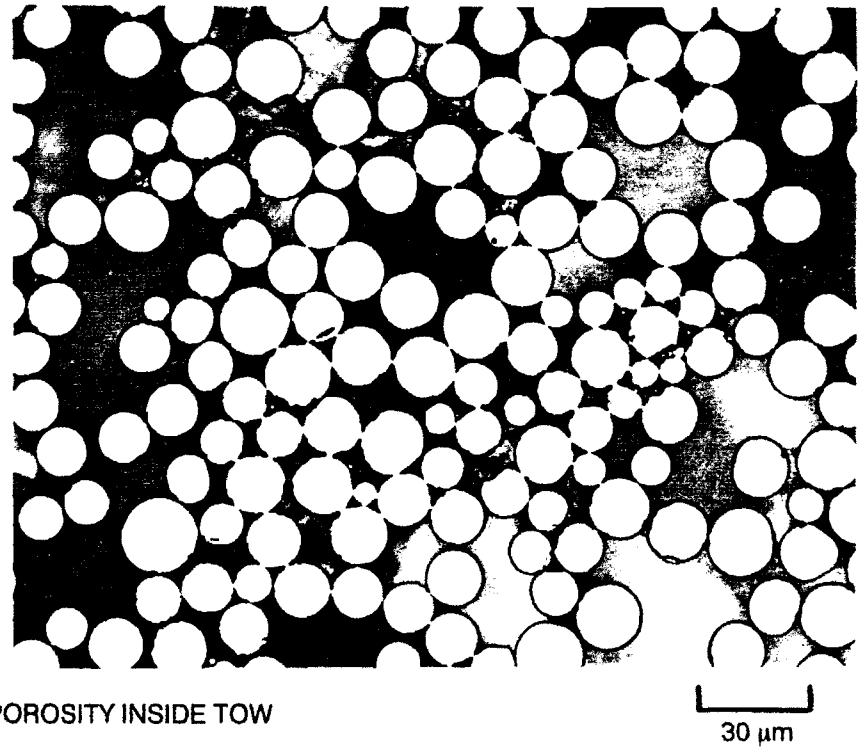

(B) POROSITY INSIDE TOW

Fig. 58 Nicalon/MAS Composite Fabricated by Glass Transfer Molding (Composite No. 102-92)

EP301-10-52

(A) SURFACE VIEW: SOME FIBER BREAKAGE

1 mm

(B) AREAS OF COATING DAMAGE <5%

20 μm

Fig. 59 Orthogonal Woven Fabric with SiC/BN Coated Fiber

EP301-10-53

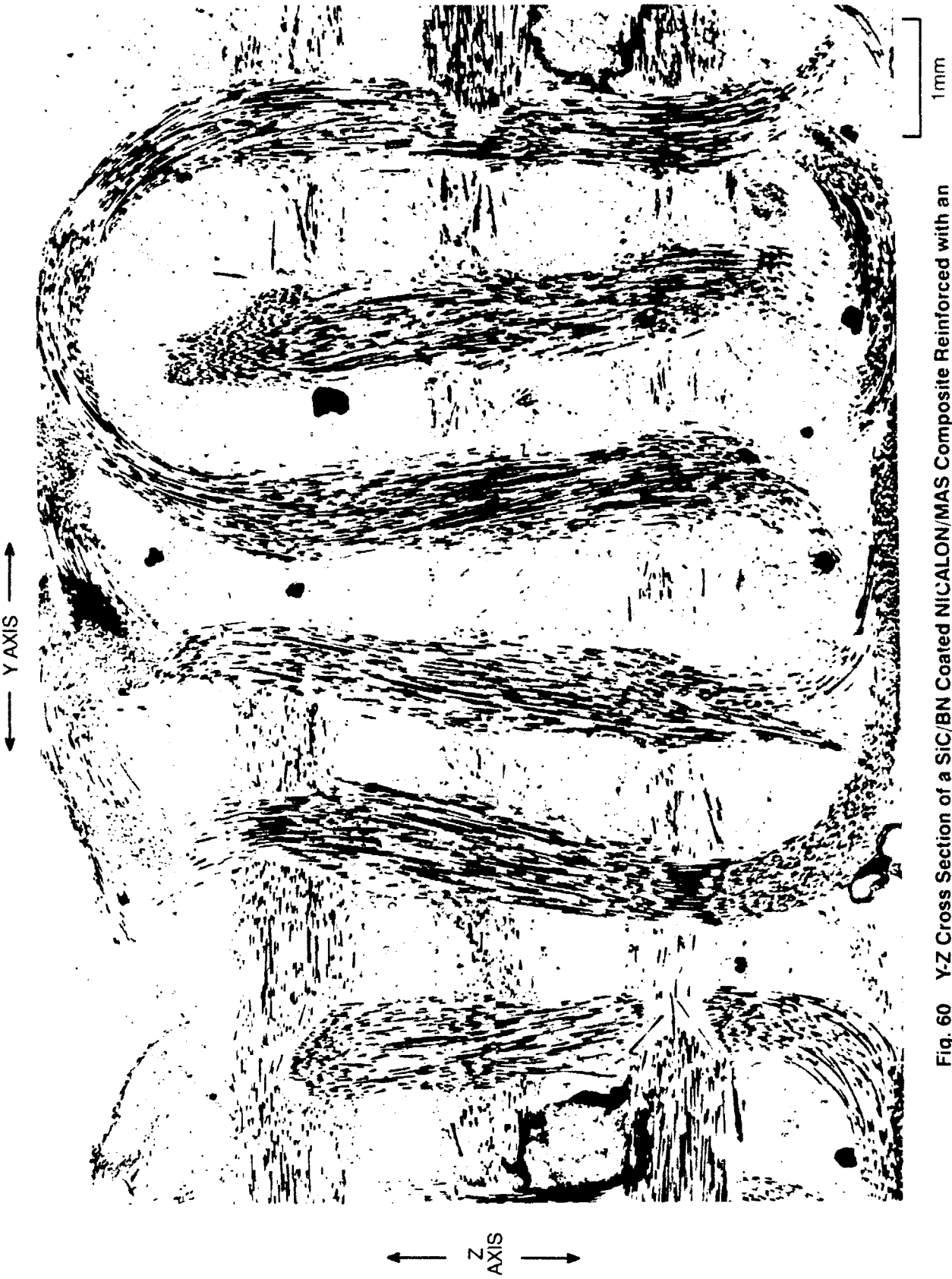

Fig. 60 Y-Z Cross Section of a SiC/BN Coated NICALON/MAS Composite Reinforced with an Orthogal Weave and Fabricated by Glass Transfer Molding (Composite No. 186-92)

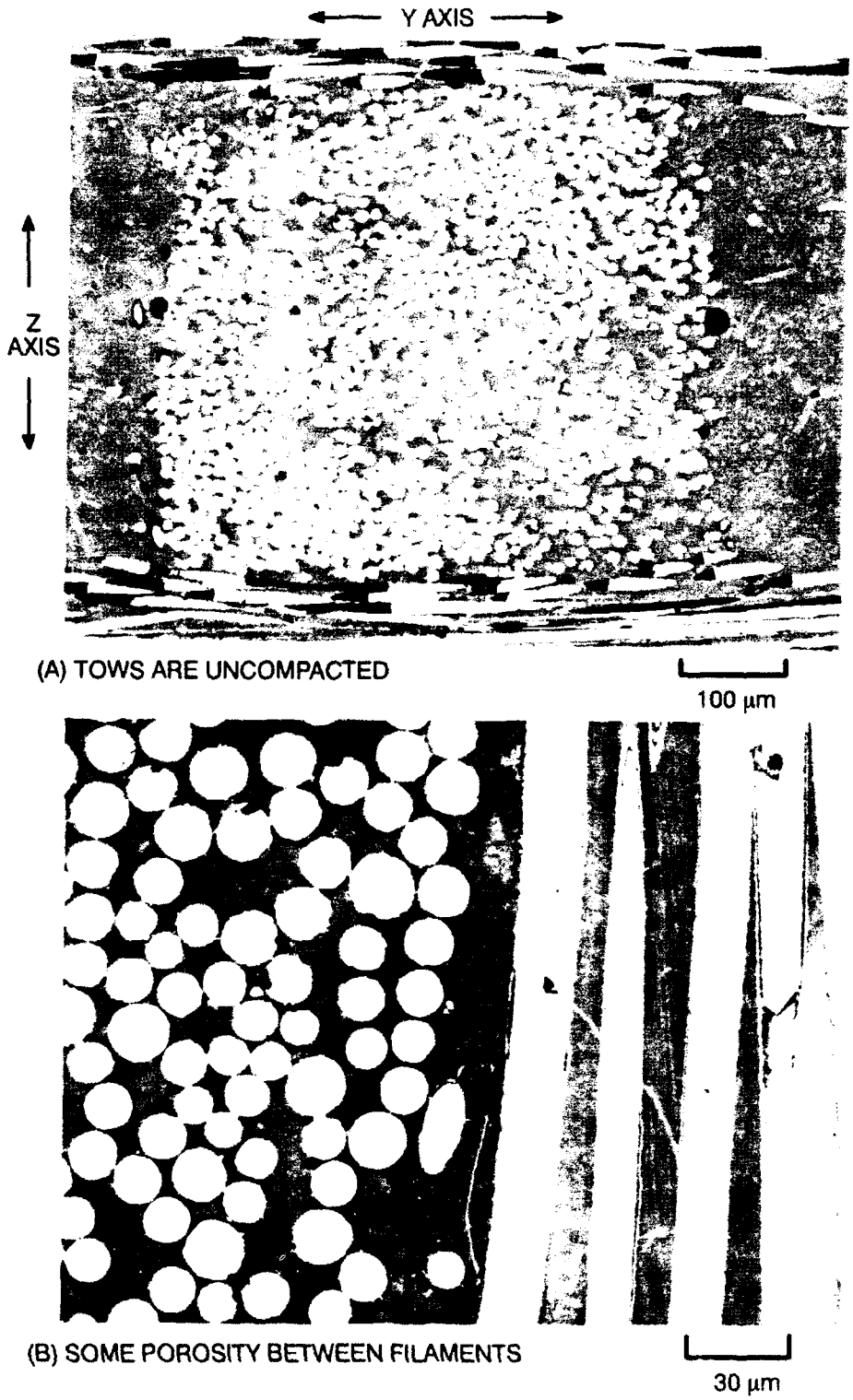

Fig. 61 SiC/BN Coated Nicalon Composite Fabricated by Glass Transfer Molding (Composite No. 186-92)

EP301-10-51

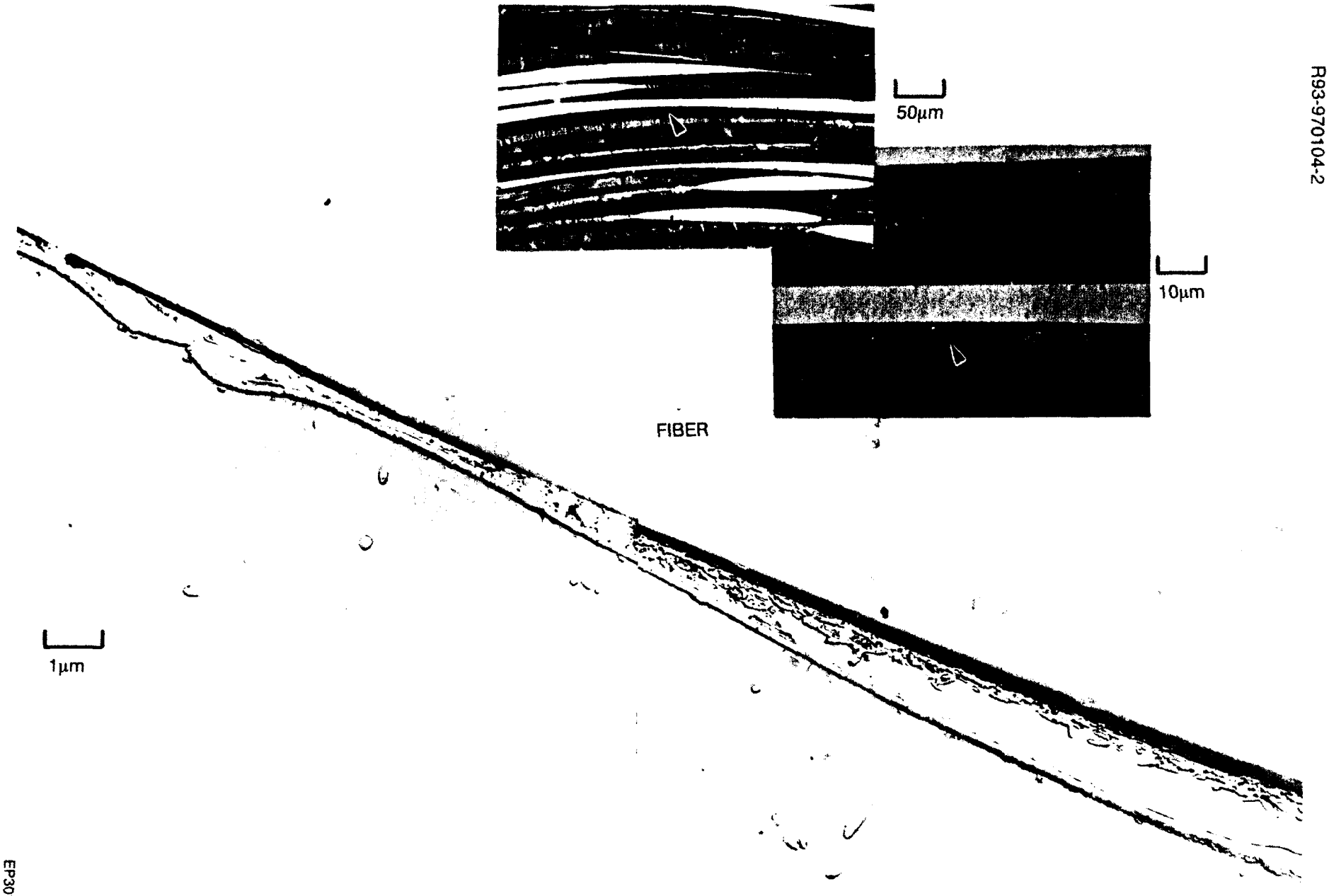

R93-970104-2

EP301-10-35

Fig. 62 Optical/TEM Micrographs of Longitudinally Sectioned MAS/SiC/BN/Nicalon Fiber "3D Weave" Composite #186-92 Showing Separation of SiC/BN Coating at Maximum Inwards Curvature of Fiber Weave

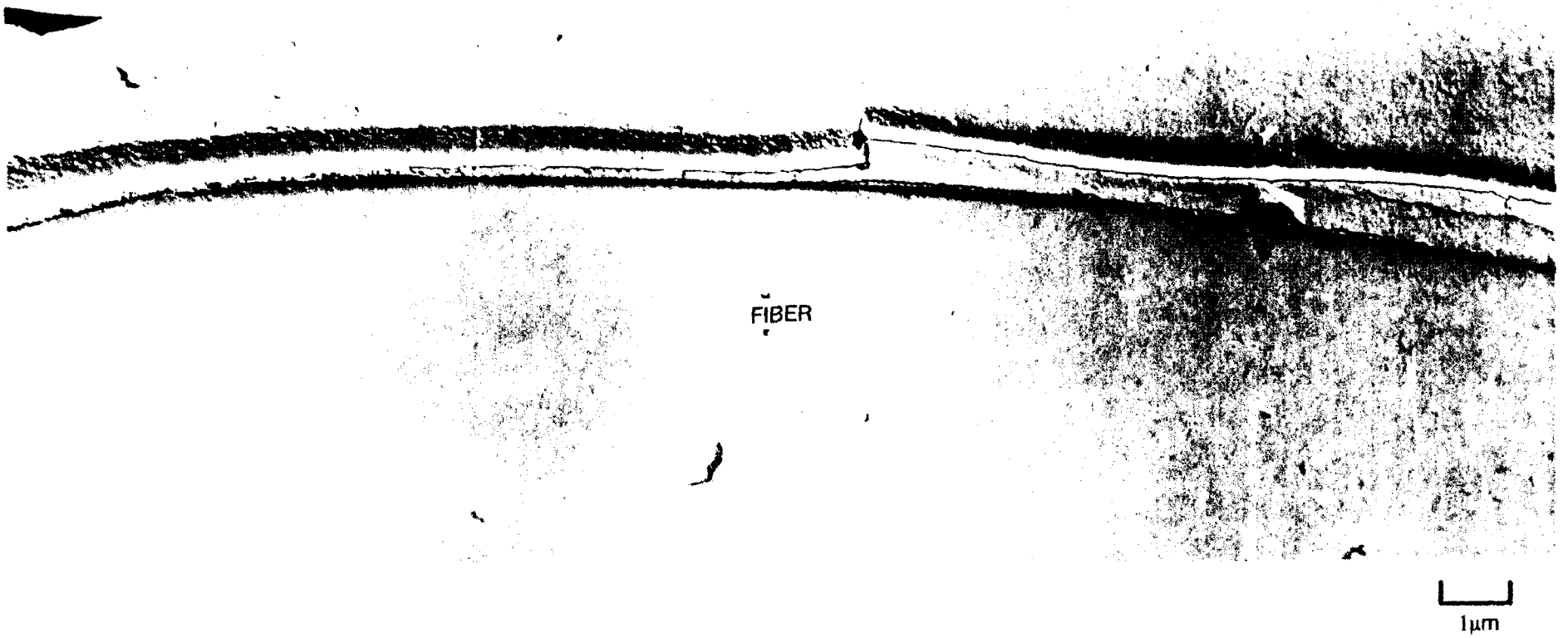

Fig. 63 TEM Micrograph of Longitudinally Sectioned MAS/SiC/BN/Nicalon Fiber "3D Weave" Composite #186-92 Showing Separation of SiC/BN Coating at Maximum Outwards Curvature of Fiber Weave